50272-101

REPORT DOCUMENTATION PAGE	1. REPORT NO. NCEER-92-0030	2.	3. PB93-198307

4. Title and Subtitle
Evaluation of Seismic Retrofit of Reinforced Concrete Frame Structures: Part I - Experimental Performance of Retrofitted Subassemblages

5. Report Date
December 8, 1992

6.

7. Author(s)
D. Choudhuri, J.B. Mander and A.M. Reinhorn

8. Performing Organization Rept. No.
-

9. Performing Organization Name and Address
Department of Civil Engineering
State University of New York at Buffalo
Buffalo, New York 14260

10. Project/Task/Work Unit No.

11. Contract(C) or Grant(G) No.
(C) BCS-90-25010
(G) NEC-91029

12. Sponsoring Organization Name and Address
National Center for Earthquake Engineering Research
State University of New York at Buffalo
Red Jacket Quadrangle
Buffalo, New York 14261

13. Type of Report & Period Covered
Technical report

14.

15. Supplementary Notes
This research was conducted at the State University of New York at Buffalo and was partially supported by the National Science Foundation under Grant No. BCS 90-25010 and the New York State Science and Technology Foundation under Grant No. NEC-91029.

16. Abstract (Limit: 200 words)
This report is Part I of a two part series on the evaluation of seismic retrofit methods for reinforced concrete frame structures. It deals with the experimental behavior of retrofitted reinforced concrete column elements and beam-column joint sub-assemblages under reversed cyclic lateral loading. A seismic retrofit/rehabilitation re-design methodology was developed, and validated in the present experimental study. Two column specimens, a one-way beam-column subassemblage and a two-way beam-column-slab subassemblage, all originally designed in accordance with ACI-318 for gravity loads only (1.4D + 1.7L), were retrofitted and tested at increasing drift amplitudes. The original specimens possessed relatively weak columns with respect to the adjacent beam strength. The retrofitted column specimens showed increased strength and a ductile post-yield behavior. Longtudinal bar buckling in the columns and low cycle fatigue failures as seen in the original/as-built specimen tests were entirely averted in the retrofitted specimens. The beam-column joint and the subassemblage retrofit, though distinct, were successful at converting the specimen failure mechanisms to a desirable strong-column/weak-beam one. Comparisons are made between the displacement response of the original/as built specimen tests and the present retrofitted test results. Conclusions are drawn on the efficacy of the retrofit schemes and the failure mechanisms observed.

17. Document Analysis a. Descriptors

b. Identifiers/Open-Ended Terms
Reinforced Concrete frames. Retrofitting. Beam column joints. Reversed cyclic loads. Lateral loads. Beam column slab subassemblages. Capacity design methods. Detailing. Partially prestressing. Gravity loads. Column jacketing. Post-tensioning. Added slab fillets. Masonry jacketing. Earthquake Engineering.

c. COSATI Field/Group

18. Availability Statement	19. Security Class (This Report)	21. No. of Pages
Release Unlimited	Unclassified	136
	20. Security Class (This Page) Unclassified	22. Price

PB93-198307

NATIONAL CENTER FOR EARTHQUAKE
ENGINEERING RESEARCH
State University of New York at Buffalo

Evaluation of Seismic Retrofit of Reinforced Concrete Frame Structures:

Part I — Experimental Performance of Retrofitted Subassemblages

by

D. Choudhuri, J.B. Mander and A.M. Reinhorn
Department of Civil Engineering
State University of New York at Buffalo
Buffalo, New York 14260

Technical Report NCEER-92-0030

December 8, 1992

This research was conducted at the State University of New York at Buffalo and was partially supported by the National Science Foundation under Grant No. BCS 90-25010 and the New York State Science and Technology Foundation under Grant No. NEC-91029.

NOTICE

This report was prepared by the State University of New York at Buffalo as a result of research sponsored by the National Center for Earthquake Engineering Research (NCEER) through grants from the National Science Foundation, the New York State Science and Technology Foundation, and other sponsors. Neither NCEER, associates of NCEER, its sponsors, the State University of New York at Buffalo, nor any person acting on their behalf:

a. makes any warranty, express or implied, with respect to the use of any information, apparatus, method, or process disclosed in this report or that such use may not infringe upon privately owned rights; or

b. assumes any liabilities of whatsoever kind with respect to the use of, or the damage resulting from the use of, any information, apparatus, method or process disclosed in this report.

Any opinions, findings, and conclusions or recommendations expressed in this publication are those of the author(s) and do not necessarily reflect the views of the National Science Foundation, the New York State Science and Technology Foundation, or other sponsors.

Evaluation of Seismic Retrofit of Reinforced Concrete Frame Structures:

Part I - Experimental Performance of Retrofitted Subassemblages

by

D. Choudhuri[1], J.B. Mander[2] and A.M. Reinhorn[3]

December 8, 1992

Technical Report NCEER-92-0030

NCEER Project Numbers 89-1001A, 90-1001A and 91-3111B

NSF Master Contract Number BCS 90-25010
and
NYSSTF Grant Number NEC-91029

1 Graduate Research Assistant, Department of Civil Engineering, State University of New York at Buffalo
2 Assistant Professor, Department of Civil Engineering, State University of New York at Buffalo
3 Professor, Department of Civil Engineering, State University of New York at Buffalo

NATIONAL CENTER FOR EARTHQUAKE ENGINEERING RESEARCH
State University of New York at Buffalo
Red Jacket Quadrangle, Buffalo, NY 14261

PREFACE

The National Center for Earthquake Engineering Research (NCEER) was established to expand and disseminate knowledge about earthquakes, improve earthquake-resistant design, and implement seismic hazard mitigation procedures to minimize loss of lives and property. The emphasis is on structures in the eastern and central United States and lifelines throughout the country that are found in zones of low, moderate, and high seismicity.

NCEER's research and implementation plan in years six through ten (1991-1996) comprises four interlocked elements, as shown in the figure below. Element I, Basic Research, is carried out to support projects in the Applied Research area. Element II, Applied Research, is the major focus of work for years six through ten. Element III, Demonstration Projects, have been planned to support Applied Research projects, and will be either case studies or regional studies. Element IV, Implementation, will result from activity in the four Applied Research projects, and from Demonstration Projects.

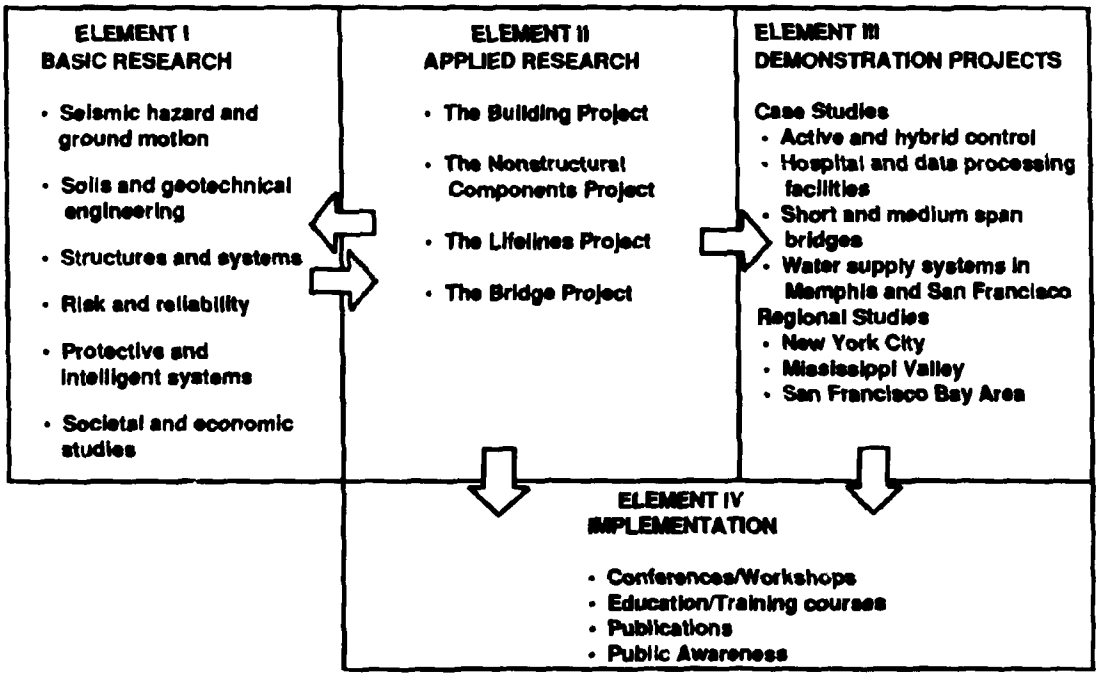

Research in the **Building Project** focuses on the evaluation and retrofit of buildings in regions of moderate seismicity. Emphasis is on lightly reinforced concrete buildings, steel semi-rigid frames, and masonry walls or infills. The research involves small- and medium-scale shake table tests and full-scale component tests at several institutions. In a parallel effort, analytical models and computer programs are being developed to aid in the prediction of the response of these buildings to various types of ground motion.

Two of the short-term products of the **Building Project** will be a monograph on the evaluation of lightly reinforced concrete buildings and a state-of-the-art report on unreinforced masonry.

The **structures and systems program** constitutes one of the important areas of research in the **Building Project**. Current tasks include the following:

1. Continued testing of lightly reinforced concrete external joints.
2. Continued development of analytical tools, such as system identification, idealization, and computer programs.
3. Perform parametric studies of building response.
4. Retrofit of lightly reinforced concrete frames, flat plates and unreinforced masonry.
5. Enhancement of the IDARC (inelastic damage analysis of reinforced concrete) computer program.
6. Research infilled frames, including the development of an experimental program, development of analytical models and response simulation.
7. Investigate the torsional response of symmetrical buildings.

This report is the first of a two-report series summarizing research on the retrofit of reinforced concrete buildings that had been designed only for gravity loadings. This first report is concerned with reduced-scale column, beam-column, and beam-column-slab specimens which were retested after retrofit. Various retrofit methods were tried, including column jacketing, post-tensioning, adding slab fillets, and masonry jacketing. The goal was to convert to weak column mechanism to a weak beam mechanism. The results of these tests served to design the model building retrofit and to aid in the development of analytical models. The second report describes the performance of the retrofitted model building.

ABSTRACT

This report is Part I of a two part series on the evaluation of seismic retrofit methods for reinforced concrete frame structures. It deals with the experimental behavior of retrofitted reinforced concrete column elements and beam-column joint subassemblages under reversed cyclic lateral loading. A seismic retrofit/rehabilitation redesign methodology was developed, and validated in the present experimental study. Part II describes the application of this method to a one-third scale model building.

In this report two column specimens, a one-way beam-column subassemblage and a two-way beam-column-slab subassemblage, all originally designed in accordance with AC1-318 for gravity loads only (1.4D + 1.7L), were retrofitted and tested at increasing drift amplitudes. The original specimens possessed relatively weak columns with respect to the adjacent beam strength.

The retrofitted column specimens showed increased strength and a ductile post-yield behavior. Longitudinal bar buckling in the columns and low cycle fatigue failures as seen in the original/as-built specimen tests were entirely averted in the retrofitted specimens.

The beam-column joint and the subassemblage retrofit, though distinct, were successful at converting the specimen failure mechanisms to a desirable strong-column/weak-beam one.

Comparisons are made between the displacement response of the original/as-built specimen tests and the present retrofitted test results. Conclusions are drawn on the efficacy of the retrofit schemes and the failure mechanisms observed.

ACKNOWLEDGEMENTS

This research was carried out at the Department of Civil Engineering at the State University of New York at Buffalo. Financial support is gratefully acknowledged from the National Center for Earthquake Engineering Research under contract numbers NCEER 89-1001A, 90-1001A, and 913111B.

The authors wish to thank Messrs. M. Pittman, P. Patarroyo, D. Walch, and R. Cizdziel for their assistance towards the construction and testing of the specimens.

TABLE OF CONTENTS

TABLE OF CONTENTS (Cont'd)

LIST OF ILLUSTRATIONS

LIST OF ILLUSTRATIONS (Cont'd)

LIST OF TABLES

SECTION 1

INTRODUCTION

1.1 Research Context

The study presented herein is part of a comprehensive research program sponsored by the National Center for Earthquake Engineering (NCEER) to assess the seismic damage potential and evaluate the performance of buildings in low to medium seismic zones, such as in the eastern and central United States. Buildings in these zones are typically designed only for gravity loads (U = 1.4D + 1.7L) according to the non-seismic detailing provisions of the code. These buildings are also referred to as lightly reinforced concrete (LRC) structures throughout this report. Although such structures are designed without consideration of lateral loads, they still possess an inherent lateral strength which may be capable of resisting some minor and moderate earthquakes. However, the deficient detailing of members can lead to inadequate structural performance during seismic activity.

The research program, entitled **seismic performance of gravity load designed reinforced concrete (R/C) frame buildings**, was developed and carried out according to the plan outlined in Fig. 1.1.

Based on a survey of typical building construction practices in the eastern and central United States (Lao 1990 and El-Attar et.al., 1991a and 1991b), a one-third scale model was constructed and tested on the shaking table in the State University of New York (SUNY) at Buffalo Earthquake Simulation Laboratory. The prototype design, model construction and similitude, initial dynamic characteristics, shaking table testing program along with the simulated ground motions, and the elastic response of the model from minor base motions are presented in Part I of the evaluation report series research program (Bracci et al., 1992a). Based on that report, analytical models can be developed and used to predict the inelastic response of the model building during more severe earthquakes.

The experimental investigation of the companion columns and beam-column components of the one-third scale model building is presented in Part II of the evaluation report series (Aycardi et al. 1992). The components were tested under quasi-static reversed cyclic loading and tests were conducted prior to testing of the model building. The results of the component tests were used to identify the behavior of localized members and subassemblages of the structure and the member properties were used to predict the overall response of the model building with analytical tools.

The experimental and analytical performance of the model building during moderate and severe ground shaking is presented in Part III of the evaluation report series (Bracci et al., 1992b). The analytical predictions of the model building during these earthquakes are presented based on member behavior developed from engineering approximations and component tests. Some of the conclusions of this study are that the response of the model is governed by weak column-strong beam behavior and large story drifts develop under moderate and severe earthquakes. A one-eighth scale model of the same prototype building was also constructed and tested at Cornell University by El-Attar et al. (1991b) as part of a collaborative study with SUNY/Buffalo. A comparison of the response behavior between the two scale models is also presented

A continuing research program was conducted on various **seismic retrofit techniques for reinforced concrete (R/C) frame structures** typically constructed in low seismicity zones. This report is Part I of the retrofit report series. In it, a capacity analysis and redesign method for seismic retrofitting of R/C structures is developed and tested. Retrofit using the concrete jacketing technique was selected and first performed on companion components. The retrofitted components were tested under quasi-static reversed cyclic loading and used to identify the behavior of the individual members. Retrofit of the components was also performed to verify the constructability of the retrofit technique for the model building.

In Part II of the retrofit report series by Bracci et.al. (1992c), the member properties from these component tests using the concrete jacketing technique were used to predict the response of the overall retrofitted model building with analytical tools. Based on analytical estimates, a global seismic retrofit for the one-third scale model building was proposed and constructed. An experimental and analytical shaking table study of the retrofitted model building was then conducted and the response behavior is presented. The main conclusions from this study are that seismic retrofit of gravity load designed R/C frame buildings: (i) can be designed to successfully enforce strong column-weak beam behavior; and (ii) is a viable economic and structural alternative as compared to demolition and reconstruction of another building.

1.2 Overall Objectives of Research Program

The objectives of the overall research program are summarized below along with the corresponding NCEER publications from Table 1.1:

1. Investigate the performance and principal deficiencies of typical LRC frame buildings during earthquakes through shaking table testing of a one-third scale model under minor, moderate, and severe earthquakes. (*Seismic Resistance of R/C Frame Structures Designed only for Gravity Loads: Parts I and III*, Evaluation report series, by J.M. Bracci, A.M. Reinhorn, and J.B. Mander)
2. Identify the potential collapse mechanisms for typical LRC frame buildings. (*Seismic Resistance of R/C Frame Structures Designed only for Gravity Loads: Part III*, Evaluation report series, by J.M. Bracci, A.M. Reinhorn, and J.B. Mander)
3. Determine the behavior and material properties of individual members and subassemblages of the structure. (*Seismic Resistance of R/C Frame Structures Designed only for Gravity Loads: Part II*, Evaluation report series, by L.E. Aycardi, J.B. Mander, and A.M. Reinhorn)
4. Determine the contribution of components in the overall response of the structure near collapse. (*Seismic Resistance of R/C Frame Structures Designed*

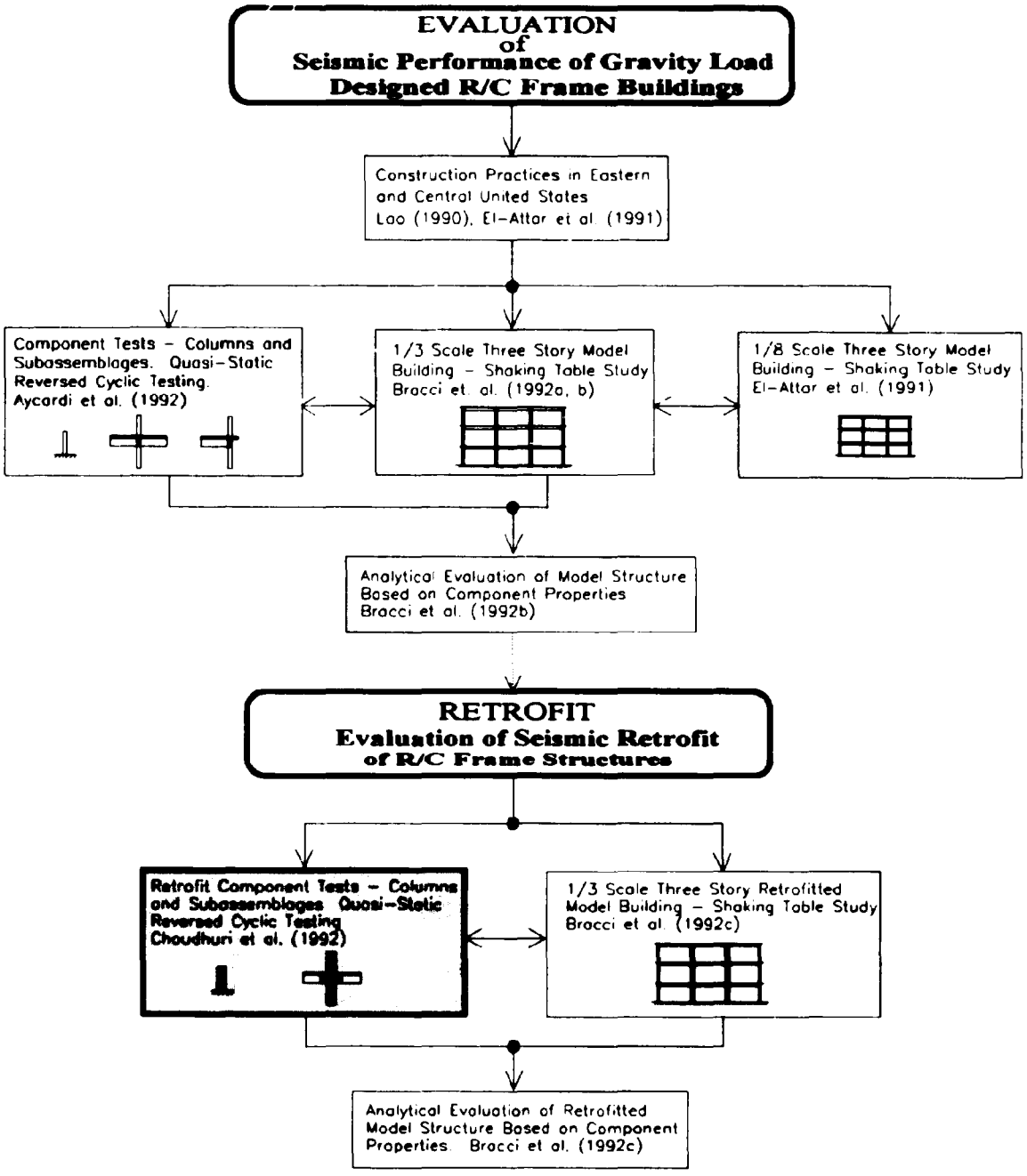

Fig 1.1 Research Context - Seismic Performance of Gravity Load Designed Reinforced Concrete Frame Buildings

only for *Gravity Loads: Parts II and III*, Evaluation report series, by J.M. Bracci, L.E. Aycardi, A.M. Reinhorn, and J.B. Mander).

5. Compare the measured response of the model building with that predicted by analytical models developed from engineering approximations or from component tests using a non-linear time history dynamic analysis. (*Seismic Resistance of R/C Frame Structures Designed only for Gravity Loads: Part III*, Evaluation report series, by J.M. Bracci, A.M. Reinhorn, and J.B. Mander)
6. Investigate appropriate local and global retrofit techniques for improving the seismic performance of LRC buildings. (*Evaluation of Seismic Retrofit of R/C Frame Structures: Part II*, Retrofit report series, by J.M. Bracci, A.M. Reinhorn, and J.B. Mander)
7. Investigate the seismic performance of the retrofitted model building and compare the measured response with the response of the original (unretrofitted) model for the same earthquakes. (*Evaluation of Seismic Retrofit of R/C Frame Structures: Part II*, Retrofit report series, by J.M. Bracci, A.M. Reinhorn, and J.B. Mander)
8. Determine the behavior and material properties of the retrofitted members and subassemblages of the structure. (*Evaluation of Seismic Retrofit of R/C Frame Structures: Part I*, Retrofit report series, by D. Choudhuri, J.B. Mander, and A.M. Reinhorn)
9. Determine the contribution of retrofitted and unretrofitted components in the overall response of the structure near collapse. (*Evaluation of Seismic Retrofit of R/C Frame Structures: Part I*, Retrofit report series, by D. Choudhuri, J.B. Mander, and A.M. Reinhorn)
10. Compare the measured response of the retrofitted model building with that predicted by analytical models developed from engineering approximations or from component tests using a non-linear time history dynamic analysis. (*Evaluation of Seismic Retrofit of R/C Frame Structures: Part II*, Retrofit report series, by J.M. Bracci, A.M. Reinhorn, and J.B. Mander)

Table 1.1 NCEER Publications Summarizing Current Study

Evaluation Report Series

Seismic Resistance of R/C Frame Structures Designed only for Gravity Loads	
Part I: Design and Properties of a One-third Scale Model Structure (by J.M. Bracci, A.M. Reinhorn, and J.B. Mander), NCEER-92-0027	
(i)	Identification of deficiencies of current engineering practice.
(ii)	Scale modeling.
(iii)	Experimental identification of structural characteristics.
(iv)	Ground motion for structural evaluation and experimental program.
Note:	This report serves as bare material for evaluation of analytical tools.
Part II: Experimental Performance of Subassemblages (by L.E. Aycardi, J.B. Mander, and A.M. Reinhorn), NCEER-92-0028	
(i)	Identify behavior and deficiencies of various components in structures.
(ii)	Identify member characteristics for developing analytical models to predict the seismic response of the one-third scale model structure.
Note:	This report serves as evaluation of structural characteristics to be incorporated in the evaluation of the entire structural system.
Part III: Experimental Performance and Analytical Study of Structural Model (by J.M. Bracci, A.M. Reinhorn, and J.B. Mander), NCEER-92-0029	
(i)	Investigate the performance and the principal deficiencies of typical gravity load designed frame buildings during earthquakes through shaking table testing of a one-third scale model under minor, moderate and severe earthquakes.
(ii)	Identify the potential collapse mechanisms for such typical frame buildings.
(iii)	Compare the measured response of the model building with that predicted by analytical models developed from (1) engineering approximations, (2) component tests, and (3) an experimental fit using a non-linear time history dynamic analysis.
Note:	This report emphasizes the structural behavior, collapse margins via damage, and efficiency of predictions using component properties evaluated from tests.

Retrofit Report Series

Evaluation of Seismic Retrofit of R/C Frame Structures	
Part I: Experimental Performance of Retrofitted Subassemblages (by D. Choudhuri, J.B. Mander, and A. M. Reinhorn), NCEER-92-0030	
(i)	Presentation of retrofit techniques.
(ii)	Identify constructability and behavior of retrofitted components
(iii)	Identify retrofitted member characteristics for developing analytical models to predict seismic response of the retrofitted model building.
Part II: Experimental Performance and Analytical Study of Retrofitted Structural Model (by J.M. Bracci, A.M. Reinhorn, and J.B. Mander), NCEER-92-0031	
(i)	An analytical seismic evaluation of retrofitted gravity load designed frame buildings using various local and global retrofit techniques.
(ii)	Shaking table testing of one of the proposed retrofit techniques on the one-third scale model under minor, moderate and severe earthquakes.
(iii)	Verify a change in the formation of the potential collapse mechanism under ultimate load from an undesirable column-sidesway mechanism to a more desirable beam-sidesway mechanism.
(iv)	Compare the measured response of the retrofitted model building with that predicted by analytical models developed from engineering approximations and component tests using non-linear time-history dynamic analysis.

1.3 Background to Present Study

Seismic design of reinforced concrete structural systems has evolved over the last several decades as a result of much research and lessons learned from earthquakes. The present state-of-the-art takes into consideration the effect of lateral design loads due to strong ground motions, and requires careful detailing of structures to ensure a ductile seismic performance. There are a large number of concrete structures, in high seismic risk zones, which were designed prior to the advent of seismic design codes (e.g. ACI 318-71) which have undergone serious damage in recent earthquakes. This category of structures has often required extensive post-earthquake repair and retrofitting to render them safe and functional. Often the structural system is modified by including structural walls in a lightly reinforced frame. Many structures are still permitted to be constructed in low to medium seismic risk zones, in the eastern and the central United States, without accounting for the seismic provisions. The majority of cities east of the Rockies do not require seismic resistant design.

Cast-in-situ reinforced concrete has a number of desirable characteristics which make it a versatile construction material. However, in comparison to structural steel, retrofit modifications or repair of damage is generally more difficult to accomplish. Structures located in seismic zones often pose problems as the usual seismic design philosophy is to achieve energy dissipation through controlled inelastic deformations in plastic hinge zones, primarily in the beams. Many non-seismically designed structures possess strong beams and weak columns, which is in conflict with the conventional wisdom of today, that requires the formation of a beam-sidesway mechanism.

This study presents an experimental investigation on the behavior of retrofitted column components, a beam to column joint and an interior beam-column-slab subassemblage of a one-third scale model of a prototype designed for gravity loads according to ACI 318 non-seismic detailing. Particular emphasis is given to the inelastic performance and the expected failure mechanism in a seismic environment.

1.4 Review of Existing Repair and Retrofit Techniques

The objective of a repair scheme is principally to bring a damaged structure back to its original condition or better in an affordable manner. This involves repairing major cracks, local spalling, and diagonal cracks which usually follow flexural cracks, and adding new load carrying paths to the structure to ensure its safety and functionality.

In contrast, a seismic retrofitting scheme aims at augmenting strength, enhancing the ductility capacity and making the structure more resilient for earthquakes. A damaged structure is not a pre-requisite for such a scheme. Some form of seismic retrofitting would generally be required for low to medium rise buildings designed only for gravity loads (e.g. U = 1.4D + 1.7L). If the structure in question is damaged, a retrofitting scheme would encompass both repair of the structure together with ensuring a favorable failure mechanism in the event of a major earthquake.

The type of repair and/or retrofitting technique to be adopted depends on the nature and the extent of damage to the structure and the original design scheme. Some commonly used techniques are mentioned below :

Epoxy injection is the simplest procedure to repair relatively small cracks of widths less than $^1/_4$". Experimental work in this area has focused on low viscosity epoxy injection which has become a fairly standard practice in the last decade for repairing cracked structural elements.

For cracks larger than $^1/_4$", and regions where the concrete has crushed, epoxy injection is inappropriate. Research on repairing this type of damage has proposed the removal of the loose concrete and replacement with expansive cement mortar, Type-III high early strength mortar or other similar material.

In some cases, earthquake loads on reinforced concrete members result in buckled, excessively yielded or fractured reinforcement. Most researchers investigating repair of this type of damage have recommended repairing the reinforcement by replacement with

new steel, butt welding or lap welding. The damaged concrete has then typically been replaced with new concrete. This method is more a retrofit method than just a repair method, since it allows special detailing of flexural and shear reinforcement for strength and ductility.

Experimental and field retrofit work has been done in the area of infill walls and concrete wing walls. To implement these methods, the entire structure must be analyzed to ensure that the loads can be transferred to the foundation and that the failure is not transferred to another undesirable area. Proper interaction and load transfer between the existing structure and the new elements is of critical importance.

Development of methods for repairing and retrofitting damaged columns in moment-resisting concrete frames and in bridges is an important problem. A considerable amount of experimental work has been conducted in repairing, strengthening and improving the ductility of damaged columns. Collapse or severe damage of a number of California bridges in recent moderate earthquakes has emphasized the need to develop retrofit measures to enhance flexural strength, ductility and shear strength of bridge columns designed before the current seismic design provisions were implemented. Recently Chai, Priestley and Seible (1991) proposed a retrofit method for circular columns by encasing plastic hinge regions with a grouted steel jacket. This method has received widespread use by Caltrans in their bridge column retrofit program. In addition to providing external steel shells, other methods of providing external steel reinforcement tested include steel straps, new closely spaced reinforcing steel ties, or welded wire fabric together with filling voids with concrete grout or shotcrete have all proved successful. It is important to perform an overall analysis to ensure that changes in stiffness introduced do not produce adverse distribution of internal forces. Column jacketing ensures that the zones of likely damage future earthquakes are confined to portions of the beams outside the connection. For jacketing, the surface of the damaged member is first roughened and new reinforcement is placed around it, then the forms are erected and the concrete is poured.

Instead of jacketing with a reinforced concrete shell as described above, reinforced masonry which encompasses the existing section can be used to provide similar retrofitted properties. A thin wire mesh can be provided in the bed joints to limit shear cracking and to ensure continuity of the masonry and existing column section. A reinforced concrete fillet in the joint area is also recommended. For details, see Part II of the retrofit report series (Bracci et al., 1992 c) of the continuing research program.

Column strength enhancement without complete obstruction of passageways can also be obtained with a partial infill constructed on each side of selected columns in a structure. The partial wall should not extend more than a few masonry units from the face of the column; the precise number of blocks will generally be governed by the required development length of the discontinuous positive beam reinforcement. Longitudinal (vertical) wall reinforcement would extend through the floor slabs, and additional transverse reinforcement and masonry joint reinforcement should be used in this design. For details, see Part II of the retrofit report series (Bracci et al., 1992 c) of the continuing research program.

1.5 Scope of Present Research

In this report, a form of the capacity design philosophy is applied to seismic retrofitting and described in Section 2. Section 3 deals with column components. Two specimens were tested, each adopting a distinct retrofit method. Section 4 addresses a one-way beam column joint and its retrofit technique. The specimen was designed for gravity loads only. The retrofit technique adopted gives due importance to the joint; often the weakest link in the structure. Section 5 describes a two-way beam column joint which includes the floor slab. Partially prestressed concrete, specifically post-tensioning, has been used together with elements of reinforced concrete to develop an effective retrofit method.

SECTION 2

CAPACITY DESIGN

2.1 Fundamentals of the Capacity Design Philosophy for New Structures

The *capacity design* method in its entirety has been based on the pioneering work of Paulay and his co-workers. He summarizes it as follows: "In the capacity design of earthquake-resistant structures, elements of primary lateral load resistance are chosen and suitably designed for energy dissipation under severe deformation. All other structural elements are then provided with sufficient strength so that the chosen means of energy dissipation can be maintained."

The *capacity design* method is a deterministic procedure where the designer "tells the structure what to do" in order to prevent the occurrence of undesirable failure mechanisms such as shear, bond or anchorage, or a column sidesway/soft story mechanism. This design procedure uses code-specified lateral static loads which are apportioned in a manner similar to the first mode shape. Elastic analysis is carried out and beam design moments assigned based on redistribution of elastic bending moments. Columns are designed based on the overstrength capacity of beam-strengths, in which an allowance is made for higher mode response. The strength of those elements are enhanced because they are not intended to participate in the primary energy dissipation process and require added protection. Thereby the designer is able to control the mode and the areas in which the structure forms its plastic mechanism.

The essence of the *capacity design* procedure lies in the formation of a weak beam-strong column sidesway mechanism. This durable form of a collapse mechanism makes it imperative for designers to insure that, when required, plastic hinges will form in the beams at many or all floors as shown in Fig. 2.1 (a). The occurrence of the soft-story sidesway mechanism, which constitutes the formation of plastic hinges in the columns of any one story, is undesirable as the plastic hinge rotational demands are excessive for

a given structure ductility.

The challenge of designing an earthquake-resistant reinforced concrete building lies in determining the expected forces and/or deformations in a preliminary design and providing resistance by appropriate proportioning of member strengths. Particular care needs to be taken in the detailing of members and their connections. This is a two-fold process: one of which is determining the expected demands and the other providing the necessary capacity for the structure in question. Special emphasis is placed on those regions whose failure can affect the integrity and stability of a significant portion of the structure.

The New Zealand loadings code (NZS4203) and concrete code (NZS3101) were among the first to explicitly adopt this philosophy of design. Subsequently the ACI Code 318 has implicitly adopted aspects of this approach by the inclusion of the following equation:

$$\sum M_e \geq (6/5) \sum M_g \qquad \textbf{(2-1)}$$

where $\sum M_e$ = sum of moments, at the center of the joint, corresponding to the design flexural strength of the columns framing into the joint. Column flexural strength shall be calculated for the factored axial force, consistent with the direction of the lateral forces considered, resulting in the lowest flexural strength and $\sum M_g$ = sum of moments, at the center of the joint, corresponding to the design flexural strength of the girders framing into that joint. It should be noted that the yield strength to be used for the girder reinforcement is to be factored up by 1.25 to give the over-strength moment. This equation was first introduced as Eq. A-1 in the 1979 edition of the ACI 318, and now exists as Eq. 21-1 in the 1989 edition.

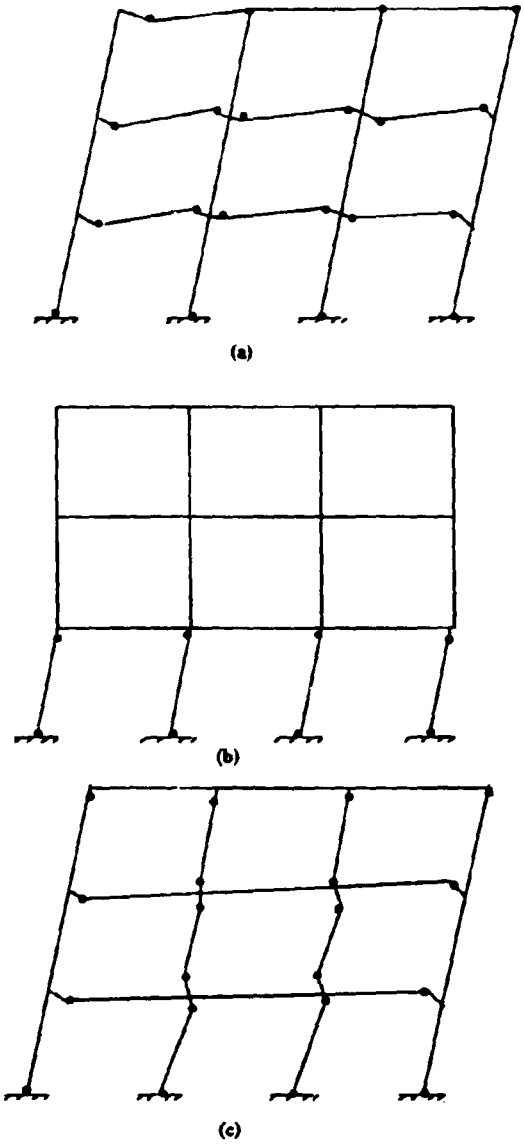

Fig. 2.1 Mechanisms of Failure of a Frame (a) Beam sidesway (b) Column sidesway (c) Hybrid Mechanism

2.2 Capacity Analysis and Redesign of an Existing Gravity Load Designed Frame

This section sets forth an application of capacity design principles for the seismic retrofit and strengthening of existing structural systems and will be referred to herein as *capacity analysis and redesign*. The primary objectives of *capacity analysis and redesign* of an existing gravity load designed frame are threefold:

1. Conversion of a weak-column/strong-beam structure to a dependable strong-column/weak-beam structure. This implies a change of the failure mechanism of the structure from a column sidesway or hybrid mechanism to a beam sidesway mechanism.
2. Upgrade the ductility capacity of the column hinges at the ground floor level.
3. Enhance the strength capacity of the beam-column joint core.

These objectives are achieved by following a sequence of design stages which are presented below:

Flexural check of beam strength distribution

In most structures that are designed for gravity loads (1.4D + 1.7L) the bottom positive reinforcement of the beams is discontinuous with only 6" embedment into the joint. It is of importance to provide a dependable positive moment capacity to ensure the negative moments are capable of being redistributed. This may be accomplished by providing a joint fillet. The design length of the fillet to be provided is dictated by the anchorage length required for the positive (bottom) reinforcement of the beam. This is calculated by using the ACI formulation:

$$l_d = 0.02 d_b f_y / \sqrt{f'_c} \qquad (2.2)$$

As the existing embedment into the column may have been damaged from previous in-service loadings, this length should be provided from the face of the original as-built column.

Check of shear strength

When a structure is redesigned, it is not the intention of the designer to increase the shear capacity of the beams to the code specified strength as required of a new structure. The designer, on the other hand, should isolate only those critical regions which are included in the active energy dissipation process, such as potential plastic hinges and assess their shear strengths. The center regions of beams also should be assessed for shear strength. Some supplementary transverse reinforcement may be necessary for beams with few or no stirrups, but this is generally too difficult to warrant implementing.

Flexural strength redesign of columns

The first objective of *capacity analysis and redesign* is achieved by augmenting the flexural strength of the existing columns. The principal aim is to minimize additional reinforcing steel that needs to be added in order to alleviate congestion when pouring concrete in a confined space. To best achieve this objective, principles of prestressed concrete can be employed. By keeping the column uncracked at all times, the intrinsic shear strength of uncracked concrete (V_{cw} or V_{ci} as applicable) should be sufficient to resist the most adverse shear force, obviating the need for transverse reinforcing steel.

Consider the stress blocks of a column under combined axial load and flexure as illustrated in Fig. 2.2. The respective equations for the outermost compression and tension fibers for concentric prestress are as follows:

$$-\frac{P}{A_g} - \frac{M}{S_x} \geq f_c \tag{2.3}$$

$$-\frac{P}{A_g} + \frac{M}{S_x} \leq f_t \tag{2.4}$$

in which P = total axial load from prestress and gravity effects ($= P_p + P_g$), M = moment demand and $S_x = A_g d/6$ = section modulus where A_g = gross cross-section area. The maximum allowable compression and tensile strength under transient earthquake loads may be taken as $f_c = -0.6f'_c$, $f_t = 12\sqrt{f'_c}$ (psi. units), respectively. By dividing Eqs.

2.3 and 2.4 by $-f_c'$ the following tension positive non-dimensional equations are obtained:

$$\frac{P}{A_g f_c'} + \frac{6M}{A_g f_c' d} \leq 0.6 \tag{2.5}$$

$$\frac{P}{A_g f_c'} - \frac{6M}{A_g f_c' d} \leq -\frac{12}{\sqrt{f_c'}} \tag{2.6}$$

where d = depth of section and f_c' = compressive strength of concrete in psi.

The optimal axial load will occur when Eqs. 2.5 and 2.6 are solved simultaneously giving:

$$\frac{P}{f_c' A_g} = \left(0.3 - \frac{6}{\sqrt{f_c'}} \right) \tag{2.7}$$

Assuming tension cracking prevails, the section can be sized from Eq. 2.6 which can be re-written as:

$$A_g d = \frac{6M}{f_c' \left(12/\sqrt{f_c'} + P/f_c' A_g \right)} \tag{2.8}$$

where the value of M = design moment is determined from Eq. 2.1. In Eq. 2.8 an axial load ratio can be assumed, or the optimum value from Eq. 2.7 can be used if minimum dimensions are desired.

Once the section size is determined, the longitudinal reinforcement is fixed. This limits the steel content for the RC column between respective minimum and maximum volumetric ratios of 0.01 and 0.03, with the latter limit being necessary to minimize steel congestion. For the PSC column, the ratio of the prestressed reinforcement for the computation of moment strength shall be such that $\omega_p = (\rho_p f_{ps})/f_c'$ is not greater

than $0.36\beta_1$ where $\rho_p = A_{ps}/bd_p$ = ratio of prestressed reinforcement, f_{ps} = stress in prestressed reinforcement at nominal strength calculated from Eq. 2.9 and β_1 = a factor to be taken as 0.85 for concrete strengths, f'_c , up to and including 4000 psi, and for strengths greater than 4000 psi, β_1 is reduced at a rate of 0.05 for each 1000 psi., but β_1 is not taken less than 0.65. The type of steel should be a high strength variety efficient in post-tensioning. The amount of prestress applied to the upper columns should be limited to 70% of ultimate strength of the prestressing bar used.

For an unbonded post-tensioned column, it is necessary to determine the dependable ultimate strength using the maximum steel stress, f_{ps} , calculated in accordance with ACI 318-89 which states:

$$f_{ps} = f_{se} + 10{,}000 + \frac{f'_c}{100.\rho_p} \qquad (2.9)$$

and the maximum value of f_{ps} in Eq. 2.9 is limited to the lesser of f_{py} and $(f_{se}+60{,}000)$, where f_{py} = specified yield strength of prestressed tendons in psi., f_{se} = effective stress in the prestressed reinforcement (after allowance for losses) psi., ρ_p = ratio of prestress reinforcement.

Once the longitudinal steel and the prestress values have been determined, Eqs. 2.4 and 2.5 may be plotted on an axial load-moment interaction diagram as shown in Fig. 2.3. The difference between the cracking and the ultimate surfaces should be checked to ensure there is a reserve strength capacity which is protection against moment magnification due to higher mode response. This reserve capacity should preferably be greater than 1.5 but need not be greater than 2. If it is observed that cracking could occur at the estimated moment demand or the axial load is less than the optimum value, additional prestressing should be used in the upper story columns.

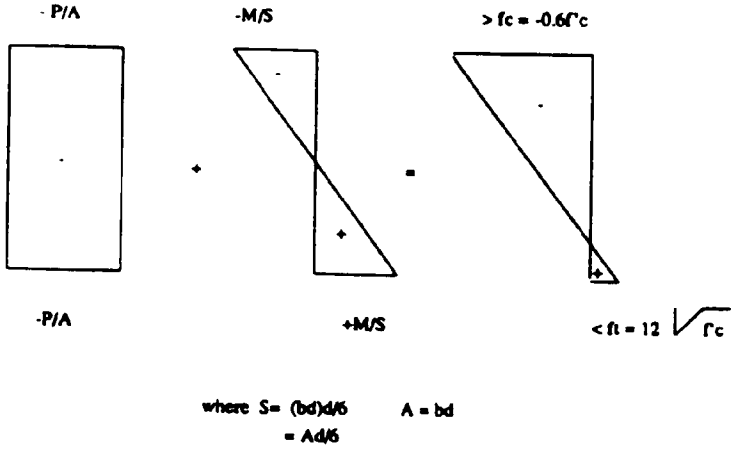

Fig. 2.2 Stress Block Diagram for Redesign

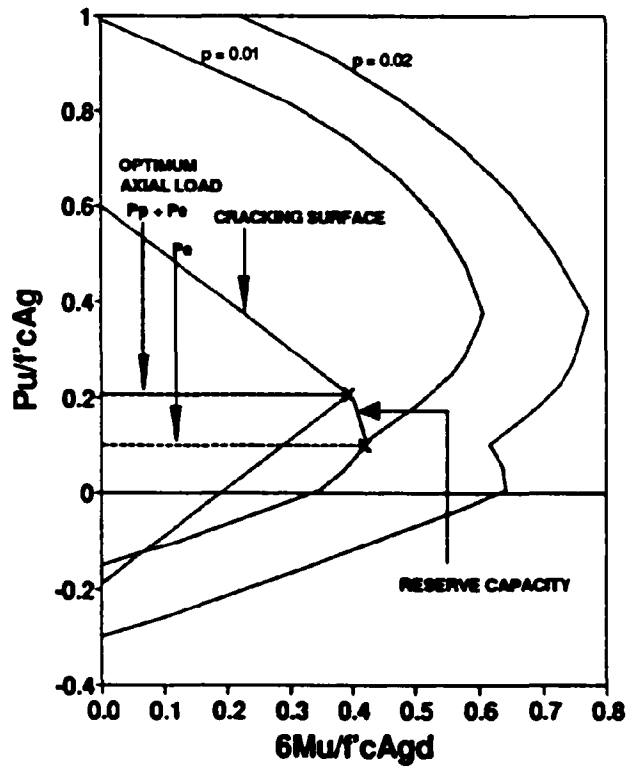

Fig. 2.3 Axial Load-Moment Capacity Interaction Diagram

The design shear on the column should be calculated from considering the critical end moments; it is given by $V_e = 2M_n / h_c$ where h_c = clear height of the column and M_n = the nominal strength of the columns with the factored axial load applied. This is used in the detailing of the transverse reinforcement of the redesigned columns.

Transverse reinforcement detailing of redesigned columns

For the lower story, where a RC column should be used at the ground floor level, the shear capacity of the section should satisfy $V_e < \phi(V_s + V_c)$ where $V_s = A_s f_y d/s$ = nominal shear strength to be provided by shear reinforcement and $V_c = 2\sqrt{f'_c} b_w d$ = nominal shear strength to be provided by concrete. The confining steel for the plastic hinge zone of the lower story column should be checked and the maximum spacing to be provided should be in accordance with $s \leq 8d_b$ where s =spacing of the hoops, and d_b =diameter of longitudinal reinforcement used.

For a PSC column without requiring transverse hoops $V_e < \phi V_c$ where V_c is the lesser of V_{ci} and V_{cw} given by:

$$V_{ci} = 0.6\sqrt{f'_c} b_w d + \frac{V_i M_{cr}}{M_{max}} \qquad (2.10)$$

but should be $V_{ci} \geq 1.7\sqrt{f'_c} b_w d$.

$$V_{cw} = (3.5\sqrt{f'_c} + 0.3 f_{pc}) b_w d \qquad (2.11)$$

where, V_{ci} = nominal shear strength provided by concrete when diagonal cracking results from combined shear and moment, f'_c = specified compressive strength of concrete in psi., b_w = web width or diameter of circular section, d = distance from the extreme compression fibre to centroid of longitudinal tension reinforcement, but not less than $0.80h$ for prestressed members, V_i = factored shear force at section due to

externally applied loads occurring simultaneously with M_{max} , M_{max} = maximum factored moment at section due to externally applied loads, M_{cr} = moment causing flexural cracking at section due to externally applied loads, f_{pc} = compressive strength in concrete at centroid of cross section resisting externally applied loads in psi.

Eq. 2.10 governs when the shear failure is initiated by flexural cracking. If the column end moments are considered then $\frac{V_i}{M_{max}} = \frac{V_e}{M_n} = \frac{2M_n}{h_c M_n}$, which when substituted in Eq. 2.10 gives the following equation:

$$V_{ci} = 0.6\sqrt{f'_c} b_w d + \frac{M_{cr}}{0.5 h_c} \qquad (2.12)$$

in contrast when the principal tensile stresses exceed the tensile strength of concrete web -shear cracking occurs and Eq. 2.11 governs.

Detailing of beam-column joint

The last step of *capacity analysis and redesign* concerns itself with the beam-column joint connection. The design length of the joint fillet (Refer Fig. 2.3a) was decided in the first stage of the redesign. However, a check should be made to ensure there is adequate anchorage of the top reinforcement against a sliding bond failure. If at least 40 longitudinal bar diameters are present between the outer faces of adjacent fillets, anchorage should not be a problem. Otherwise, it is recommended that the fillet length be extended to accomodate this anchorage necessary to avoid a sliding bond failure.

The horizontal joint shear should be calculated from the equilibrium of the subassemblage (Refer Fig. 2.3b). This is computed as:

$$V_{jh} = \frac{M_g^+ + M_g^-}{jd} - V_{col} \qquad (2.13)$$

where jd = depth of internal lever arm $\approx (d-d')$, $\sum M_g = M_g^+ + M_g^-$ = over strength capacity of girders = $(A_s + A_s')(1.25f_y)jd$, hence Eq. 2.13 can be written as:

$$V_{jh} = \sum M_g \left(\frac{1}{jd} - \frac{L/L_b}{h_s}\right) \tag{2.14a}$$

$$V_{jh} = (A_s + A_s')(1.25f_y)\left(1 - \frac{L}{L_b}\cdot\frac{jd}{h_s}\right) \tag{2.14b}$$

The horizontal joint shear V_{jh} is resisted by V_{ch} = horizontal joint shear resisted by concrete alone through a strut mechanism and by V_{sh} = horizontal joint shear resisted by the fillet reinforcement. This can be represented by the following equation:

$$V_{jh} = V_{ch} + V_{sh} \tag{2.15}$$

This method of *capacity analysis and redesign* includes a fillet which provides anchorage for the bottom reinforcement. If the structure in question has unbonded positive (bottom) beam reinforcement adjacent to the columns due to previous seismic activity, a layer of steel in the fillet of equal area as the positive beam reinforcement needs to be provided as shown in Fig. 2.4(a). It is important to realize that the presence of the joint fillet precludes the formation of any plastic hinge at the joint. Thus for an elastic joint, if $V_{jh} \le \phi V_{cw}$ (where V_{cw} is determined from Eq. 2.10), no additional joint steel need be provided. If however $V_{jh} \ge \phi V_{cw}$, Eq. 2.15 will apply and V_{ch} can be determined using Eq. 2.10, or by the following equation suggested in the New Zealand code NZS 3101:

$$V_{ch} = 0.5\frac{A_s'}{A_s}\left(1 + \frac{P}{0.4 f_c' A_g}\right)V_{jh} \tag{2.16}$$

where $\beta = A'_s/A_s$ = ratio of the beam/fillet compression to tension reinforcement where $0.5 \le \beta \le 1$. For the remainder of the horizontal joint shear force resisted by fillet steel, V_{sh} , the required area is calculated from Eq. 2.17.

$$A_{sj} = \frac{V_{jh} - V_{ch}}{\phi_s f_{yh}} \qquad (2.17)$$

2.3 Summary of the Design Processes

This section summarizes the aforementioned design methodologies. Note that in each scenario there is a parallel set of steps that progress through the design process.

CONVENTIONAL CAPACITY DESIGN	CAPACITY ANALYSIS AND REDESIGN
Step 1 : Longitudinal Beam Reinforcement	
D.1 Flexural design of beams:	**R.1 Flexural check of beam strength distribution:**
Beams are designed and propotioned for moments which are a result of applying the moment redistribution process to the elastic design code actions. Beam plastic hinges are generally located at the column face and adequately detailed for ductility. From the actual reinforcement provided the beams flexural overstrength capacity is assessed. This is used in beam shear and column strength design.	The anchorage of the positive reinforcement at the beam-column joint connection should be particularly considered. If the bottom bars are discontinuous then a means of providing dependable positive moment capacity needs to be devised for enhancing seismic resistance. A beam joint fillet is a recommended solution. From the actual reinforcement provided the beams flexural overstrength capacity is assessed. This should include the full effects of the floor slab steel on the negative moment capacity.

Step 2: Transverse Beam Reinforcement

D.2 Shear design of beams:

This is achieved by providing shear strength for the entire beam to be greater than the shear corresponding to the maximum possible flexural strength at the plastic hinge region of the beam. The underlying premise being that inelastic shear deformation does not provide the essential charecteristics for energy dissipation.

R.2 Check of shear strength:

It may not be the intent to bring beam shear capacity up to code strength for new design. However, critical regions such as potential plastic hinge zones and the centers of beams which may have little or no shear reinforcement should be assessed for shear strength and supplementary stirrups provided,if necessary.

Step 3: Longitudinal Column Reinforcement

D.3 Flexural Strength design of columns:

The nominal flexural strength of the columns is computed by considering the beam overstrengths. This ensures a weak-beam/strong-column failure mechanism. It should be mentioned that the beam flexural overstrengths are determined and then an additional allowance is made to account for possible higher-mode structural response. From the actual longitudinal reinforcement provided the flexural capacity is assessed. This is used in the next step for column shear design.

R.3 Flexural strength redesign of columns:

The required flexural strength of the columns is computed from the assessed beam overstrengths. The optimum axial load ratio is computed which helps size the column section. The lower story column is designed as a conventional RC section. If the imposed axial load due to gravity for the upper story columns is less than the optimum amount, prestress is applied to the upper story columns. The cracking surface for the prestressed columns is plotted on a column interaction diagram and the reserve capacity is computed. The ultimate shear to be resisted by the columns should be calculated for the transverse reinforcement design.

Step 4: Transverse Column Reinforcement

D.4 Transverse reinforcement detailing for the columns:

From the most adverse combination of column end overstrength moments the maximum possible shear force in the columns is computed. Transverse shear reinforcement is provided over the entire column height. Additional shear steel and/or confinement or antibuckling steel is generally also required in the potential plastic hinge zone.

R.4 Transverse reinforcement detailing for the redesigned columns:

For the lower story RC column step D.4 applies for the shear steel design. For the upper story PSC columns use the prestressed concrete code equations to determine the shear resisted by the concrete. Generally the intrinsic shear strength of the compressed concrete would be greater than the ultimate shear to be resisted, else provide supplementary transverse shear reinforcement.

Step 5: Beam Column Joint

D.5 Detailing of the beam-column joint:

The beam column joint is a poor source of energy dissipation and thus needs to be detailed to resist the high shear input from the beam and column actions. In this step the designer should attempt to keep the joint elastic by reducing if not eliminating any inelastic deformation due to the joint shear forces and bond deterioration.

R.5 Detailing of the beam-column joint:

Check that there is adequate longitudinal beam bar anchorage through the joint core. Since the length of the joint fillet has been decided in the Step 1 of the redesign, the designer should attempt to detail fillet reinforcement in this step. The joint may be considered to behave in an elastic manner and the shear resisted by concrete in elastic joints is computed. If the input shear forces from the beams and columns exceed that resisted by concrete via strut action provide the necessary reinforcement.

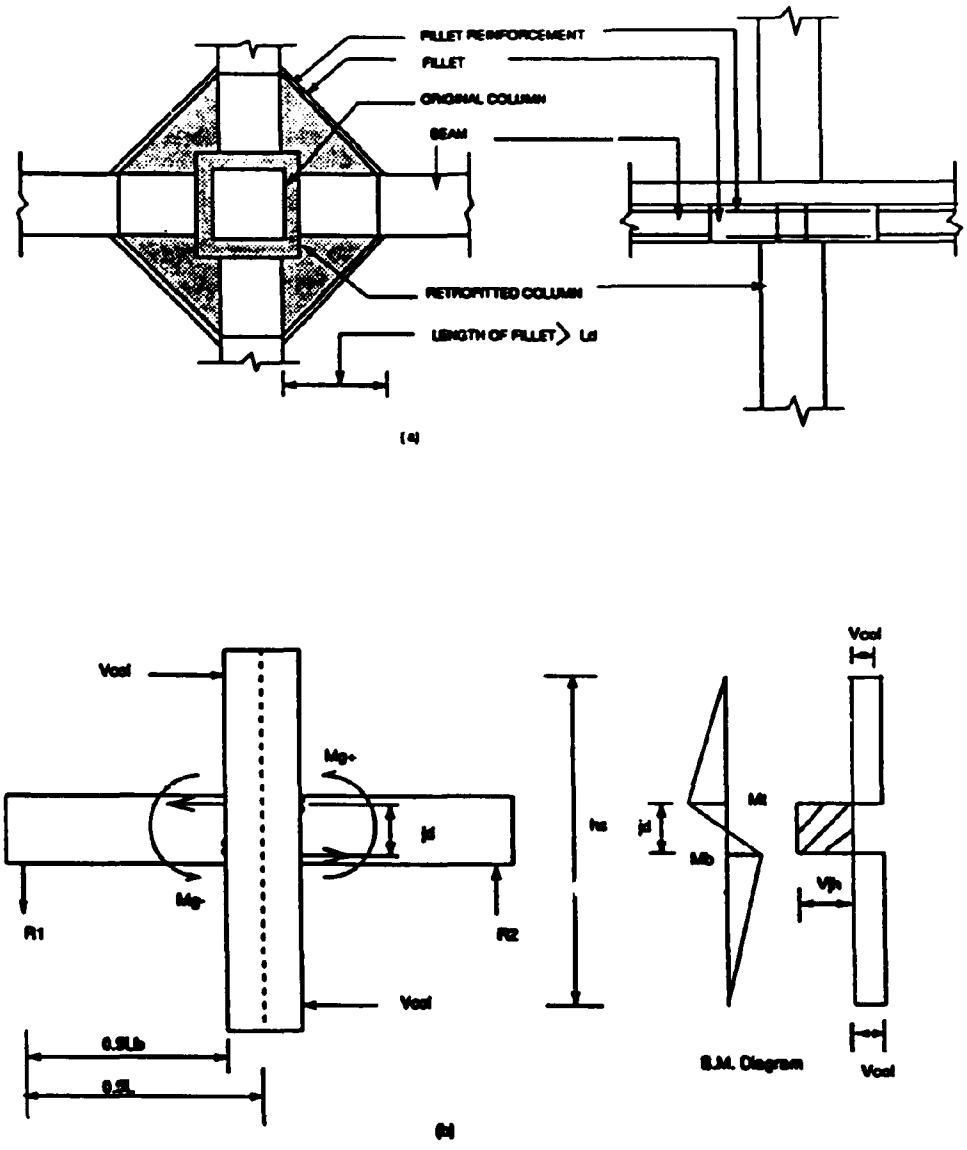

Fig. 2.4 (a) Diagram of Joint Fillet (b) Equilibrium of Subassemblage

SECTION 3

EXPERIMENTAL STUDY ON GRAVITY LOAD DESIGNED COLUMNS

3.1 Introduction

In this section an experimental study of two retrofitted columns is presented. The original/as-built specimens were one third scale model columns of a prototype building. These specimens were constructed, tested and presented in Part II of the evaluation report series (Aycardi et al. 1992). The results of these original tests are reviewed to furnish an appropriate basis for evaluating the post-retrofit performance of the specimens. Both specimens were tested under increasing amplitudes of reversed cyclic lateral loading to simulate the effect of strong ground motions in order to investigate their strength and ductility capability. Conclusions are drawn on the failure mode and the ultimate capacity of the specimens before and after the retrofit/rehabilitation.

3.1.1 Materials

A high strength concrete mix was used for the retrofit process. The mix was a propriety Magnesium Ammonium Phosphate concrete of the high strength early setting type. Additional information about the mix is given in Section 5.3.2.

The reinforcement of the original/as-built specimen consisted of two types of steel, annealed and regular. The annealed steel comprised of D4 bar with yield strengths (f_y) of 65 ksi. The regular steel consisted of plain round #11 gauge wire with a measured yield strength of f_y value of 54 ksi.

In addition to the longitudinal D4 bars and #11 gauge wire hoops used in the as-built specimens the reinforcement for the retrofitted specimens, consisted of:

1. High strength thread-bar with a nominal diameter of 3/8". The d_b was 5/16" based on the root thread diameter, hence A_b=0.077 in^2 and f_y=120 ksi.
2. D1 wire (A_b=0.01 in^2.) for transverse reinforcement f_y=140 ksi.

The results of the coupon tests for all the steel types are shown in Fig. 3.1.

3.2 The Original/As-built Specimen Performance

3.2.1 The Specimen

The experimental testing configuration presented in Part II of the evaluation report series (Aycardi et al. 1992) for the original/as-built specimens is shown in Fig. 3.2. Fig. 3.3 presents the original model, reinforcement for the columns and the column bases. The value of f'_c for the original/as-built specimens was 4.35 ksi.

3.2.2 Testing and Results

The specimen was tested with a constant axial load of 21.2 kips. This was based on $P=0.3f'_cA_g$. Flexural cracks were first observed at the end of the ±1% drift cycles; with progressive drift cycles cracking increased. During the ±3% drift cycles the cover concrete in the bottom 6 in. of column started spalling. Buckling of the longitudinal bars was observed at the end of the 4% drift cycles. The column failed due to buckling of the longitudinal bars and crushing of the core concrete during the ±5% drift cycle.

The force-drift and the lateral load-rotation graphs for the as-built/specimen are shown in Fig. 3.4.

3.3 Retrofit of the Damaged Columns

3.3.1 Retrofitting Techniques

The previous testing of the as-built/original columns showed that although the columns attained drift amplitudes of 5% while still maintaining their nominal strength, they subsequently failed on cycling due to buckling of longitudinal bars and crushing of the core concrete. For column retrofits in buildings which possess strong beams and weak columns, it was decided that the primary objective of the retrofit scheme should aim at increasing strength. The ductility demand on the columns would effectively be reduced due to an increase in strength. For the lower story columns where a hinge is expected to occur at ground floor level, ductile reinforced concrete detailing should be used.

Two identical specimens previously tested, as described in the preceding sections, were retrofitted. One of the damaged specimens was retrofitted using the principles of conventional reinforced concrete - herein refered to as the RC specimen. The other specimen was retrofitted using the concepts of partially prestressed concrete and referred to herein as the PSC specimen. The retrofitting scheme for both the specimens entailed a minimal enlargement of the columns from 4"x4" to 6"x6" square section.

3.3.2 Construction of the Retrofitted Specimens.

The residual plastic deformation of the column specimens resulting from previous testing was eliminated using a jack. All loose concrete primarily around the bottom 6" of the column was removed and the surfaces were thoroughly cleaned. A steel plate $16x8x^3/_8$ in. with a central 4"x4" hole, to accommodate the as-built column, was fabricated and placed in position. This plate served as the base for the placement and anchorage of additional longitudinal steel which was accommodated in appropriately threaded holes. For the PSC column the longitudinal thread-bar steel was sleeved in plastic tubes. This ensured that later post-tensioning could be applied to the unbonded tendons.

The longitudinal reinforcement for the retrofits consisted of four high-strength thread-bars (d_b=0.3125", A_b=0.077 in^2 and f_y=120 ksi.); Refer to Fig. 3.1 for the stress-strain relationship.

The transverse reinforcement consisted of a wound square spiral of D1 wire at a center-to-center spacing of 2 in.(Refer Fig. 3.5). Transverse reinforcement was not required for the PSC column due to the high intrinsic shear strength of compressed concrete. Lateral ties were only placed in the top 6" of the column to prevent any local failure at the point of application of the lateral load (Refer Fig. 3.5).

The wooden formwork was placed around the new reinforcement cage and the concrete was cast in one pour. The average value of f'_c at the time of testing was 4.8 ksi.

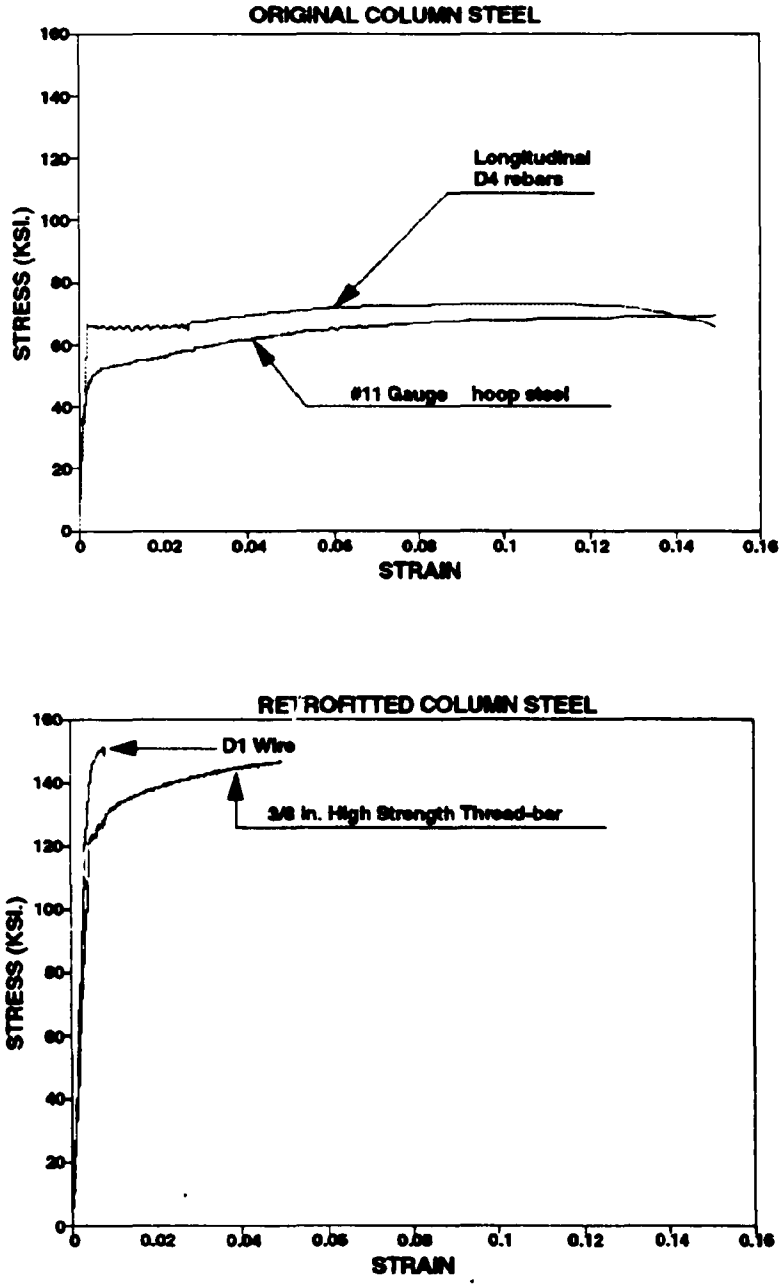

Fig. 3.1 Stress-Strain Graphs for Reinforcement

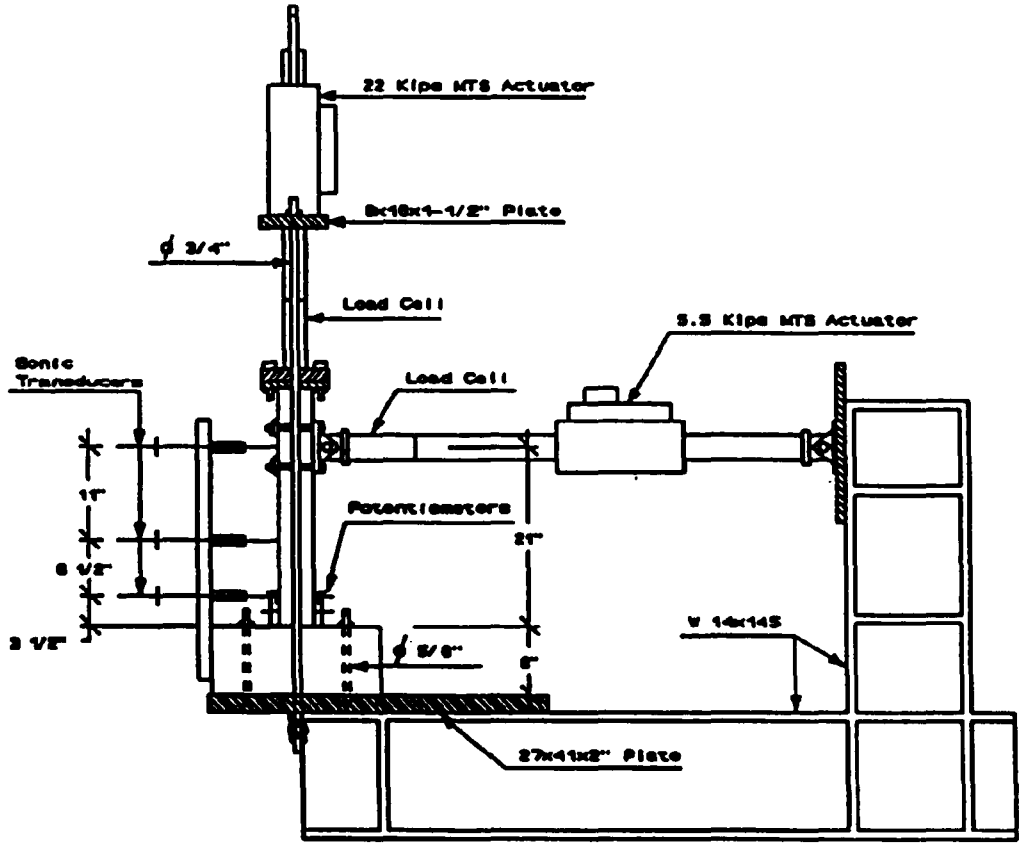

Fig. 3.2 Configuration of the Original/As-built Specimen.

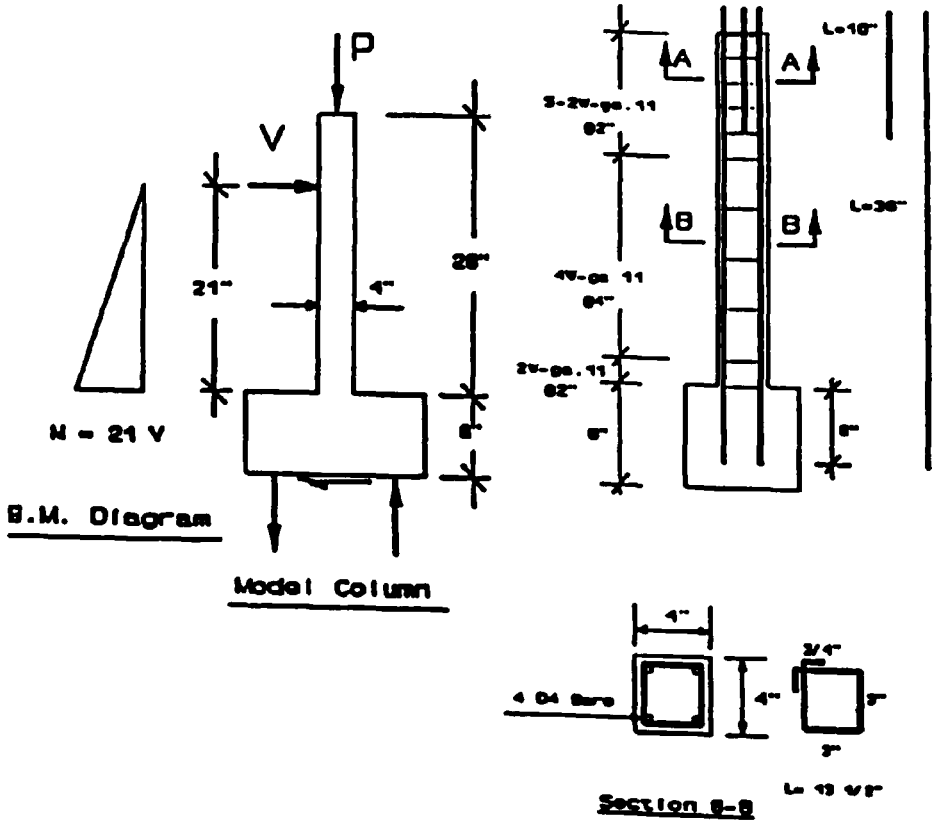

Fig. 3.3 Reinforcement Diagram for the Original/As-built Specimen

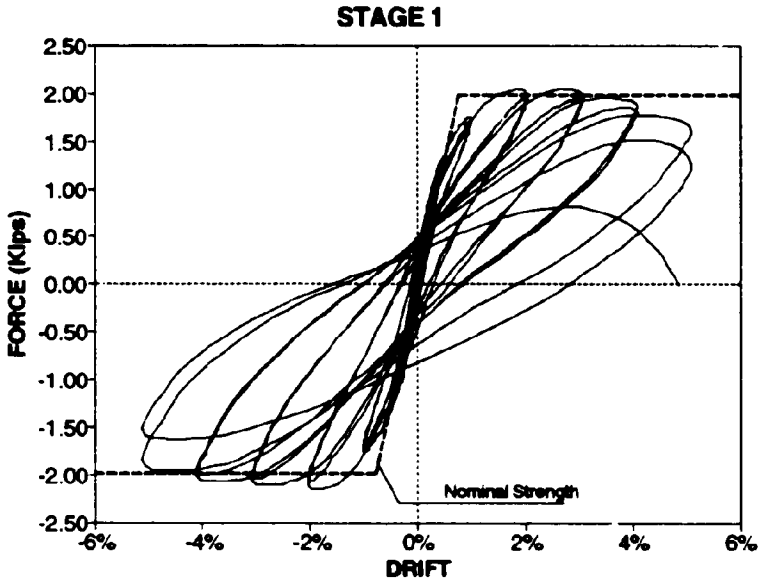

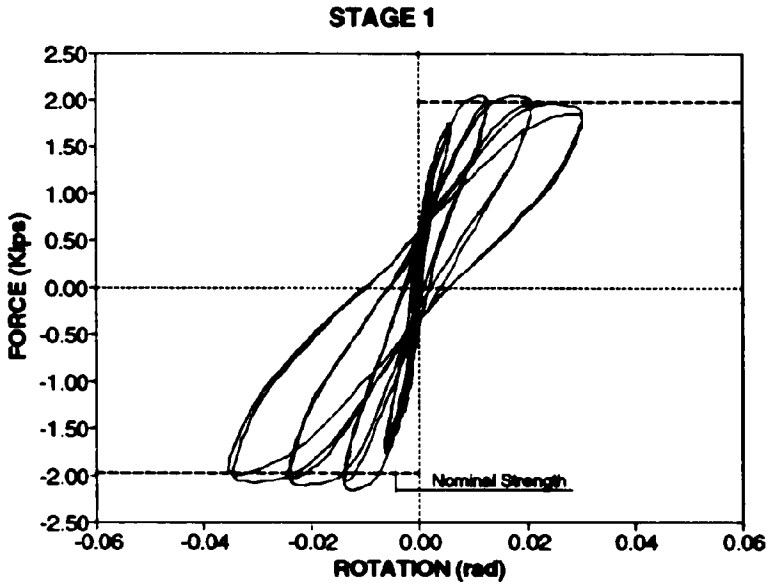

Fig. 3.4 Force-Drift and Lateral Load-Rotation Graphs for the Original/As-built Specimen

3.4 Experimental Set-up and Instrumentation

The general set-up of the test rig was the same as the one used for experiments on the original/as-built specimen shown in Fig. 3.2.

The axial load for the RC specimen was applied with a 22 kip servo-controlled hydraulic actuator. This was held in place with the help of two $^{3}/_{4}$ in. tie down bars which were used to apply the axial load by transferring the reaction onto a plate and the reation frame.

Post-tensioning of the PSC column was applied with a 60 kip hydraulic jack. A total post-tensioning force of 28 kips was applied using an under-stress/over-stress relaxation technique. The total prestress was 60% of the ultimate strength of the thread-bars.
Lateral load was applied to the specimen by a 6 kip servo-controlled hydraulic actuator. Loads were measured by a load cell calibrated to an accuracy of ±0.01 kips. Rotations were measured by two series of linear potentiometers which were attached in pairs, one to each side of the column. These potentiometers had a calibrated resolution accuracy of ±0.001 in.

Data from all channels was recorded on a 486 PC computer at a sampling rate of 1 Hz. using Labtech Notebook software. A backup lateral load vs. displacement plot was recorded on a 7090A analog Hewlett-Packard X-Y plotter during each test. The recorded data was exported to a spreadsheet program for analysis.

The comparative strength of the original/as-built and the retrofitted specimens is shown in the form of an interaction diagram in Fig. 3.6.

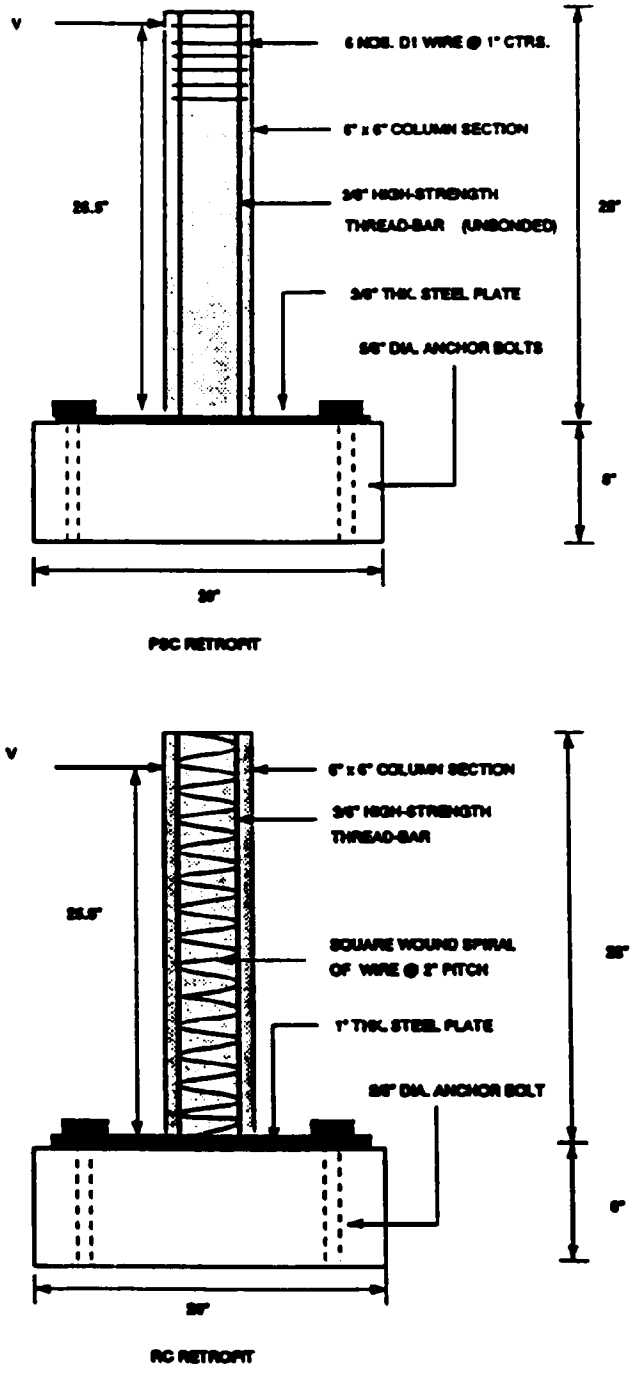

Fig. 3.5 Reinforcement Diagram for the Retrofitted Specimens

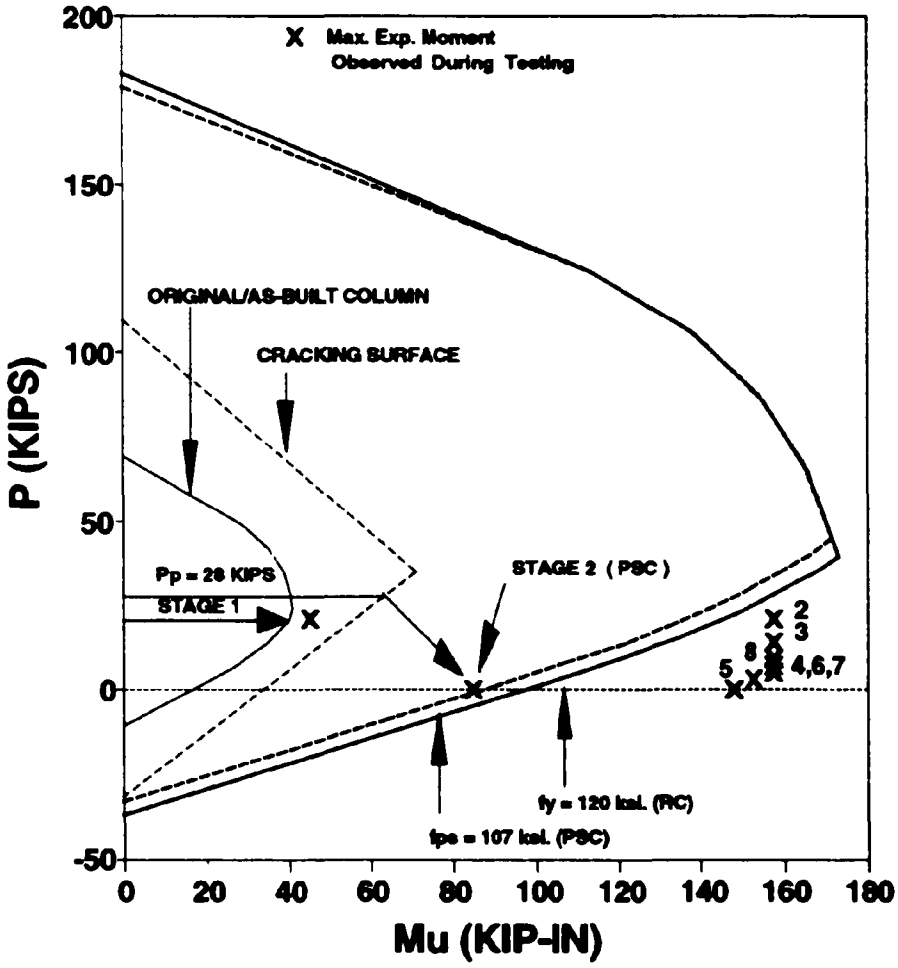

Fig. 3.6 Interaction Diagram for the As-Built and Retrofitted Specimens.

3.5 Experimental Testing of the RC Retrofit

Due to high strength of the RC column and the force limitations of the lateral load jack, it was necessary to quasi-statically test the specimen in seven stages with decreasing levels of axial load. This was followed by a quasi-dynamic test on the same specimen. The input signal for the horizontal actuator for all quasi-static tests and the quasi-dynamic test was a sine wave with cycling frequencies of 0.01 and 0.5 Hz., respectively. Stage 1 refers to the testing of the original/as-built specimen.

In Stage 2 of testing the applied axial load was 21.2 kips the same applied to the original/as-built specimen in Stage 1. The specimen was tested at ±0.25%, ±0.5%, ±1% drift amplitudes. The horizontal actuator capacity was reached at this stage.

The Stage 3 of testing was carried out at ±0.25%, ±0.5%, ±1%, ±2% drift amplitudes. The axial load on the specimen was reduced to 14.3 kips to represent the load in the 3 story model. Prior to attaining the 2% drift amplitude, the horizontal actuator load capacity of 6 kips was reached at a drift amplitude of ±1.25%.

The axial load on the specimen was further reduced to 9.5 kips for Stage 4 of testing. The actuator capacity limited testing to drift amplitudes of ±1% and ±1.5% at the maximum load of 6 kips.

For Stage 5 the specimen was tested under proportional axial loading with $P=(6.95+2H)$ kips similar to Aycardi's specimens 3 and 4. The specimen was tested at increasing drift amplitudes of ±0.5%, ±1%, ±2% after which the horizontal actuator capacity was reached.

The specimen was tested with an axial load of 7 kips and 5 kips for Stage 6 and Stage 7 respectively. The capacity of the horizontal actuator limited testing to drift amplitudes of ±1%, ±2% for this stage.

A comparison of the elastic stiffness' of the original/as-built and RC specimen shown in Fig. 3.7. It is evident that the elastic stiffness of the RC retrofit was 300% of the original/as-built specimen.

The RC specimen behaved elastically during the Stages 2, 3, 4 of testing as seen in Fig. 3.8. In Stage 5, of testing of the RC column there was reasonable amount of hysteresis in the reverse direction since the column specimen became weaker due to reduction of axial load. There were flexural cracks at the bottom 6" of the column. Fig. 3.8 also shows Stages 6 and 7 of testing in which the specimen displayed some energy dissipation indicated by comparatively wide hysteresis loops. This is attributed to cracked response behavior rather than steel yielding.

The axial load on the specimen was further reduced to 3 kips for the Stage 8 of testing and subsequently tested at increasing drift amplitudes of ±1%, ±2%, ±3%, ±4% and ±5%. The force vs. drift and the lateral load vs rotation relationships for Stage 8 is shown in Fig. 3.9. During this stage there were extensive shear and flexural cracking at the base of the column. The column strength exceeded the nominal capacity in both directions though a gradual drop in lateral force is observed in the reverse direction.

The RC specimen under quasi-dynamic at a drift amplitude of ±4%. The column strength dropped to 75% of its value before the test in four cycles at ±4% drift. The sinusoidal input signal had a frequency of 0.5 Hz. (Refer Fig. 3.10).

3.6 Experimental Testing and Results for the PSC Retrofit

The PSC specimen was quasi-statically tested at increasing drift amplitudes of ±0.25%, ±1%, ±2%, ±3%, ±4% and ±5%. The initial half-cycle of loading for all tests was in the reverse direction followed by the forward cycle.

The PSC specimen performed very well up to the ±3% drift amplitude with no visual cracking observed. At this juncture the $^{3}/_{8}$" base plate cracked due to fatigue of threadbar

attachments and there was a large loss of axial prestress hence a major drop in the lateral force was observed.

The behavior of the PSC specimen was essentially elastic at the 0.25% drift. A comparison of the elastic stiffness of the original/as-built and the PSC specimen is shown in Fig. 3.7. The elastic stiffness of the PSC retrofit was 150% of the original/as-built specimen.

3.7 Conclusions

The following conclusions are made based on the observations of the previous testing of the as-built specimens and the testing of the retrofitted specimens:

1. The principal objective of the seismic retrofit redesign was the augmentation of strength. This was achieved for both RC and PSC specimens.

2. A second objective for the RC column was to ensure a ductile post-yield behavior through the provision of transverse reinforcement. The specimen behaved well showing excellent energy dissipation up to drift amplitudes of 5%.

3. Although it was not the intention of ensuring ductile inelastic response for the PSC column, nevertheless it behaved well showing a surprisingly good energy dissipation capability up to 3% drift amplitudes. In spite of absence of transverse reinforcement there was only a modest decay in strength due to shear.

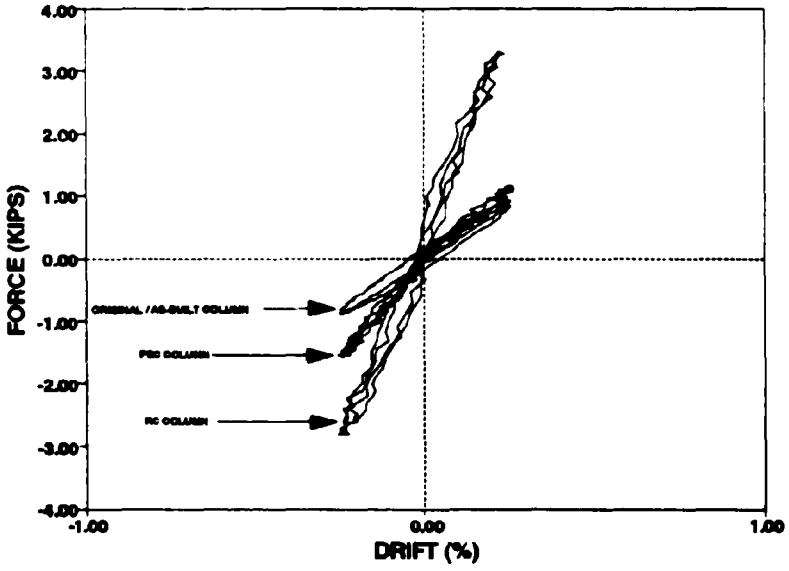

Fig. 3.7 Comparison of the Elastic Stiffness of the As-built and Retrofitted Specimen

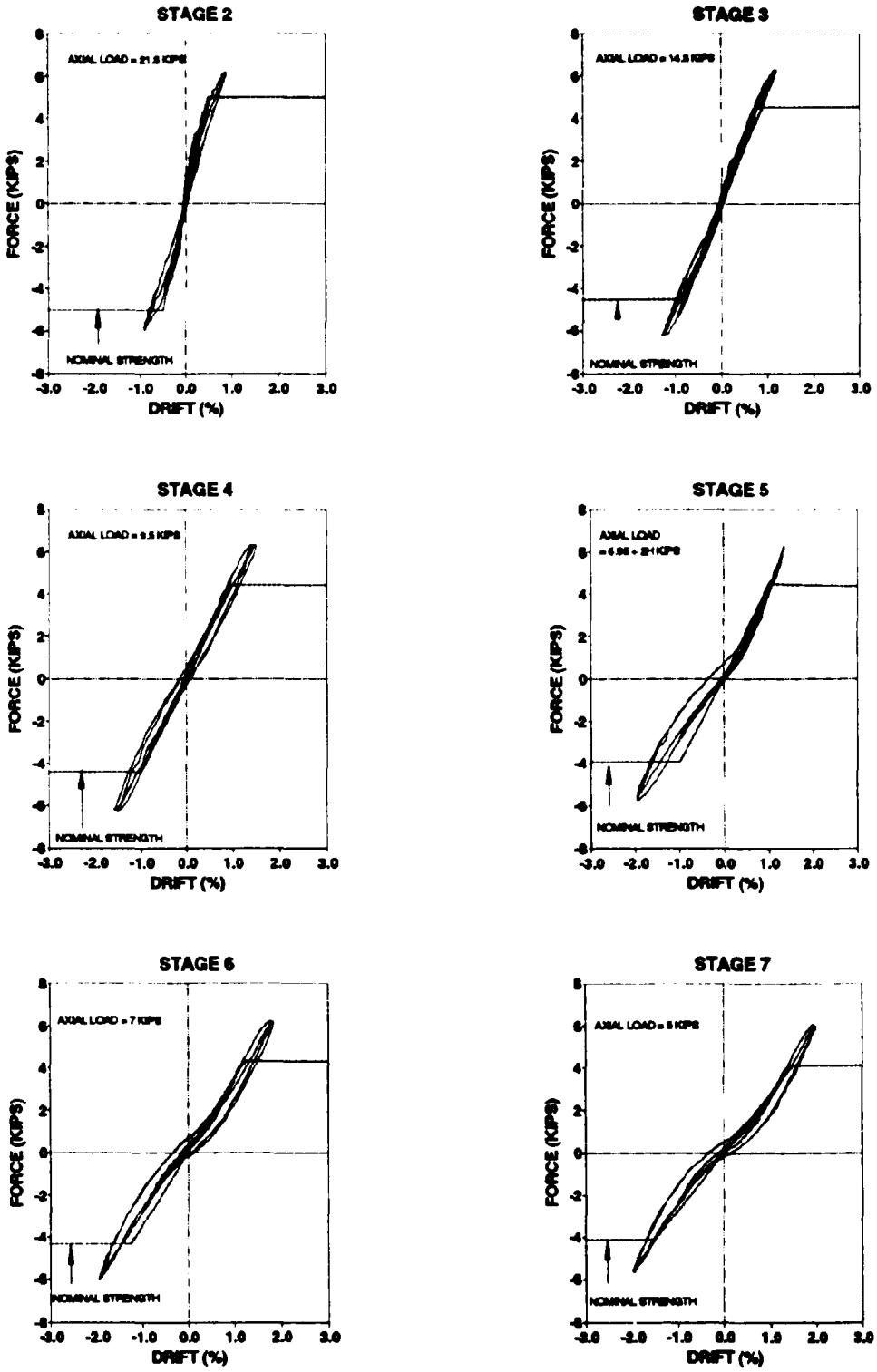

Fig. 3.8 Force-Drift Plots for Stages 2, 3, 4, 5, 6, 7

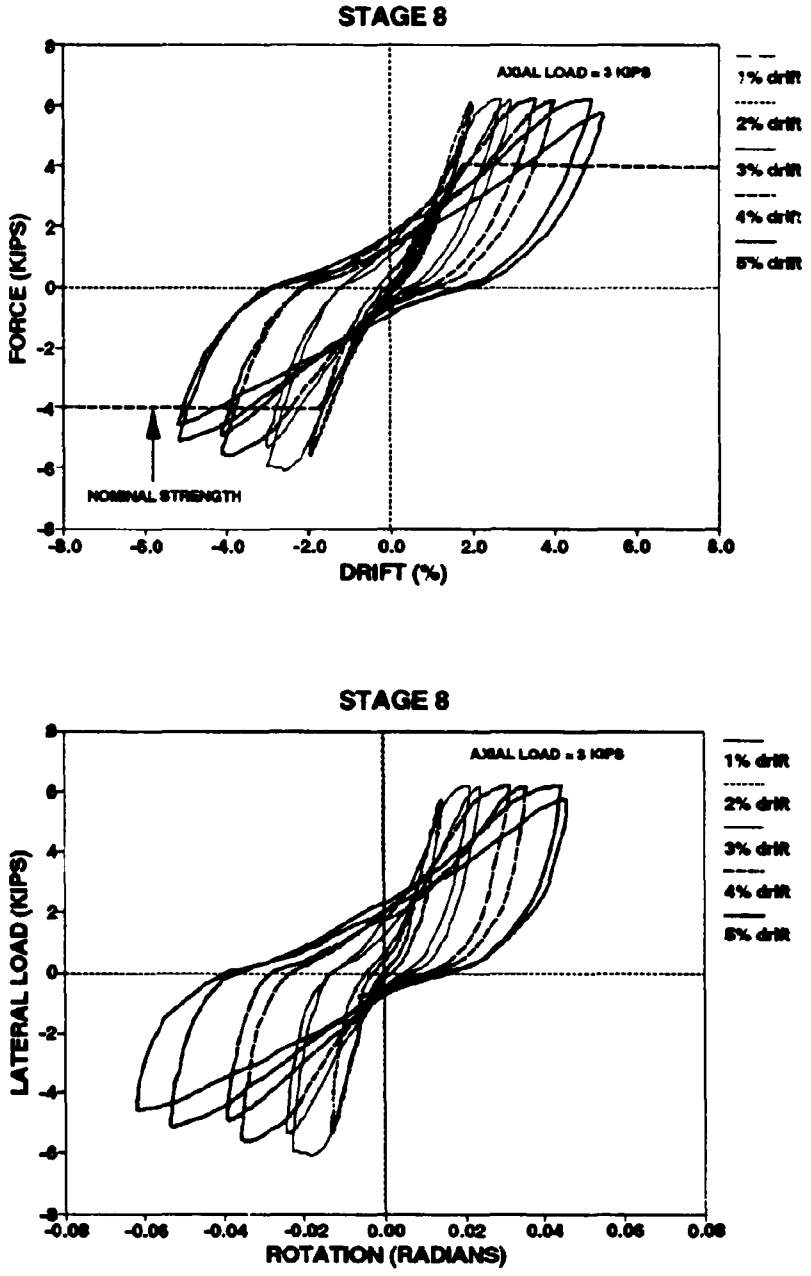

Fig. 3.9 Force-drift and Force-rotation graphs for Stage 8

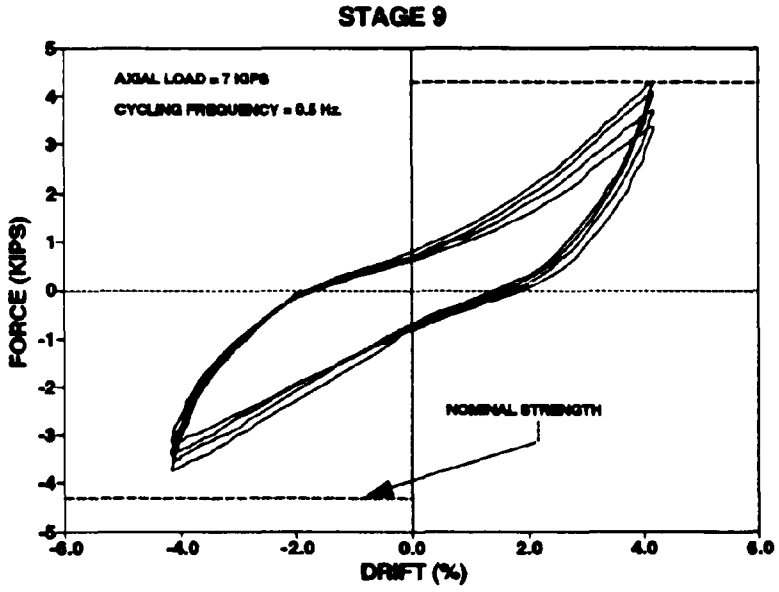

Fig. 3.10 Force-Drift for Quasi-Dynamic test at 4% drift

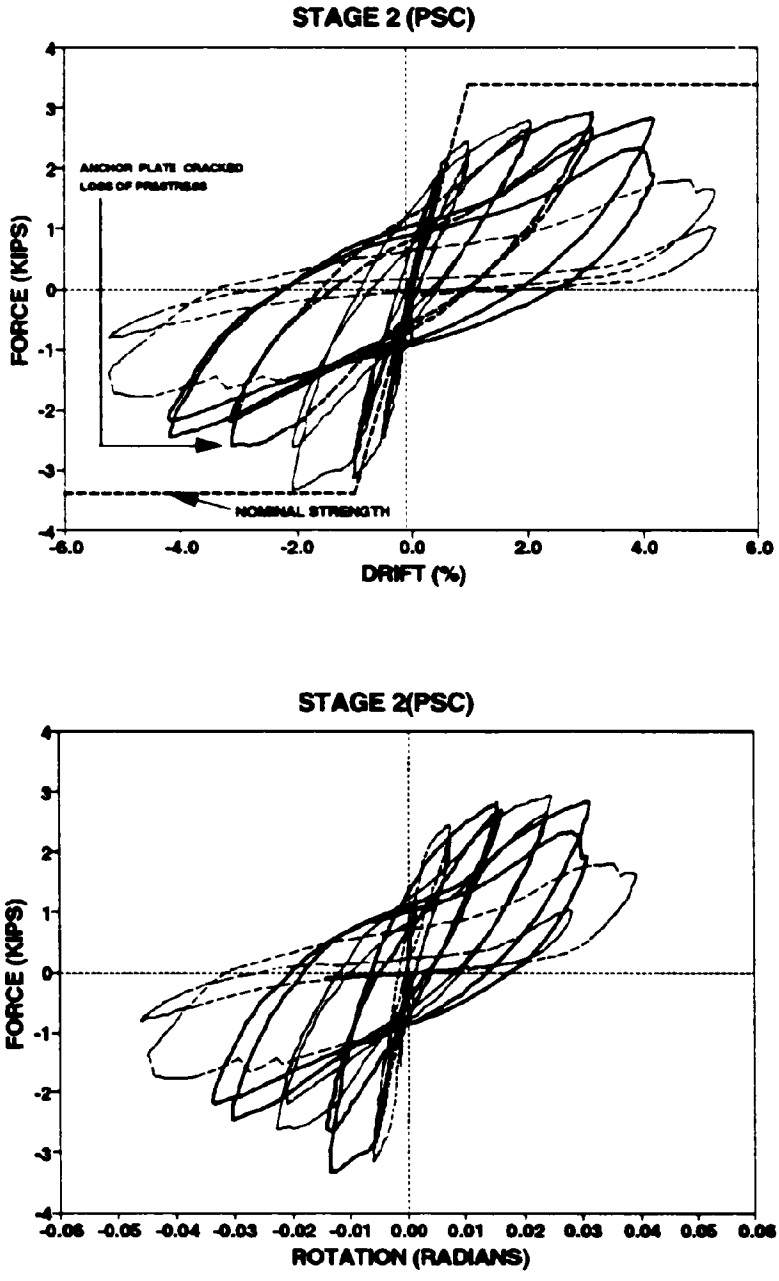

Fig. 3.11 Force-drift and Force-rotation graphs for Stage 2 (PSC)

SECTION 4

EXPERIMENTAL STUDY ON GRAVITY LOAD DESIGNED ONE-WAY BEAM COLUMN JOINTS

4.1 Introduction

In this section, an experimental study of a retrofitted one-way beam column joint is presented. The original/as-built beam-column joint was a one-third scale specimen designed in accordance with the ACI 318-89 for wind and gravity loads (e.g. U = 1.4D + 1.7L) only. This non-seismic design is typical of the eastern and central United States. The results of the original test are reviewed herein to provide an appropriate basis for evaluating the performance of the retrofitted/rehabilitated beam-column joint. Conclusions are drawn on the failure mode and the ultimate capacities of the specimen before and after the retrofit/rehabilitation.

4.1.1 Materials

The concrete for the original/as-built specimen consisted of Type III - Rapid hardening cement, Type I crushed stone, coarse sand and water. A 440 N super plasticizer was added and air-entrainment upto 3.0% was allowed. The average compressive strength of concrete was 4.3 ksi.

The reinforcement of the original as-built specimen consisted of two types of steel; annealed and regular. The annealed steel comprised of D4 bars with a yield strength, f_y, of 65 ksi. The regular steel consisted of plain round #11 gauge wire with an f_y value of 54 ksi.

The mix for the retrofitted specimen was a propriety Magnesium Ammonium Phosphate concrete of the high strength early setting type. Additional information about the mix is given in Section 5.3.2.

In addition to the longitudinal D4 bars and #11 gauge wire hoops used in the original/as-

built specimen, the reinforcement for the retrofitted specimen consisted of D1 wire (A_b = 0.01 in^2) for transverse reinforcement which had a f_y value of 140 ksi.

The results of the coupon test for all the steel types are presented in Fig. 3.1 of the previous section.

4.2 The Original/As-built Specimen Performance - STAGE 1

4.2.1 The Specimen

A schematic diagram of the test set-up for the original/as-built specimen is shown in Fig. 4.1. The rig used for testing was the same as the one described in Section 5 and shown in Fig. 5.1. Fig. 4.2 presents the reinforcement diagram for the beams and columns of the original/as-built specimen.

4.2.2 Testing and Results

The original/as-built specimen was tested quasi-statically without any axial load at increasing drift amplitudes of ± 0.1%, ±1%, ±2%, ±3% and ±4%.

The behavior of the specimen was essentially elastic at the ±0.1% drift cycles. In subsequent cycles the specimen exhibited wider hysteresis loops in the subsequent as shown in Fig. 4.3. The nominal capacities presented in Fig. 4.3 represent three states of full anchorage, partial anchorage and no anchorage of the bottom positive beam reinforcement. For the first state $A_s^* = 2A_b$, the second state assumes $A_s^* = 2A_b * \frac{column\ embedment}{development\ length}$, and finally $A_s^* = 0$ for the no anchorage state where A_s^* = the area of positive beam (bottom) reinforcement used for calculating the nominal capacity and A_b = area of positive beam reinforcement. The pinched appearance of the hysteresis loops is predominantly seen in the ±3% and ±4% drift amplitudes. This is attributed to pull-out of the positive (bottom) discontinuous beam reinforcement which commenced at the ±3% drift cycles.

Fig. 4.4 shows the load-rotation plots for the beams; clearly the mechanism exhibited by the specimen was predominantly in the form of a beam-sidesway one, although an appreciable amount of inelastic behavior is also evident adjacent to the joint. The behavior of the top and bottom columns is seen in Fig. 4.5.

The beam-column joint behavior is shown in Fig. 4.6. The original/as-built specimen had inadequate joint shear strength because of the absence of confining/joint shear steel.

4.3 Retrofit of the Damaged Beam-Column Joint

4.3.1 Retrofit Technique

The previous testing of the original/as-built beam-column joint showed that although the specimen developed a beam-sidesway mechanism, it left the joint thoroughly weakened. The lack of joint shear reinforcement and core confinement in gravity load designed members make it inadequate to resist large rotations associated with plastic hinge zones without the occurrence of crushing. The main objective of the retrofit was to rehabilitate the damaged joint core. Prior testing of the original/as-built specimen had also caused damage to the south beam at the point of discontinuity of the top (negative) reinforcement. To prevent additional damage localized in that region it was decided to bond plates on both the north and south beams to augment their negative moment capacity. It was also decided to increase the column size minimally from a 5"x5" to a 6"x6" section. This would help increase the strength and proportionately reduce the ductility demand on the columns.

4.3.2 Construction of the Retrofitted Specimen

The residual plastic deformation of the beam-column specimen resulting from previous testing was eliminated using a jack. All loose concrete primarily around the beam-column joint was removed and the surface was thoroughly cleaned.

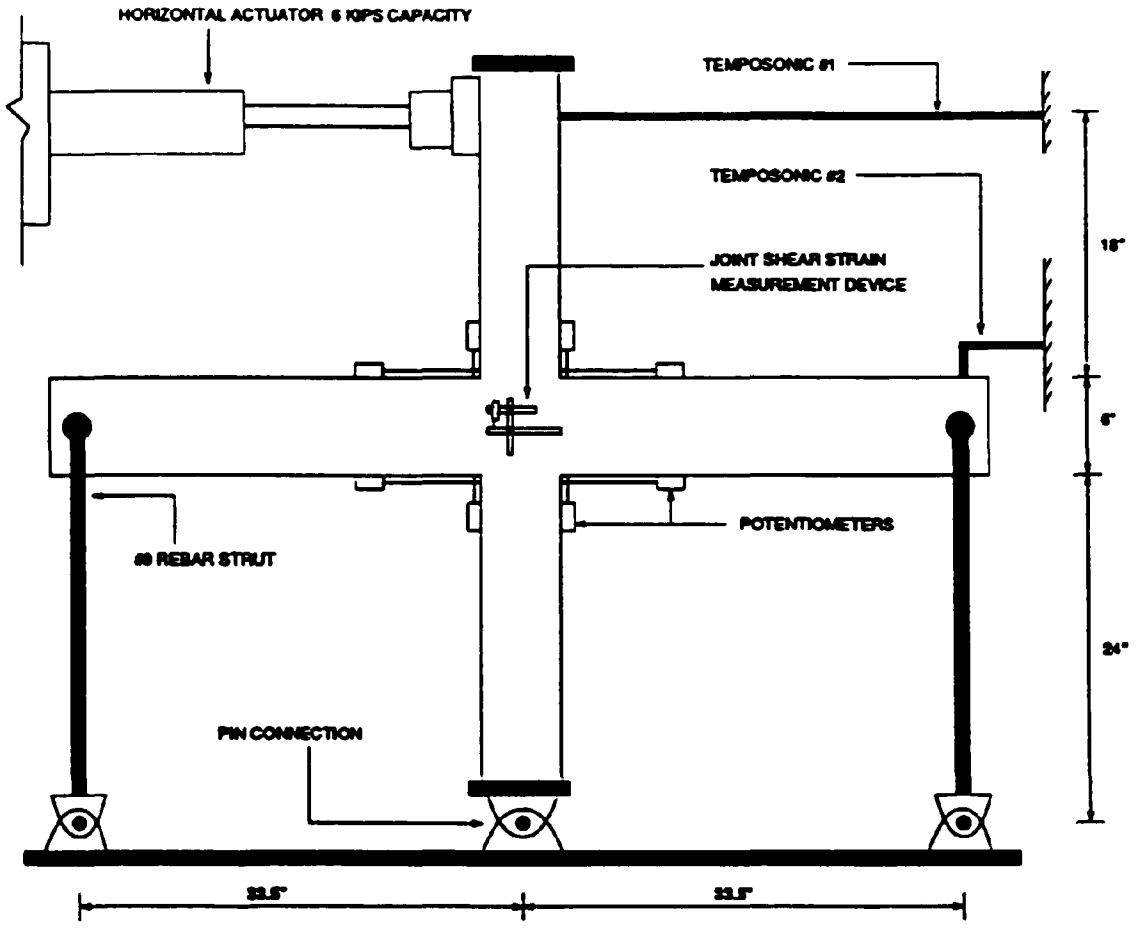

Fig. 4.1 Test Set-up for the Original/As-built Specimen

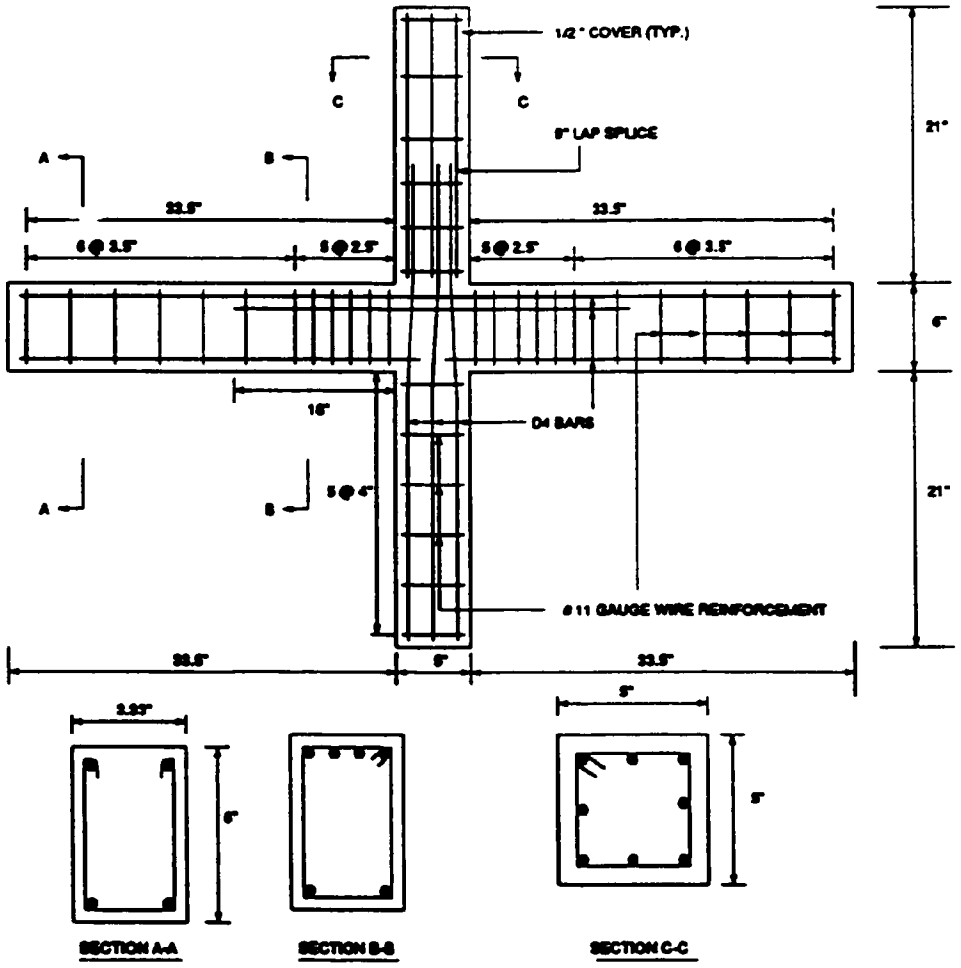

Fig. 4.2 Reinforcement Diagram for the Original/As-built Specimen

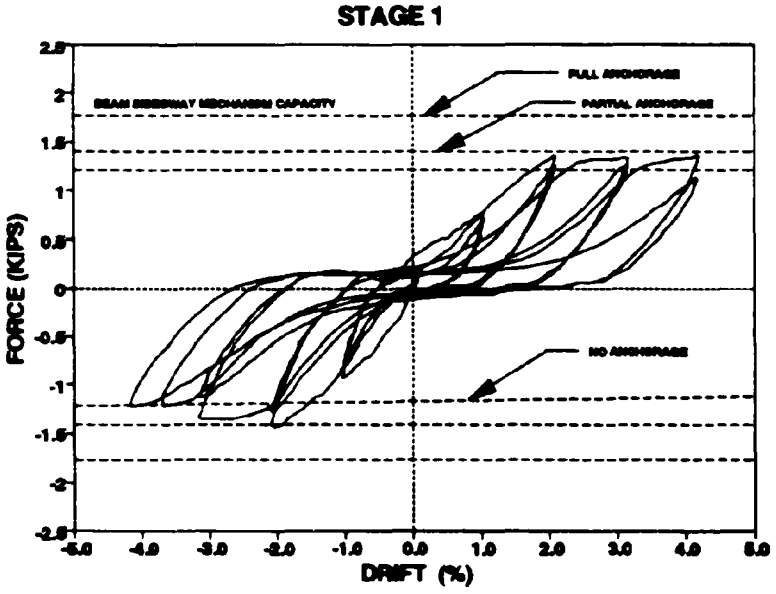

Fig. 4.3 Force-Drift of the Original/As-built Specimen

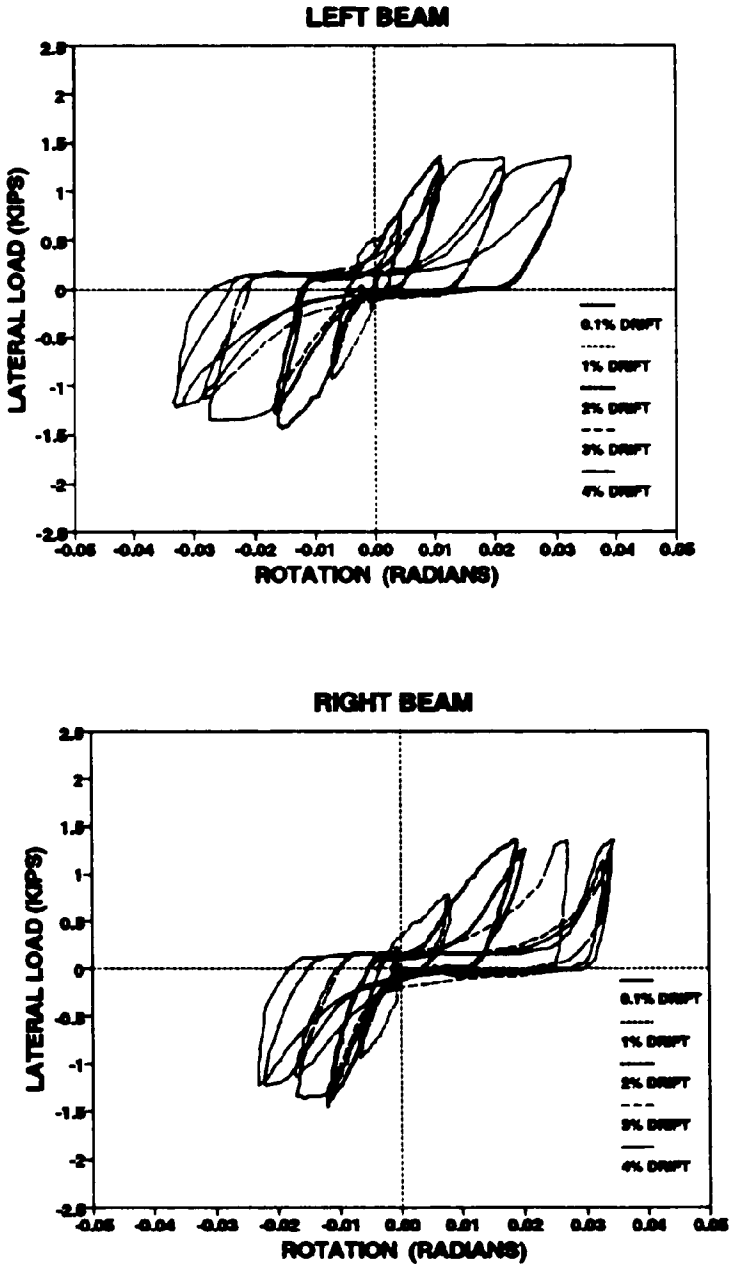

Fig. 4.4 Lateral Load vs. Rotation for the Beams of the As-built Specimen

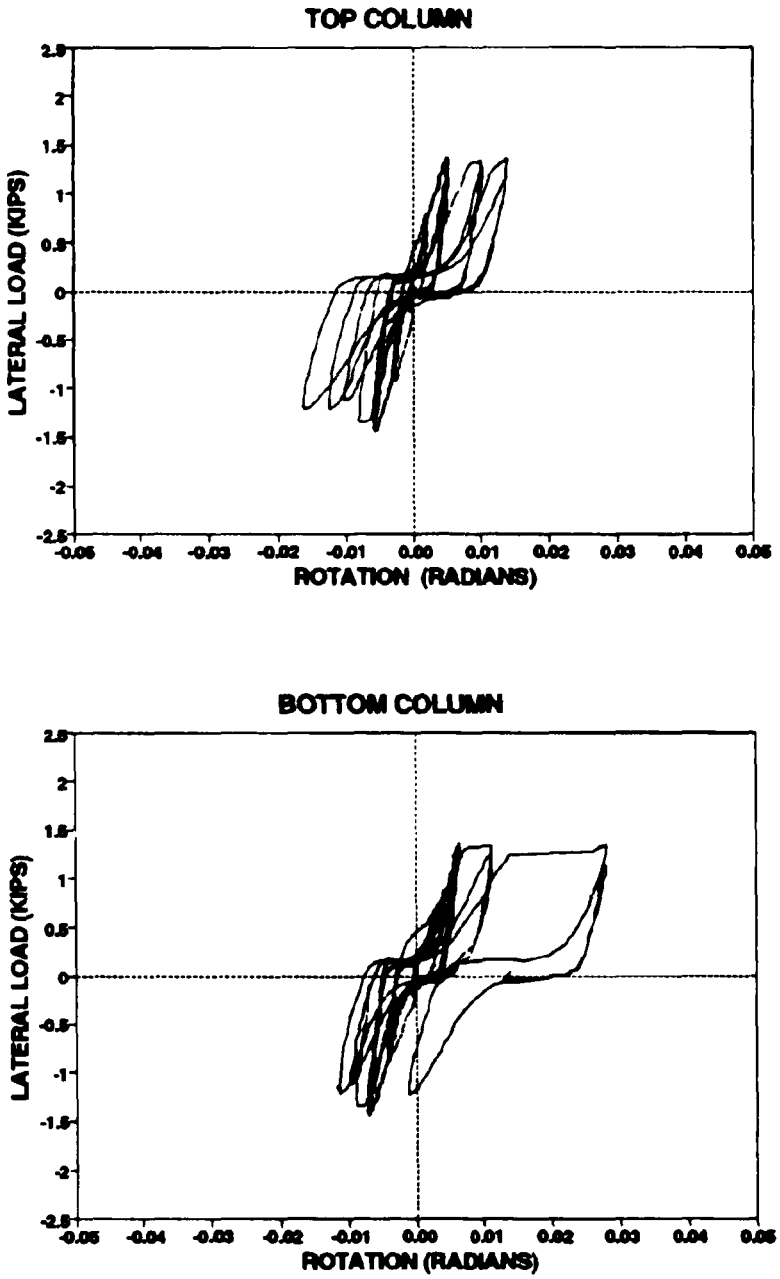

Fig. 4.5 Lateral Load vs Rotation for the Top and Bottom Columns of the Original/As-built Specimen

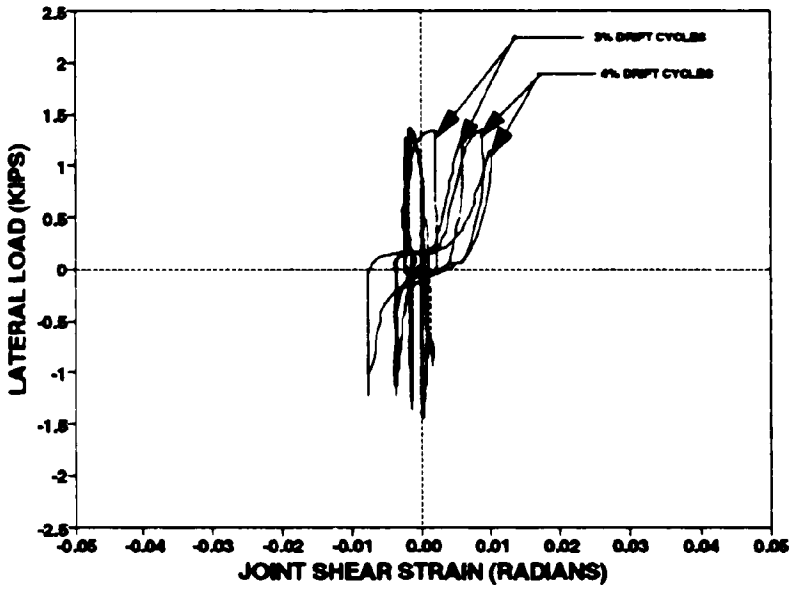

Fig. 4.6 Lateral Load vs. Joint Shear Strain for the Original/As-built Specimen

Appropriate holes were made on both the north and the south beams at 7.5" from the original column face to accommodate three layers of joint shear reinforcement for the fillet.

Additional longitudinal reinforcement consisting of eight D4 bars was placed around the original/as-built 5"x5" column held in place with tie wire. The stress-strain relationship for the D4 bars is presented in Fig. 3.1 of the previous section. The three layers of joint shear reinforcement was then placed and welded for continuity as seen in Fig. 4.7. The transverse reinforcement consisted of a wound spiral of D1 wire at a center-to-center spacing of 2" (Refer to Fig. 4.7). The spiral was wound for the entire column length.

Formwork made out of 22 ga. galvanized sheet metal was placed around the columns and fillet and the specimen was concreted in three stages; first the bottom column, followed by the joint fillet and finally the top column was poured. The average value of f_c' at the time of testing for the three pours was 4.8 ksi.

4.4 Experimental Set-up and Instrumentation

The rig used to test the retrofitted specimen was the same as the one used for the original/as-built specimen. A schematic diagram of the test set-up for the retrofitted specimen is shown in Fig. 4.8.

Lateral load was applied to the specimen by a 6 kip servo-controlled hydraulic actuator. Loads were measured by a load cell calibrated to an accuracy of ±0.01 kips.
Rotations were measured by sets of linear potentiometers which were attached in pairs, one to each side of the columns and beams. These potentiometers had a calibrated resolution accuracy of ±0.0001 in.

Joint shear strain was monitored with a purpose built device which measured the angular deformation of the beam-column joint using a 1/2" linear potentiometer. This gave a joint

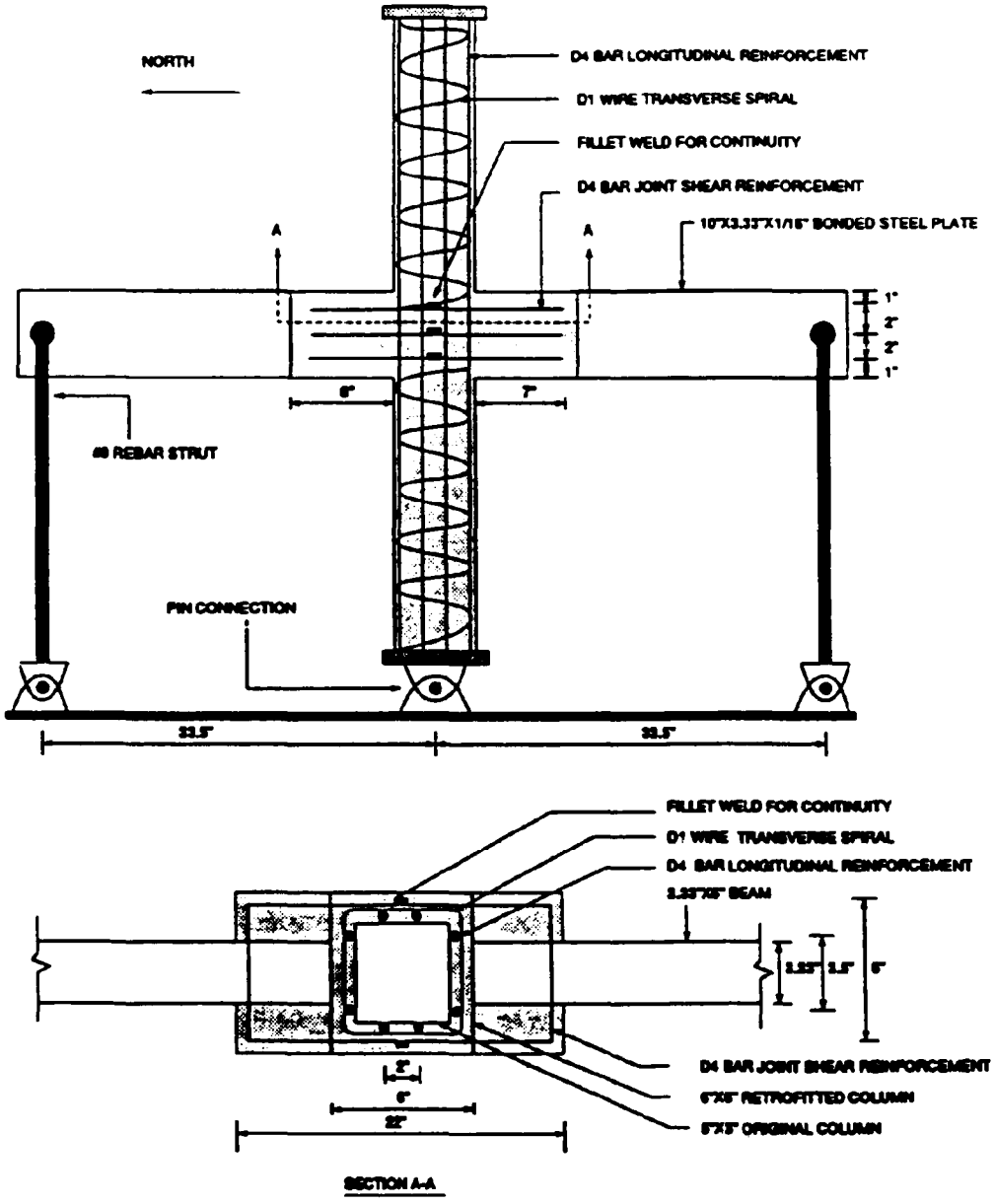

Fig. 4.7 Reinforcement Diagram for the Retrofitted Specimen

shear strain resolution accuracy of 0.00002 radians.

Data from all channels was recorded on a 486 PC computer 24 channel data acquisition system at a data sampling rate of 1 Hz. using Labtech Notebook software. A backup lateral load vs. displacement plot was recorded on a 7090A analog Hewlett-Packard X-Y plotter during each test. The recorded data was exported to a spreadsheet program for further analysis.

The comparative strength of the original/as-built and the retrofitted specimens is shown in the form of an interaction diagram in Fig. 4.9.

4.5 Experimental Testing and Results for Retrofitted Specimen - STAGES 2 and 3

The retrofitted specimen was quasi-statically tested at ±0.25%, ±1%, ±2%, ±3% and ±4% drift level which constituted Stage 2 of testing. This was followed by Stage 3 a monotonic pull test of the top column.

At the ±0.25% drift level the specimen behaved elastically, as observed by the narrow hysteresis loop shown in Fig 4.10. A comparison of the elastic stiffness of the original/as-built and the retrofitted specimen is shown in Fig. 4.10. It is evident that the elastic stiffness of the retrofitted specimen was approximately double the original/as-built specimen.

The 1% drift cycles show comparatively wide hysteresis loops which is attributed to cracked response behavior rather than steel yielding. Fresh flexural cracks developed just outside the region of the joint fillet.

This was followed by the 2% drift cycles in which wide hysteresis loops were observed. Cracking outside the fillet region was more pronounced. The lateral force in this cycle reached the beam-sidesway mechanism capacity as observed from Fig. 4.11. At the end

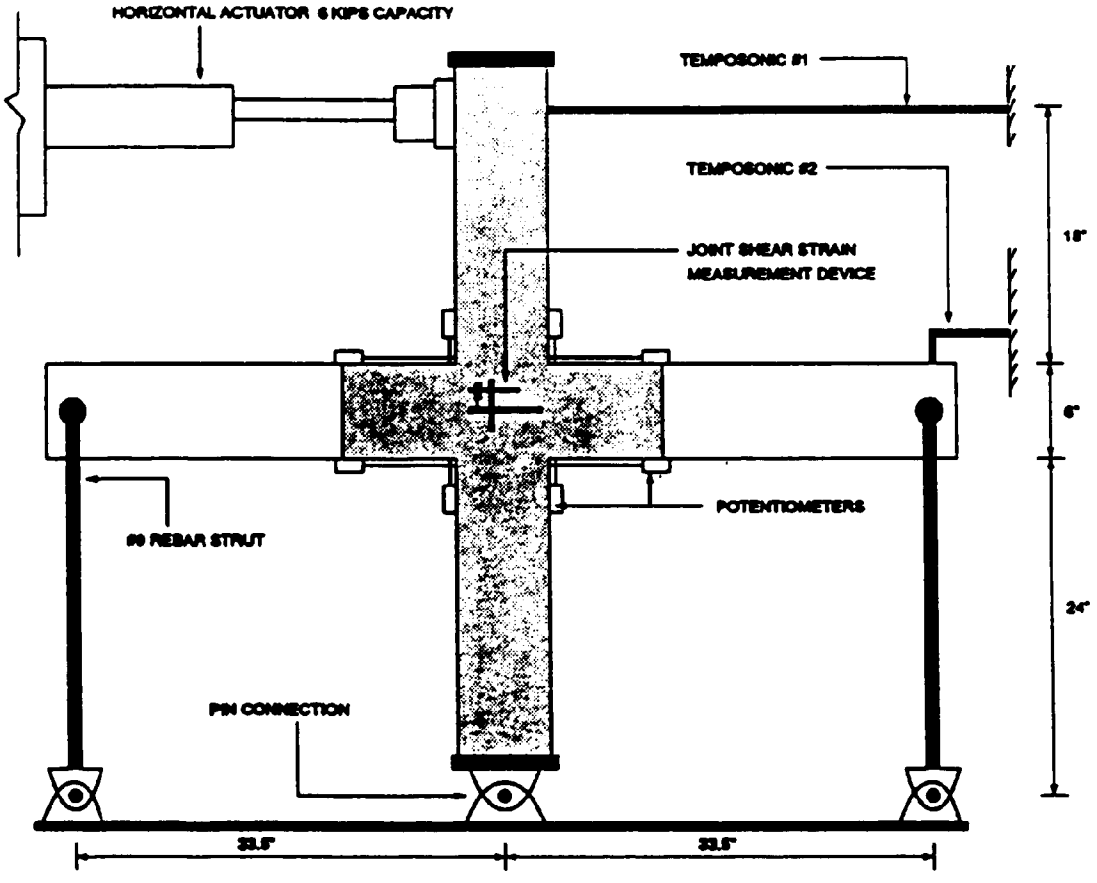

Fig. 4.8 Test Set-up for the Retrofitted Specimen

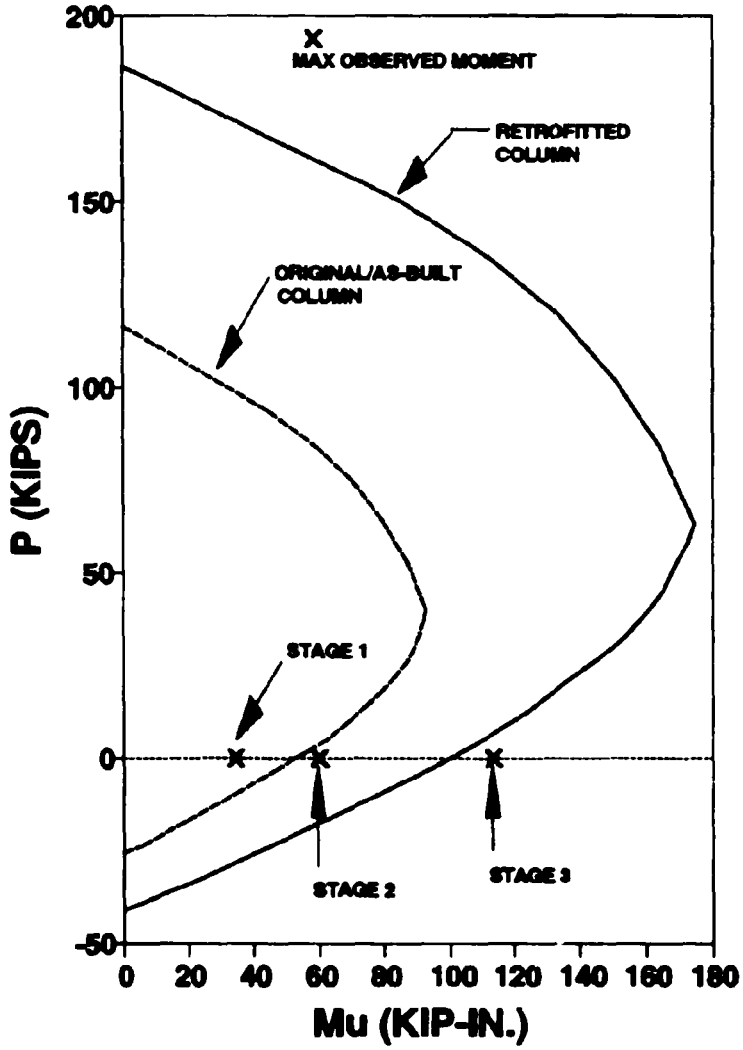

Fig. 4.9 Interaction Diagram for the As-Built and Retrofitted Specimen

of the ±2% drift cycles upon inspection of the specimen it was noticed that the 10"x $3^1/_3$"x $^1/_{16}$" bonded steel plate on the south beam tended to pry out at this stage.

At the 3% drift cycle, the bonded plate on the south beam partially pried off. There was an appreciable loss in strength and stiffness, causing a drop in lateral force resistance of the specimen in the reverse direction. The cover concrete on both sides of the fillet began to spall and extensive flexural cracks developed at the face of the fillets in the beams. The columns showed no signs of damage.

The bonded plate on the south beam completely pried out and took with it some of the cover concrete of the south beam at the ±4% drift cycles. There was additional flexural cracking on both beams outside the joint fillet. The bonded plate on the north beam was intact and showed no signs of any localized damage. The columns continued to show no signs of damage.

Fig. 4.12 shows the lateral force vs rotation plots for both the north and south beams. The columns showed no signs of distress. This is confirmed by Fig. 4.13, the lateral load vs rotation plots, which shows essentially elastic behavior for both the top and bottom columns.

The joint behavior was mostly elastic as shown in Fig. 4.14. It appears from this plot however, that due to load cycling, there was a strength decay in the concrete resistance mechanism. Some apparent joint yielding occurred under positive loading at 2.8 kips where the hoops appear to be providing a plastic truss resistance mechanism.

In general, the overall response was satisfactorily met the design objectives which were to enhance the strength of the columns and the joint core, and to concentrate any damage in the beam hinges. It is evident however, that the bonding of steel plates with epoxy resin to the beam (in order to enhance the flexural strength) only has a limited life and that after only a few reversals to maximum strength (about 4 in this case) the bond is lost.

The Stage 3 of testing consisted of blocking the beams to avoid any sidesway movement and then monotonically pulling the top column with the objective of determining the ultimate lateral load carrying capacity of that column. Fig. 4.15 shows the results of this test as a force vs displacement plot. The nominal ultimate strength presented in Fig. 4.15 is exceeded due to strain hardening of the longitudinal column reinforcement.

4.6 Conclusions

The following conclusions are made based on the previous testing of the as-built specimen and the retesting of the retrofitted specimen:

1. The principal objective of the seismic retrofit and redesign was to augment joint and column strength. This was achieved as confirmed by the essentially elastic behavior of the joint. Column strengths of the subassemblage was also adequately increased preventing them from actively participating in the energy dissipating process.

2. The joint fillet design successfully shifted the potential plastic hinge zone away from the column face to the edge of the joint fillet and at the same time provided adequate development length to prevent pull-out of the bottom longitudinal beam reinforcement.

3. The bonding of the steel plates was successful at reducing the localized damage in the top portion on the south beam which was badly damaged due to previous testing. However, such a repair is good for only a limited number of load reversals.

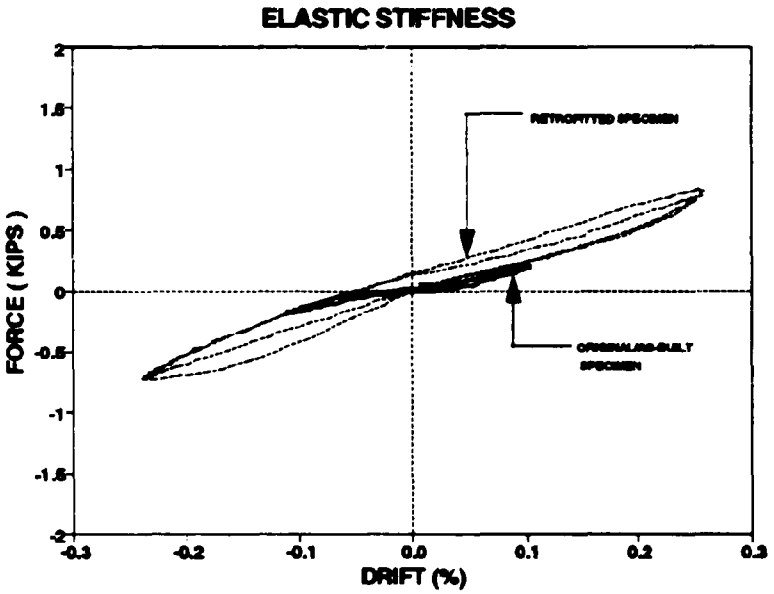

Fig. 4.10 Comparison of the Elastic Stiffness of the Retrofitted and Original/As-built Specimen

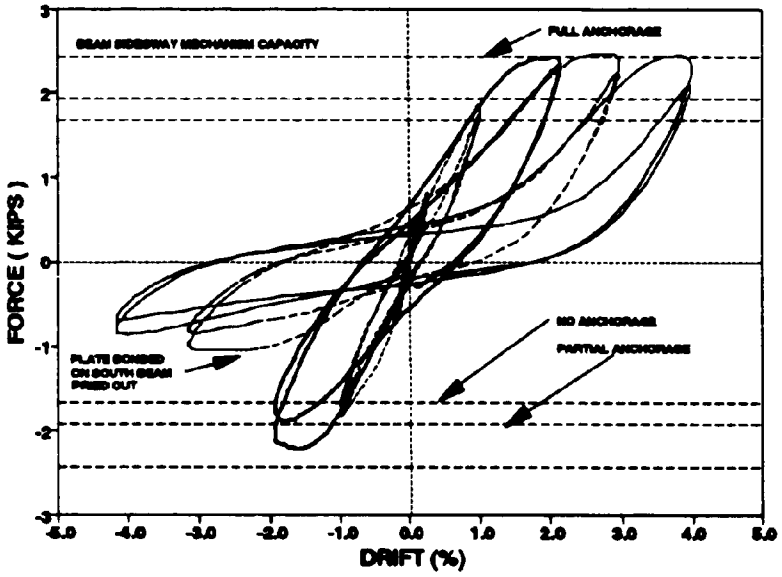

Fig. 4.11 Force-Drift for the Retrofitted Specimen

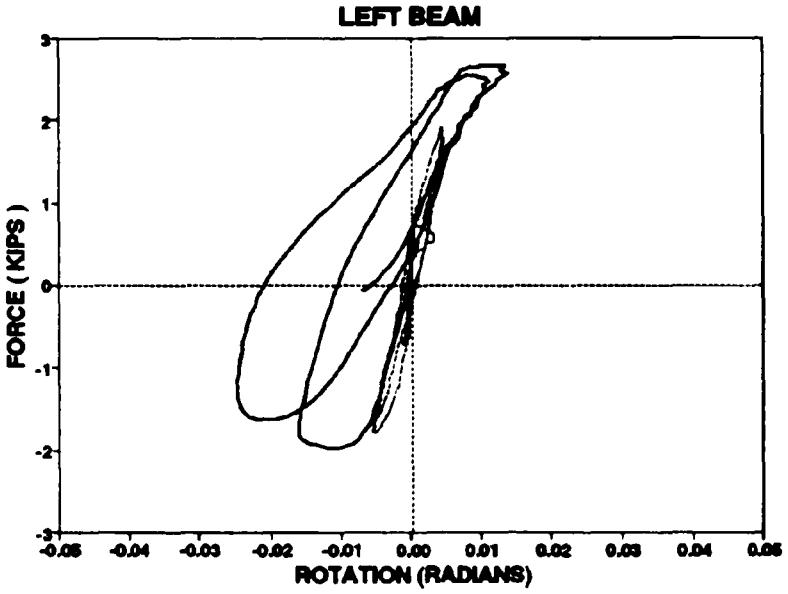

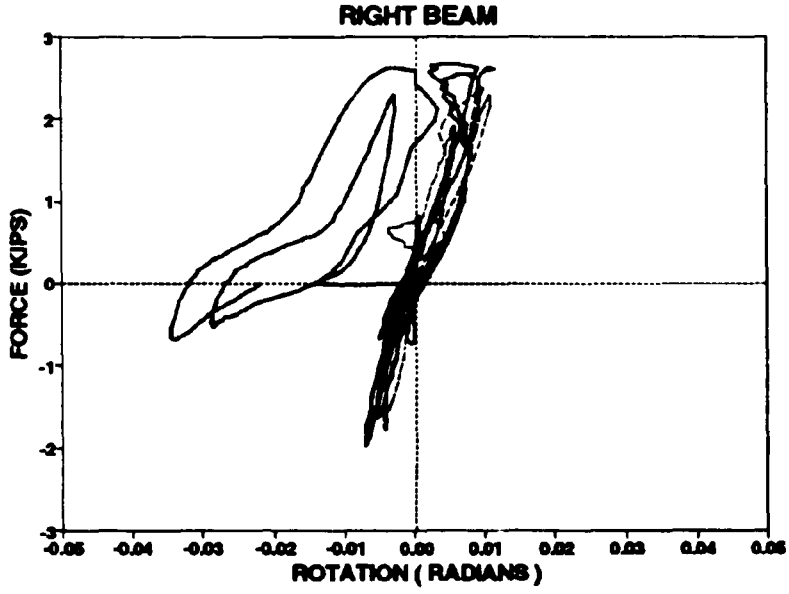

Fig. 4.12 Lateral force vs. Rotations for the Beams of the Retrofitted Specimen

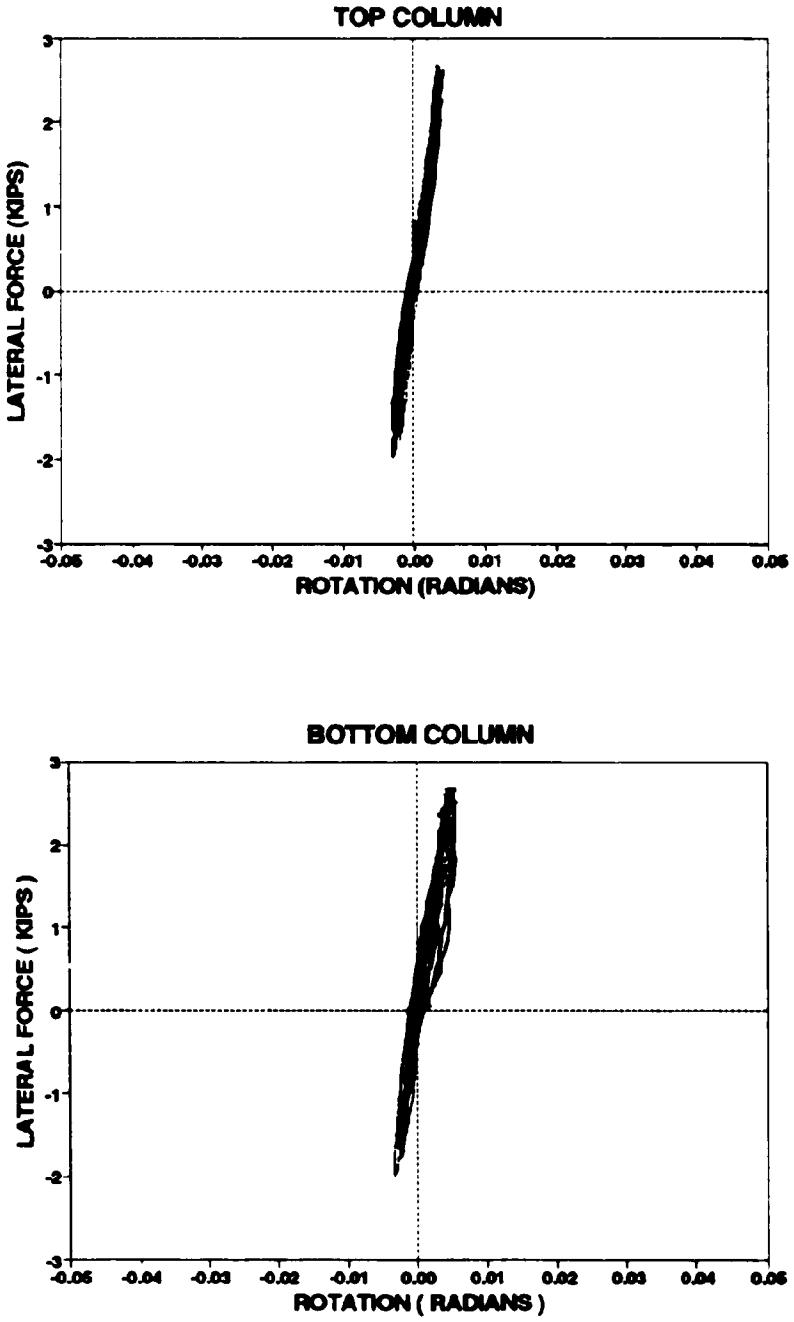

Fig. 4.13 Lateral load vs. Rotation for the Columns of the Retrofitted Specimen

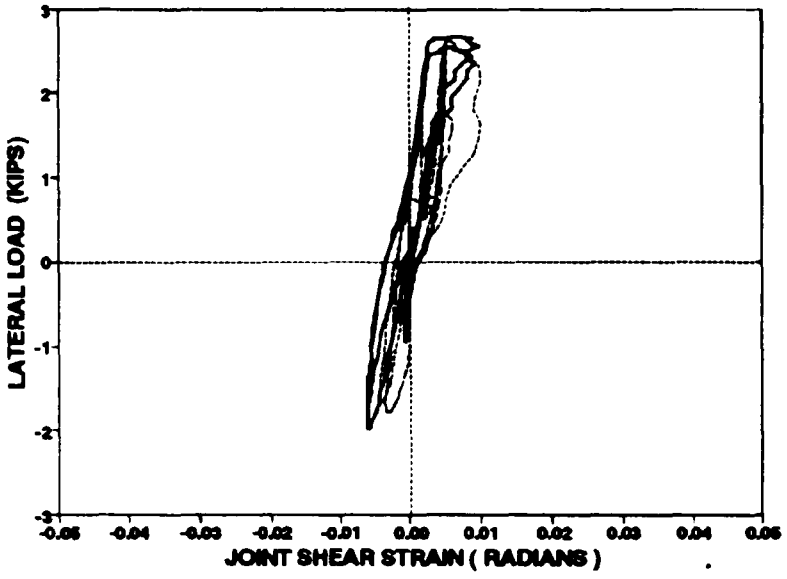

Fig. 4.14 Lateral Load vs. Joint Shear Strain for the Retrofitted Specimen

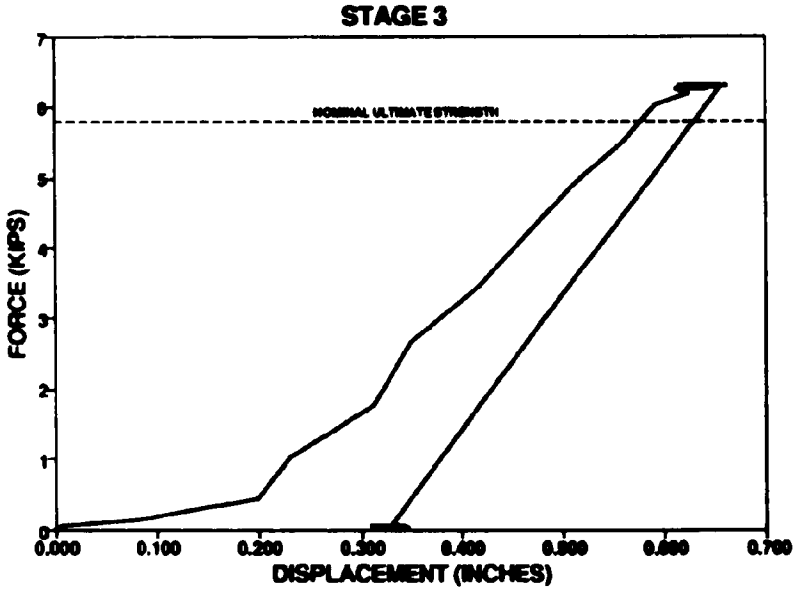

Fig. 4.15 Results of the Pull test of the Retrofitted Specimen

SECTION 5

EXPERIMENTAL STUDY ON A SLAB-BEAM-COLUMN SUBASSEMBLAGE

5.1 Introduction

In this section, an experimental study of a retrofitted interior slab-beam-column-joint subassemblage is presented. The original/as-built specimen was a one-third scale model of an interior subassemblage of a prototype building. The full-size prototype structure was originally designed in accordance with the ACI-318-89 code for gravity loads (U=1.4D+1.7L) only. The original subassemblage specimen was tested by Aycardi (1992), and cast simultaneously with a companion one-third scale model building which has been tested by Bracci (1992b). The subassemblage specimen included the floor slab and the transverse beams and was tested with additional kentlages to create similar initial bending moments and shears near the joint connections with respect to the prototype. For the purpose of comparison, the results of Aycardi's (1992) original test are summarized herein to provide a basis for objectively evaluating the effectiveness of the retrofit scheme considered in the present study. Conclusions are drawn on the implications of the failure modes observed in the subassemblage both before and after the retrofit.

5.2 The Original/As-built Specimen Performance

5.2.1 The Specimen

The dimensions of the specimen were based on the interstory height and the typical spans of the prototype building; the underlying assumption being that points of contraflexure occur at mid column heights and approximately mid-span. The top column of the specimen was sufficiently high to allow connection of both the horizontal and vertical actuators.

The value of f'_c was 4.35 ksi. for the columns; for the beams and slab the value was 5.00 ksi. The details of the reinforcement used for the original/as-built subassemblage are given in Table 5.1.

Table 5.1 Reinforcement for Original/As-built Specimen

Steel Type	f_y (ksi)	E_s (ksi)
D4	65	31050
D5	42	31050
#1 Gauge	53	29800
#12 Gauge	54	29900

The configuration of the original/as-built specimen is presented in Fig. 5.1. The layout of the slab, column and beam reinforcement is shown in Figs. 5.2, 5.3, 5.4 respectively.

5.2.2 Testing and Results - STAGES 1, 2 and 3

The as-built specimen was tested in three stages. The axial load was kept at a constant of 9 kips for all the three stages.

The signal for the horizontal actuator was a sine wave with a frequency of 0 20 Hz. for three drift levels below 2% and 0.01 Hz. for all other cycles. The control was made using the measured displacement coming from the sonic transducers at the level of the applied load. Readings from all instruments were recorded continuously using a Megadac data acquisition system with a data sampling rate of 100 samples per cycle of loading.

The *Stage 1* of testing consisted of two complete displacement controlled cycles at drift levels of ±0.25%, ±0.50%, ±1%, ±2%, ±3% and ±4%. This stage of testing resulted in some cracks located only in the upper column at the end of the ±2% drift cycles. After the ±3% drift cycles were completed, flexural cracks increased and some spalling was observed. The ±4% drift cycles resulted in damage principally concentrated in the upper column lap splice region. Little damage, apart from some superficial cracking was apparent in the beams and the lower columns.

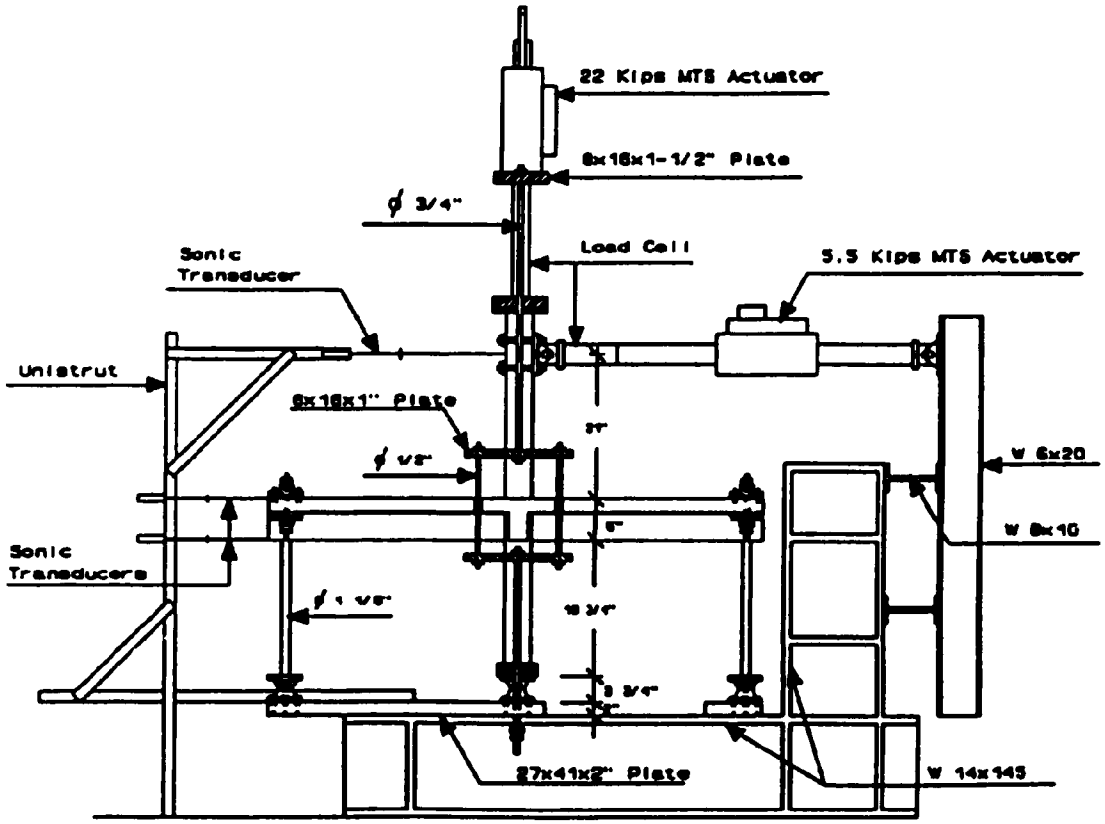

Fig. 5.1 Configuration of the Original/As-Built Specimen

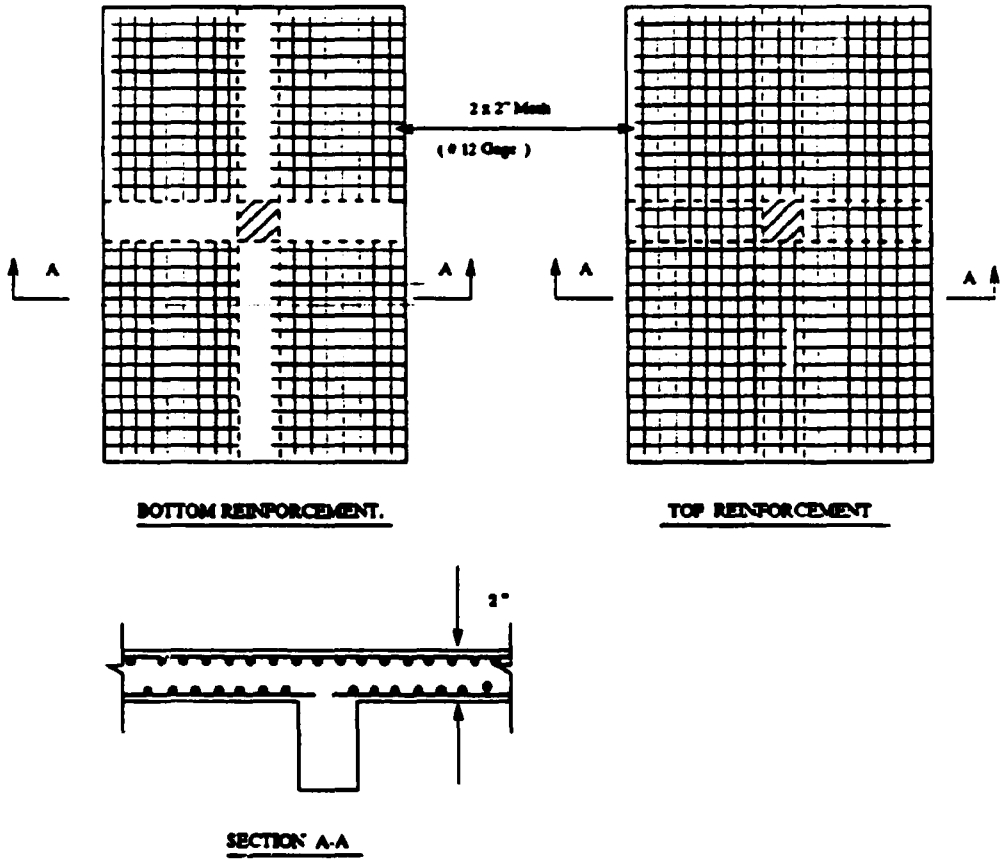

Fig. 5.2 Slab Reinforcement

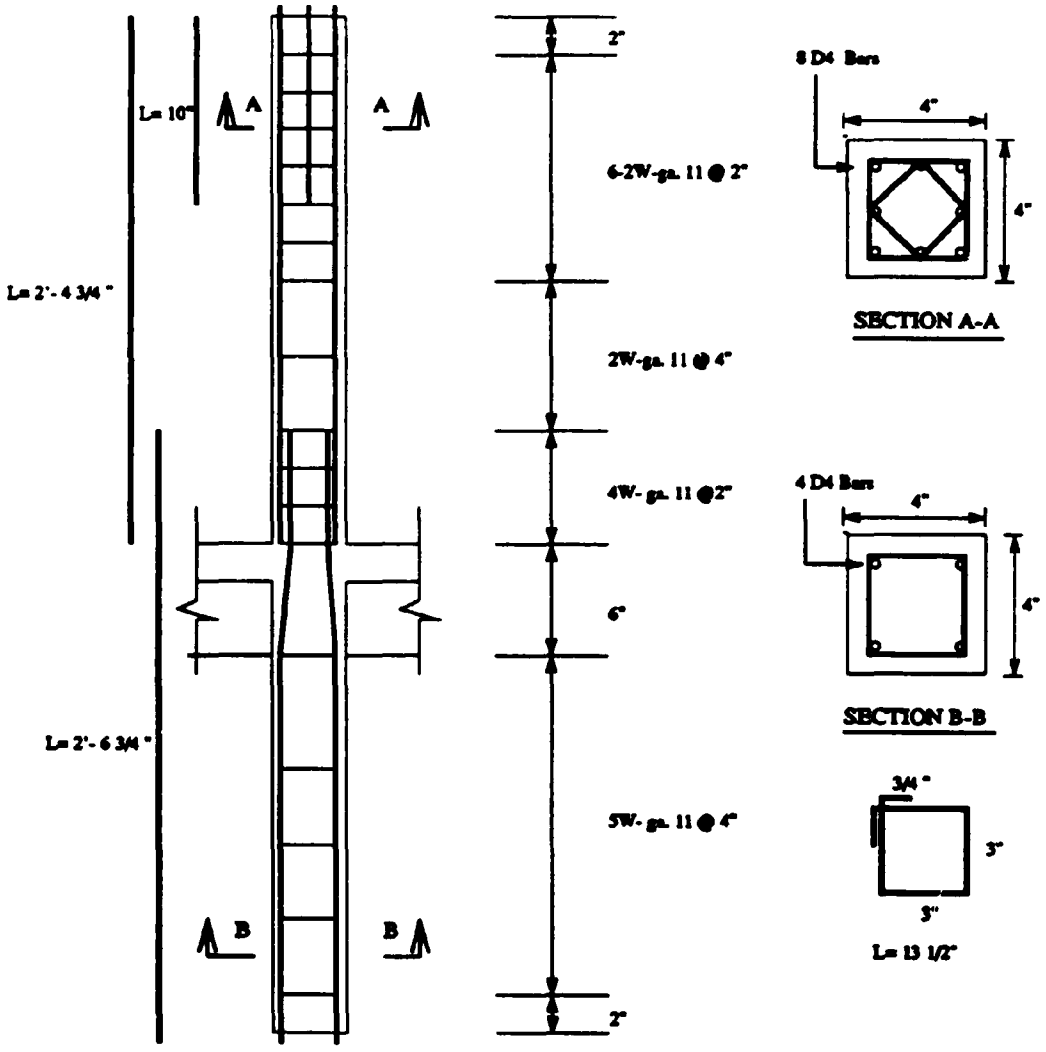

Fig. 5.3 Reinforcement Details of the Columns

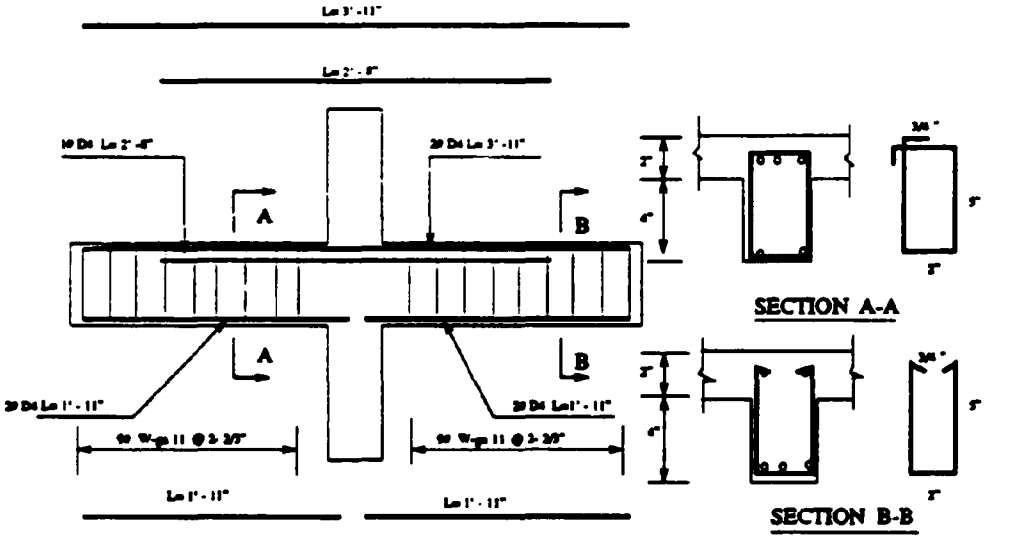

(a)

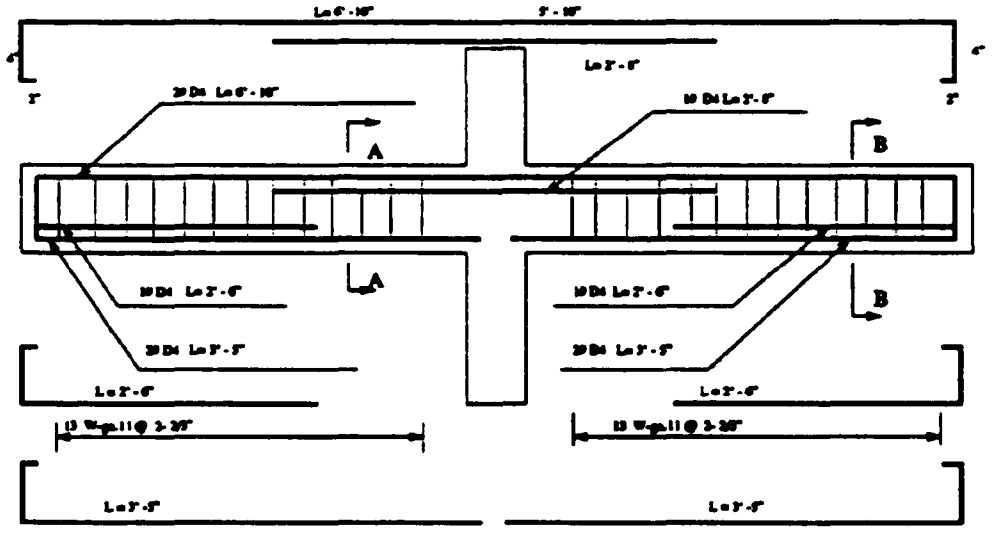

(b)

Fig. 5.4 Reinforcement detail (a) Transverse Beam ,(b) Longitudinal Beam

In *Stage 2* of testing, the horizontal actuator was moved down to apply the load 10 in. from the top of the slab. This was to simulate the downward movement of the point of contraflexure in the second story due to early formation of a column hinge. This second stage followed a different test sequence: two complete drift cycles at each drift levels of ±1%, ±2%, ±4%. On completion of this stage, spalling and flexural cracks were observed in the upper and lower columns of the as-built specimen and the buckling of longitudinal bars of the lower columns had commenced. No further damage was apparent in the beams. It was thus evident that a weak column-strong beam mechanism had occurred.

Stage 3 of the test was designed to determine the positive and negative moment capacity of the beams. The vertical actuator was fixed using two MC 6x18 beams which were connected to the W 8x31 columns of the safety frame and to the steel plate to which the actuator was bolted. The lower column was disconnected and the hinge was removed. Hence the subassemblage was free to move when the vertical load was applied. The monotonic test was executed pushing down and pulling up the upper column with the vertical actuator at the rate of 0.005 in./sec. The Stage 3 of testing caused a large crack at the beam-column interface and a pullout of the bottom bars. Most of the top steel layer of the slab was fractured along a yield line.

The force vs. drift plots for Stage 1, Stage 2, and the moment vs. curvature plot for Stage 3 of the as-built specimen is presented in Fig. 5.4. The force vs. rotation plots for the top column, bottom column, right beam, left beam and the drift contributions from each component of the as-built specimen are presented in Figs. 5.5 -5.7.

This clearly shows that the failure mechanism of the as-built specimen was a weak column-strong beam one, which is undesirable according to present day seismic design philosophy.

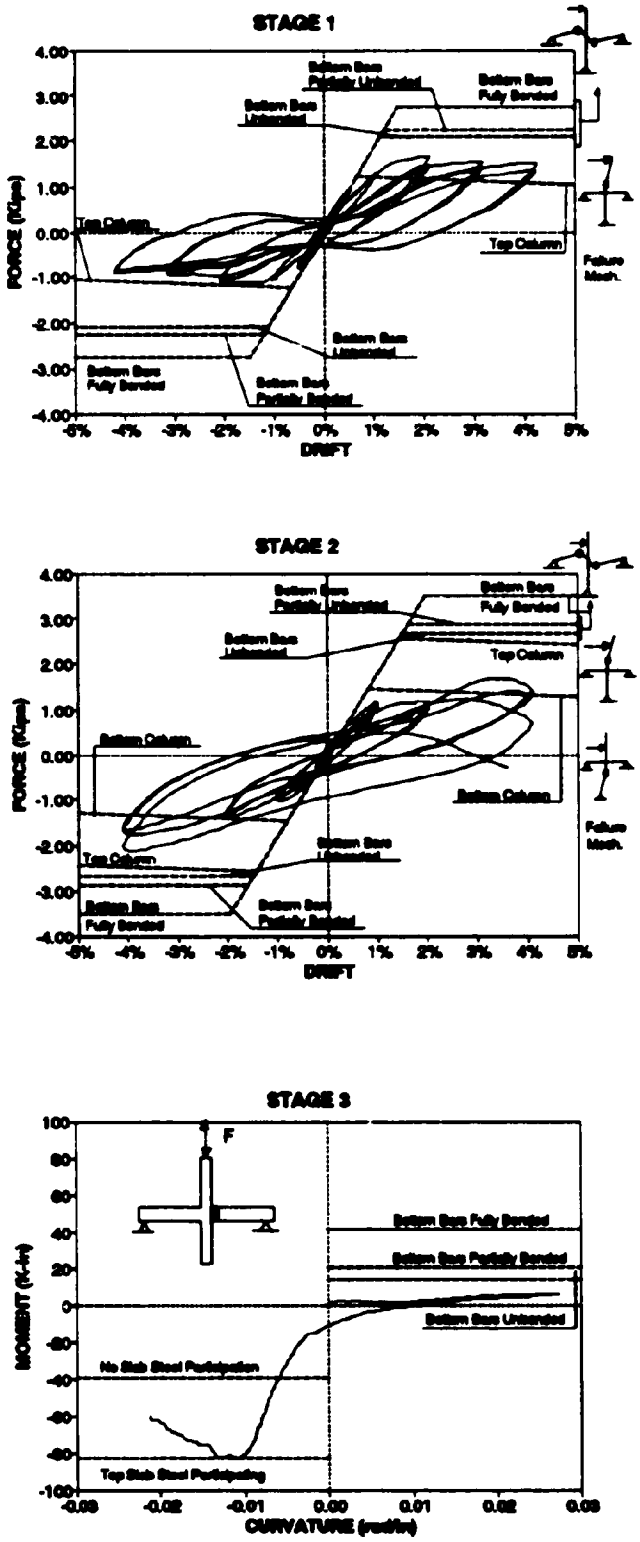

Fig. 5.5 Stage 1, 2, 3 of Testing of the As-Built Subassemblage

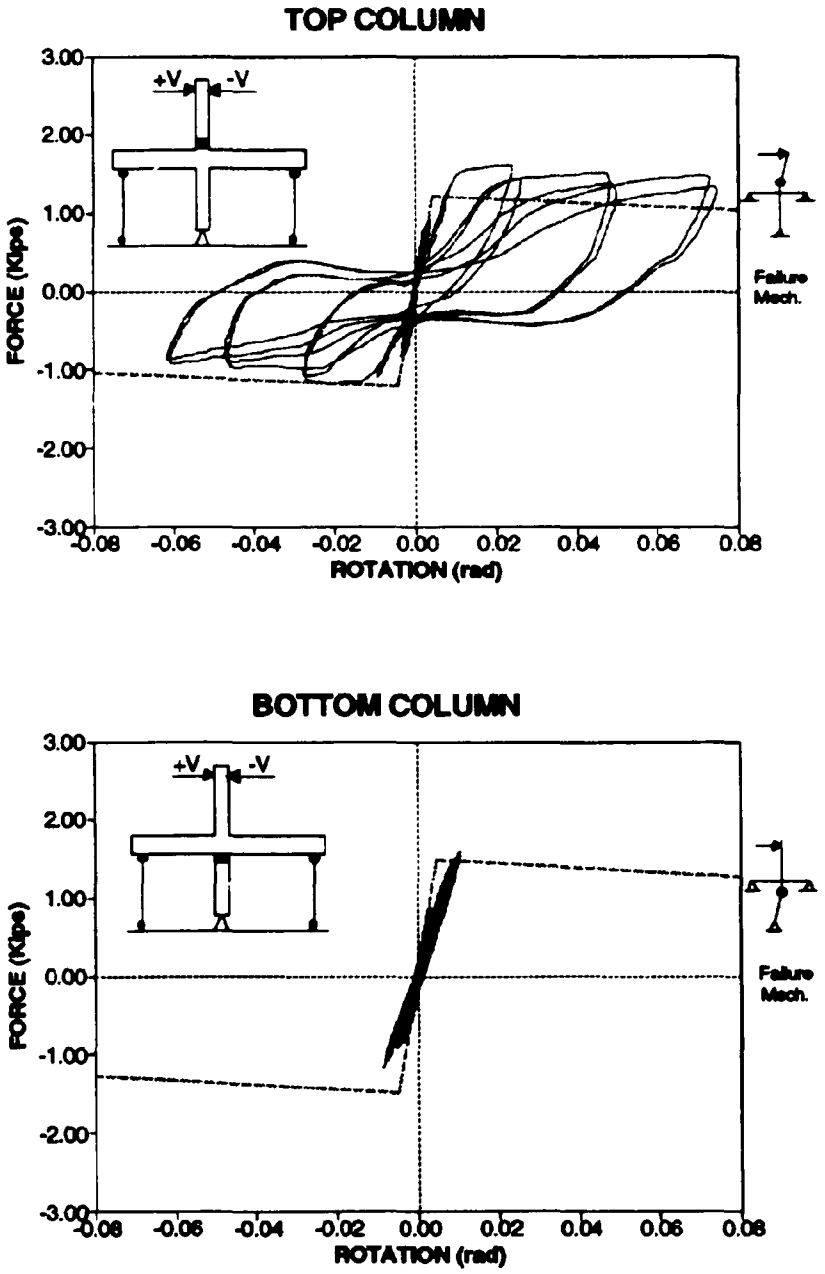

Fig. 5.6 Lateral Load -Rotation graphs for Top and Bottom Columns of As-Built Specimen (Stage 1)

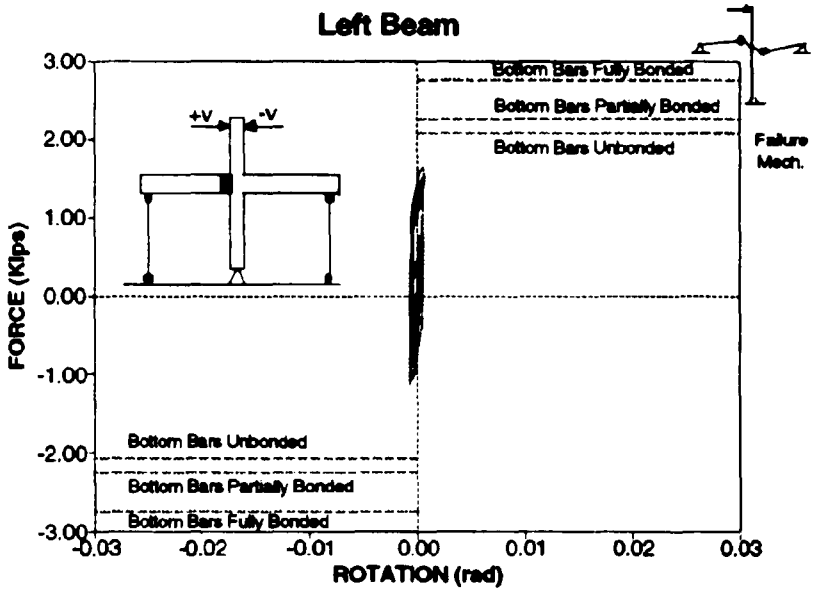

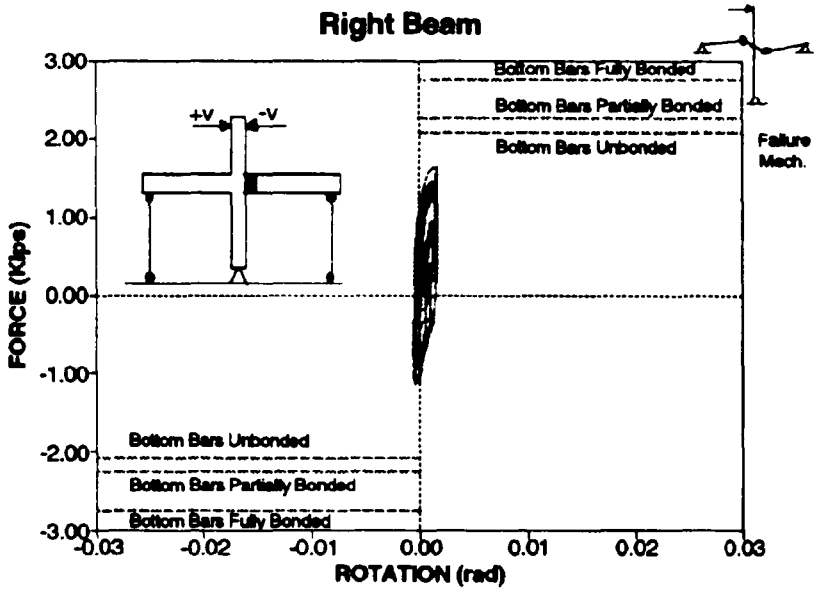

Fig. 5.7 Lateral Load-Rotation for Longitudinal Beams of As-Built Specimen (Stage 1)

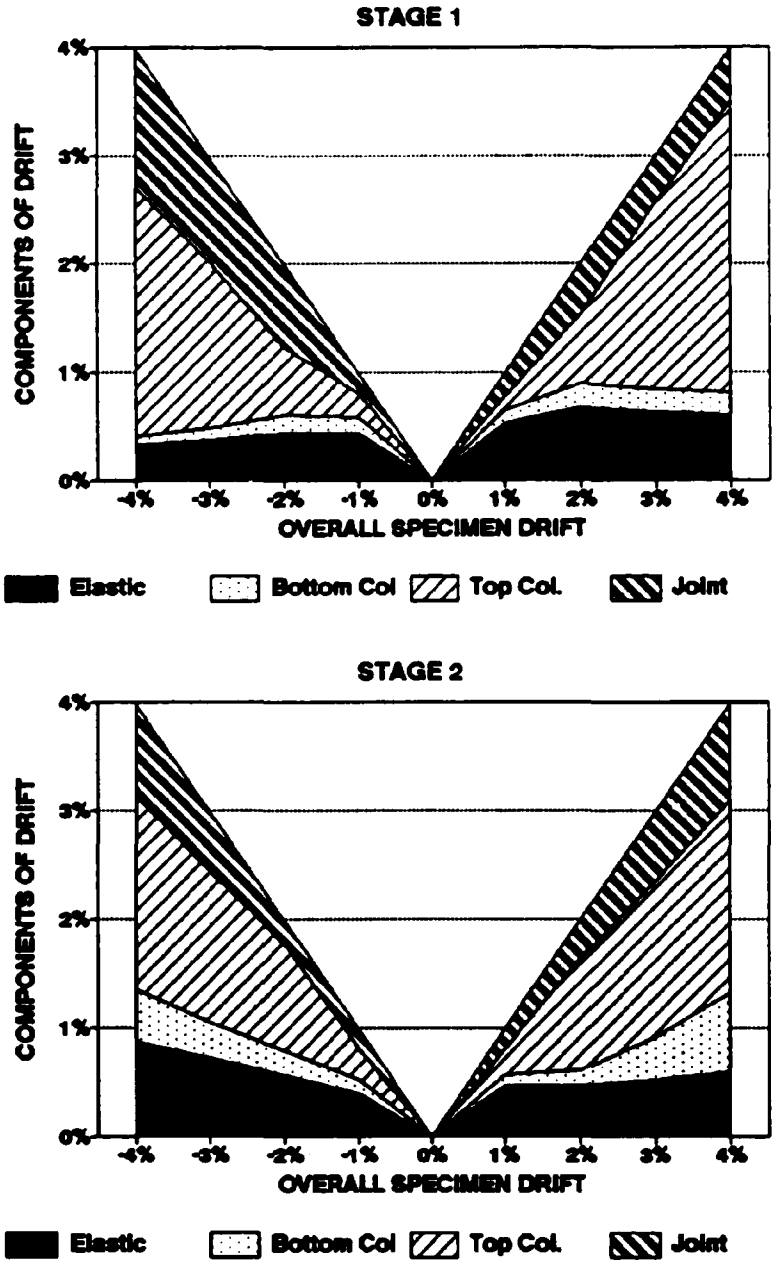

Fig. 5.8 Drift Contribution from each component of the As-Built Specimen

5.3 Retrofit of the Damaged Subassemblage Specimen

5.3.1 Retrofitting Technique

The specimen was retrofitted in accordance with the guidelines outlined in Section 2. A combination of reinforced and prestressed concrete was adopted for the retrofit of the damaged specimen. The top column of the subassemblage was prestressed. By effectively increasing the axial compression of the column through prestressing the strength was enhanced such that the response was primarily in the elastic range. Prestressing also provided a construction advantage as no transverse hoops were needed in the column due to the high intrinsic shear strength of uncracked concrete.

The bottom concrete column was conventionally reinforced. This was selected in preference to prestressed concrete on the premise that in the event of an earthquake, the base of the lowest story column of a structure would form a plastic hinge. A reinforced concrete section with adequate transverse reinforcement would ensure adequate energy dissipation in the cracked state. Also, enhanced strength by using post-tensioning at the lowest story of a structure may not be desirable since any increase in strength of these heavily loaded columns could induce excessive moments into the foundation system. The lower story also acts as a zone in which the prestressing bars can be anchored (bonded) for the upper stories that are post-tensioned.

The construction of the joint fillet served two purposes. First, it provided adequate development length for the positive (bottom) longitudinal steel of the beams; and second, it accommodated the much needed shear steel in the beam-column joint region.

5.3.2 Construction of the Retrofitted Specimen

The occurrence of a weak column-strong beam failure mechanism during the previous testing on the as-built specimen justified concrete jacketing of the columns of the subassemblage. This entailed a minimal enlargement of the columns from 4"x4" to a 6"x6" square section.

The steps adopted in the retrofit process were as follows: All the loose concrete around the column area and the beam adjacent to the column face was removed. Triangular holes were made through the slab in each of the four quadrants adjacent to the longitudinal and transverse beam junctions. This was to facilitate easy pouring of concrete to the bottom column, the joint fillet and also to allow the passage of longitudinal threadbar reinforcement. A set of two 0.5 in. dia. holes were made on each of the four beams centered at 5 in. from the face of the original 4x4 in. column to accommodate the joint shear/fillet reinforcement. These areas were thoroughly cleaned so that there would be adequate bond between the old concrete, fresh concrete and the new joint shear steel.

The longitudinal reinforcement was placed for the entire length of the top and the bottom column. The reinforcement was securely screwed onto the specially designed couplers to connect to the base plate on the bottom column. Above the slab level, the unbonded threadbar reinforcement for the top column was sleeved in a $^{3}/_{8}$ in. dia. plastic tube.

The transverse steel for the bottom reinforced concrete column consisted of a square wound spiral which was wound at a pitch of 2" and secured to the longitudinal threadbars by tie wire. The joint shear/fillet reinforcement was placed in two layers through the 0.5 in. dia. holes made in the beams. Each layer was placed in four parts and the laps fillet welded for continuity in a single pass. Transverse hoops were only placed in the top portion of the upper column to prevent local failure due to stress concentration at the point of application of the lateral load.

The column formwork was constructed from 22 ga. galvanized sheet metal. The entire formwork was split into two halves, which folded into each other to form the appropriate shape.

The concrete mix used for the retrofitting process was a proprietary Magnesium Ammonium Phosphate concrete of the high-strength early setting type (Set-45, Hot Weather, supplied by Master Builders Inc.). This type of concrete product was chosen

because it provided material properties that were ideal for the retrofitting operation. To state a few advantages of this concrete: The water content was low, only 8.34% by weight, resulting in minimal shrinkage. This ensured a good bond between the old and new concrete. According to the manufacturers specification, the compressive strength of the mix is expected to be 3000 psi. and 5000 psi. at 2 and 24 hours respectively. This high early strength enables a rapid turn around of formwork and minimum interference time in a building being rehabilitated. The concrete mix had its own pre-mixed aggregate of size $^1/_8$ in. down. Up to 60% extension is permitted using $^1/_4$ in. down aggregate without expecting any significant loss of compressive strength. The mix afforded the attainment of its maximum flexural strength of 1000 psi. in 20 hours. The mix had an adequate amount of super-plasticizer which gave it an inherently high slump mix resulting in easy pouring over the tall height with narrow cavities.

The retrofitted subassemblage was poured in three stages. Firstly the lower column, secondly the joint fillet and the triangular holes in the floor slab and finally the upper column was poured. The average value of f_c' for the retrofitted specimen, obtained from testing three 4x2 in. cylinders of each stage, was 4.8 ksi. at the time of testing.

5.3.3 Reinforcement for the Retrofitted Specimen

Four 0.375 in. dia. high-strength threaded rods were used to longitudinally reinforce the upper and lower columns (see stress-strain diagram Section 3.1.1). The reinforcement for the bottom column was bonded giving a 6x6 in. reinforced concrete column. The reinforcement for the top column was unbonded, sheathed in a plastic tubing giving a post-tensioned prestressed column.

Transverse reinforcement was provided only in the top portion of the top column, to prevent local failures, by way of stirrups of D1 wire at 1 in. center-to-center spacing. For the bottom column transverse reinforcement consisted of a wound square spiral of D1 wire at 2 in. center to center (Refer Fig. 5.9).

The joint region consisted of a fillet which extended 6 in. from the face of the original 4x4 in. column. This distance was determined on the basis of the development length required for the bottom bars of the longitudinal beams. The reinforcement consisted of two layers of unannealed D4 bar reinforcement as shown in Figs. 5.9 and 5.10.

5.4 Experimental Set-up and Instrumentation

The general set-up of the test rig was the same as the one used for experiments on the original specimen and is shown in Fig. 5.1. The retrofitted specimen, in contrast with as-built specimen test by Aycardi et. al. (1991), was tested without any superimposed axial load. Axial load provides some beneficial effects in that it enhances the reinforced concrete column capacity, improves joint strength by enhancing the concrete strut capacity, and improves bond of the beam's longitudinal reinforcement. Thus by ignoring the beneficial effects of axial load an adverse loading scenario was created particularly for the joint region itself. This is similar to what may be encountered in the upper stories of a frame structure. If axial load was present, then a correspondingly smaller amount of prestress could be applied to the upper column.

A 60 kip capacity hydraulic jack was used to post-tension the upper column. A total post-tensioning force of 32 kips was applied to the four threadbars using an under stress-over stress relaxation technique. The total prestress level of 32 kips for the top column was based on post-tensioning the threadbars to 70% of their ultimate strength. Fig. 5.11 shows the specimen during the post-tensioning process.

The comparative strength of the original as-built and the retrofitted specimen is shown in the form of an interaction diagram in Fig. 5.12. The moment capacity of the prestressed column was determined using strain compatibility technique for unbonded tendons. The value of f_{ps} is calculated from Eq. 2.9 of Section 2. The bottom column was treated as a conventionally reinforced section. The $\frac{\Sigma M_{col}}{\Sigma M_{beam}}$ ratios for the original as-built and the retrofitted specimen were 0.78 and 1.6 respectively.

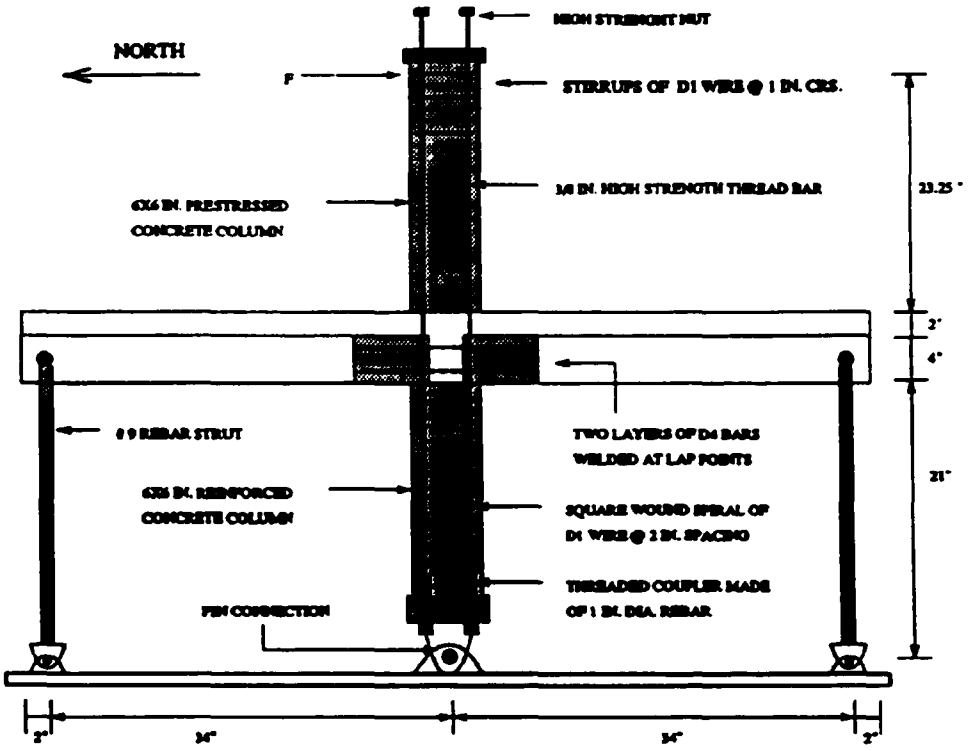

Fig. 5.9 Reinforcement Diagram for the Retrofitted Specimen

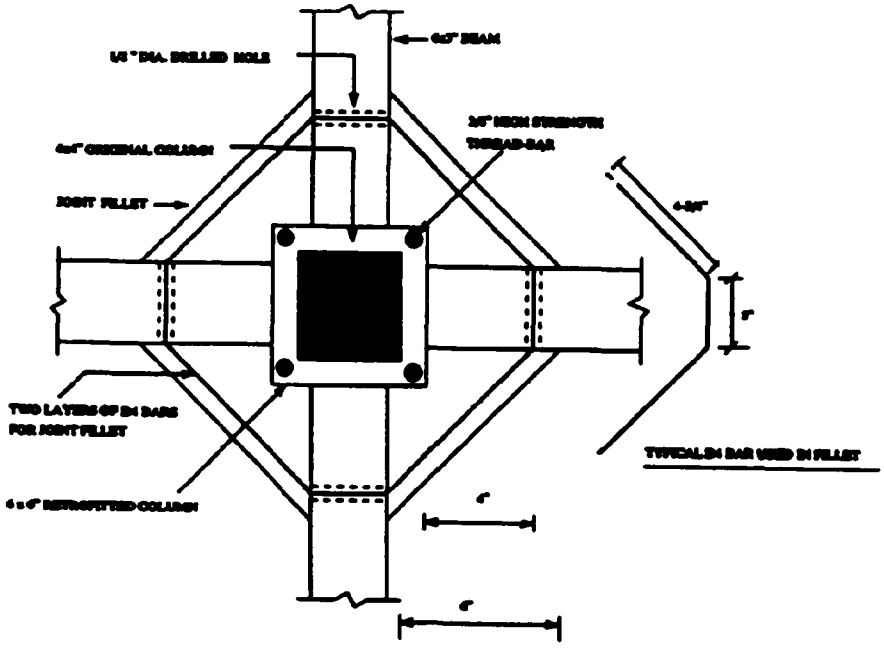

Fig. 5.10 Detail of Fillet Reinforcement for Specimen

The lateral load was applied to the specimen by a 6 kip servo-controlled hydraulic actuator. Loads were measured by a load cell calibrated to an accuracy of ±0.01 kips.

Rotations were measured by a pair of linear potentiometers which were attached in pairs, one to each side of the columns and the longitudinal beams. These potentiometers were mounted onto an aluminum chassis and epoxied to the concrete. Rotations in the longitudinal beams were measured in the hinge zones adjacent to the joint fillet as shown in Fig. 5.13. Potentiometers had a resolution of ±0.0001 in.

All channels were recorded using Megadac 5533A data acquisition system at a sampling rate of 1 Hz. Lateral load vs. displacement plots were recorded on a Type 7090A analog Hewlett-Packard X-Y plotter during the test. The data from the Megadac was exported to a PC computer for analysis using spreadsheet programs.

5.5 Testing Procedure

The retrofitted subassemblage was tested quasi-statically with two cycles of loading at increasing drift amplitudes of ±0.25%, ±1%, ±2%, ±3%, ±4%. A sinusoidal wave form was used with an input of 0.01 Hz. for the horizontal actuator. The initial half cycle of loading was in the reverse direction or the north direction followed by forward cycle or loading in the South direction.This constituted Stage 4 of testing.

This was followed by Stage 5, which comprised of 50 cycles of quasi-dynamic loading at 0.5 Hz. to a drift amplitude of 4%. The only data recorded at this stage of testing was the lateral force and the corresponding displacement.

After the entire sequence of testing, a monotonic pull test was done on the top column. This was Stage 6, the final stage of testing. Data was recorded on a X-Y plotter.

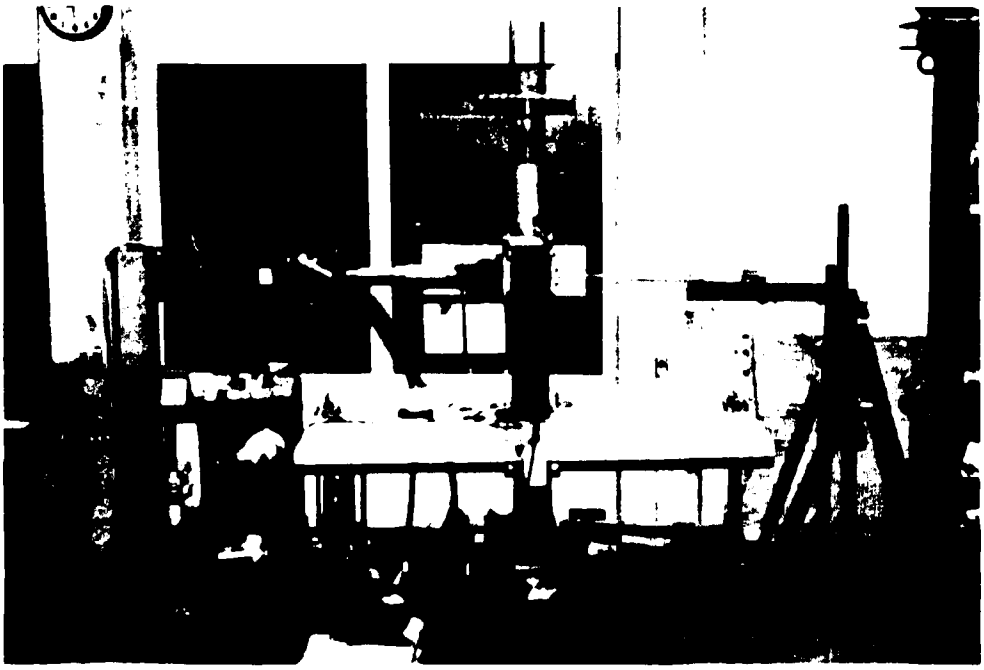

Fig. 5.11 Retrofitted Specimen before Testing during post-tensioning ofthreadbars of the Upper Column

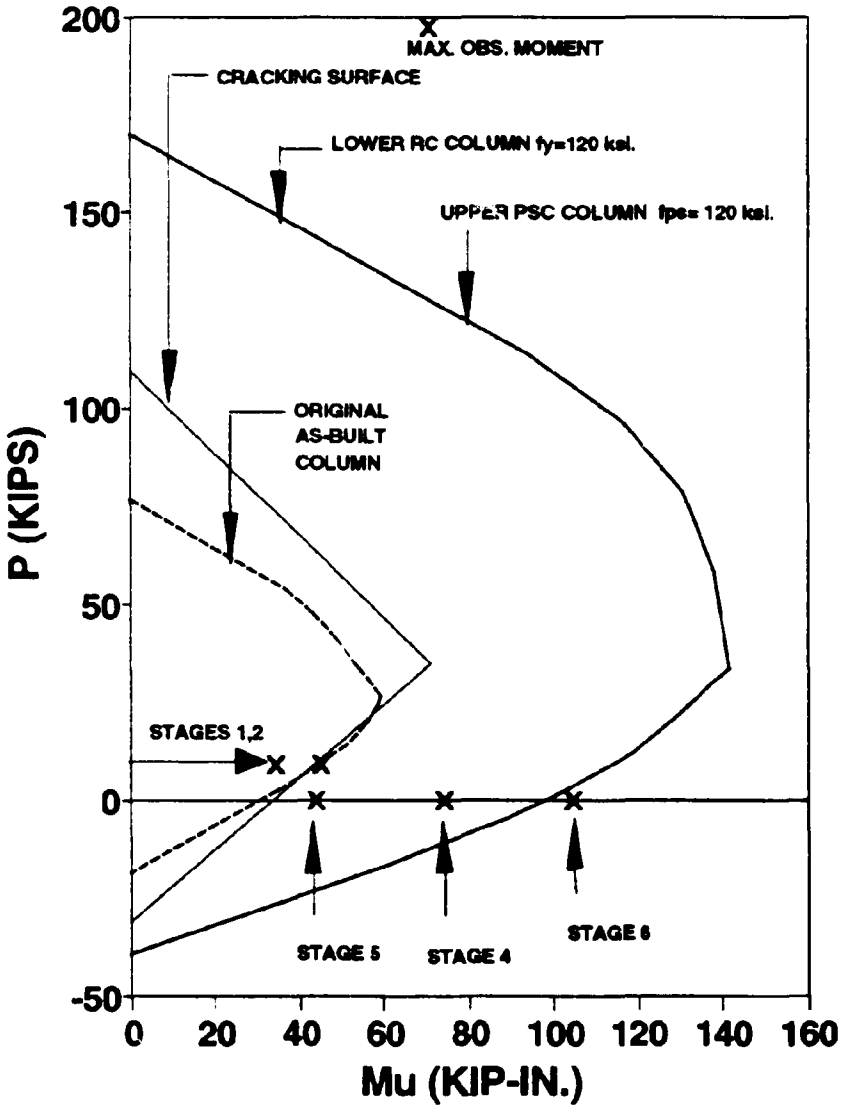

Fig. 5.12 Interaction Diagram for both the As-built and Retrofitted Specimen

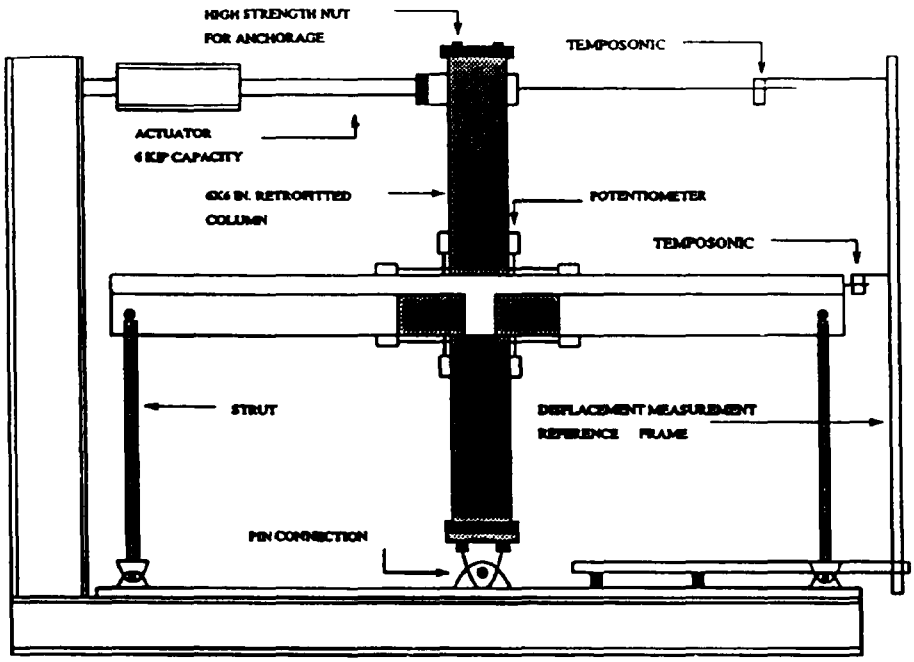

Fig. 5.13 Experimental Set-up for the Retrofitted Specimen

5.6 Experimental Results - STAGES 4, 5 and 6

5.6.1 Observed Performance at Successive Load Cycles

STAGE 4

The behavior of the specimen at the initial 0.25% level of drift was essentially elastic. The secant slope of the narrow hysteresis loops shown in Fig. 5.13 represents the elastic stiffness of the subassemblage. The slight hysteresis is attributed to cracking resulting from previous damage done to the beams.

The moment of inertia of the retrofitted columns was approximately five times that of the original columns resulting a 170% increase in the subassemblage stiffness. The comparative elastic stiffness of the original as-built and retrofitted specimen can be seen in Fig. 5.14. This increase in stiffness is due to an increase in column size should not be viewed as critical; since a structure's overall stiffness also depends on other components which may not need retrofitting when rehabilitating an entire structure. The hysteretic force-drift behavior of the subassemblage for the remainder of the quasi-static cycles of testing is shown in Fig. 5.19.

It should be mentioned that no special repair method was adopted for the slab. The large crack across the width of the slab, as a result of previous testing, was filled with a cement slurry. This would suffice as an aesthetic treatment only. It should be noted that the slab bars were fractured due to previous testing.

At the 1% drift cycles there was an indication of cracks initiating in the joint fillet region near the beam face. There was no diagonal shear cracking or flexural cracking in the columns.

There were no signs of flexural or shear cracking in the columns at the 2% drift cycles. The cumulative joint shear distortion, as observed by the appearance of cracks in the fillet region closer to the beam face, was more pronounced at this drift level. Fresh flexural

cracks developed in the beams just outside the joint fillet region.

There was no evidence of any column shear or flexural cracking at the end of the 3% drift cycles, though there was some superficial spalling of cover concrete at the top of the bottom column. The increased distortion of the fillet observed at the face of the beams indicated that the plastic hinge region had shifted into the beams.

The joint fillet area, closer to the beam face, exhibited additional spalling of cover concrete at the end of the 4% drift cycles. Fig. 5.15 is the evidence of this damage.

STAGE 5

The strength of the retrofitted specimen degraded to 75% of its initial value in the first 10 of the 50 quasi-dynamic cycles. Extensive damage was observed outside the joint fillet region in the beams and the slab above it. A force vs. drift plot of this stage is presented in Fig. 5.22 and shows the first and last 10 load cycles of testing respectively.

STAGE 6

This stage of testing consisted of blocking the beams against horizontal movement and then monotonically pulling the top column with the objective of determining its ultimate load carrying capacity. Fig. 5.23 shows the results of this test as a force vs. displacement plot. The nominal ultimate strength shown in Fig. 5.23 is exceeded due to strain hardening of the longitudinal column reinforcement.

5.6.2 Component Rotation Contributions

The idealized plastic geometry can be seen in Fig. 5.16. Total drift is the relative displacement of the temposonic at the top column level with respect to the hinge connection at the base (Refer Fig. 5.13). From geometry the total applied drift can be expressed as:

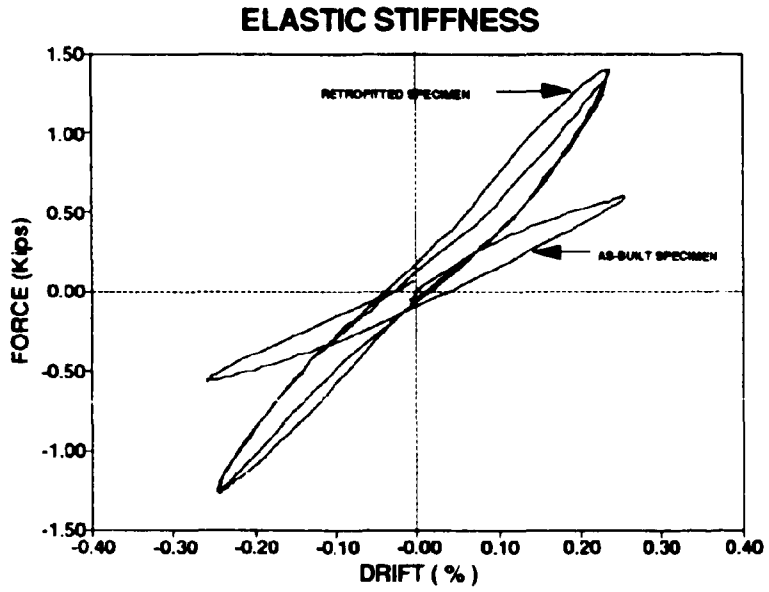

Fig. 5.14 Comparison of the Elastic Stiffness of As-built and Retrofitted Specimen

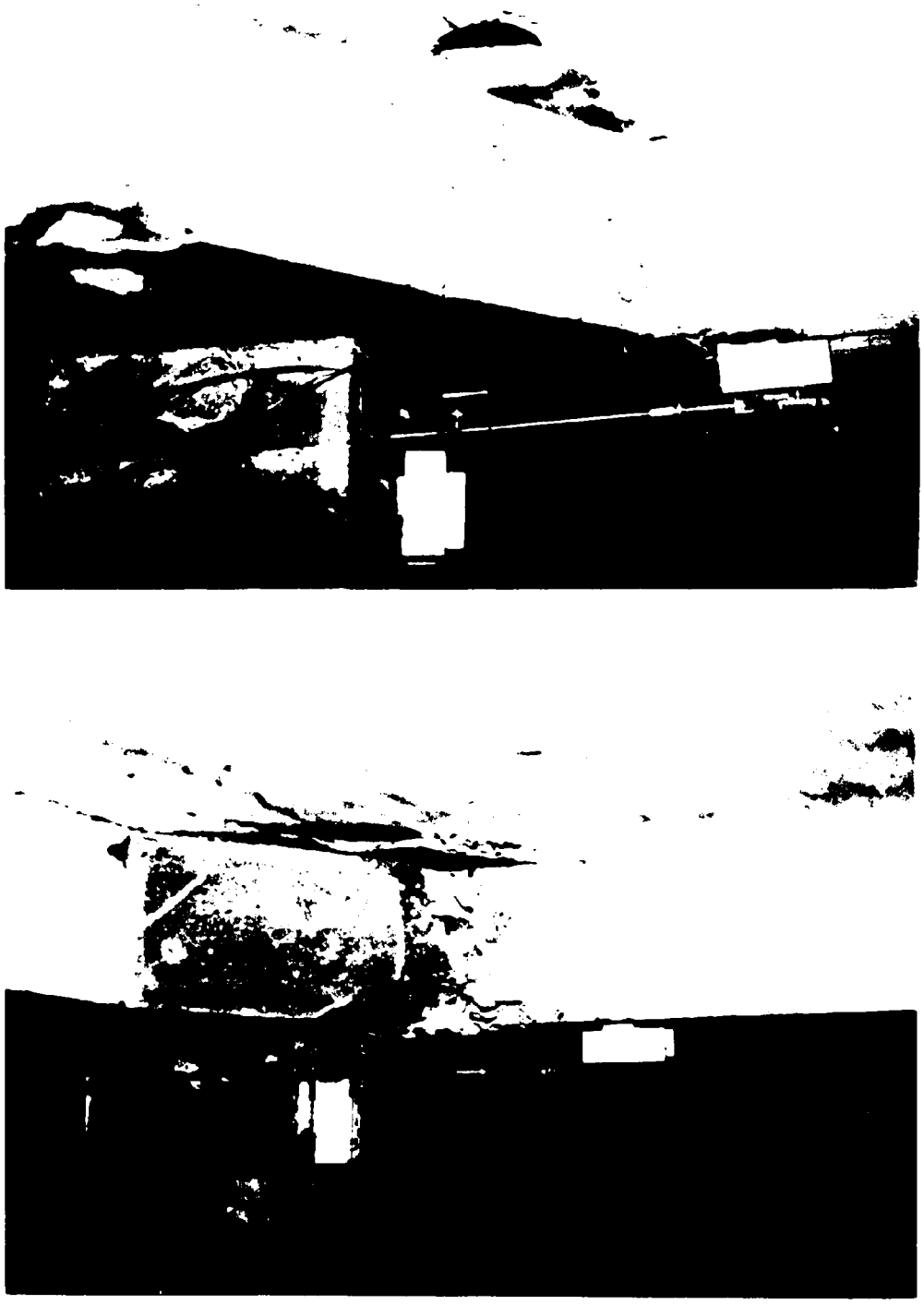

Fig. 5.15 Damage after 4% Drift Cycles

$$D=\frac{\Delta}{H}=\theta_e+\theta_{br}\cdot\frac{L_{br}}{L}+\theta_{bl}\cdot\frac{L_{bl}}{L}+\theta_{ct}\cdot\frac{H_{ct}}{H}+\theta_{cb}\cdot\frac{H_{cb}}{H}+\gamma_j \qquad (5.1)$$

where,

$D=\frac{\Delta}{H}=$ Total applied drift.

$\theta_e=$ Elastic component of drift for the subassemblage.

$\theta_{br},\theta_{bl},\theta_{ct},\theta_{cb}=$ Plastic rotation of the right beam, left beam, top column, bottom column.

$L=$ Length of beams from the specimen centerline to the point of contraflexure = 34 in.

$H=$ Height of Subassemblage between the bottom hinge and the point of lateral load application = 50.25 in.

$L_{br},L_{bl}=$ Distance from plastic hinge zone to the end of right and left beams = 26 in.

$H_{ct},H_{cb}=$ Distance from the plastic hinge zone to the end of the top column, bottom column = 22.375 in., 20.125 in.

$\gamma_j=$ Plastic shear distortion of the joint.

The elastic drift component was evaluated as $\theta_e=(0.00178).F$, where $F=$ lateral load. The plastic drift components for the individual beams and columns were evaluated from Fig 5.20 and Fig. 5.21. It was not possible to directly measure joint shear with the type of gauge shown in Fig. 4.1 due to the presence of transverse beams. However, using the relevant geometry in Eq. 5.1 it is possible to infer a plastic distortion of the joint as follows:

$$\gamma_j = [D - 0.00178F] - [0.765(\frac{\theta_{br} + \theta_{bl}}{2}) + 0.445(\theta_{ct}) + 0.4(\theta_{cb})] \qquad (5.2)$$

The first and second bracketed portions of Eq. 5.2 represent components of; the total plastic drift, and the plastic drift from the beam and column hinges respectively. The difference of the bracketed components give the joint shear distortion γ_j . The various components of drift are tabulated in Table 5.2.

Table 5.2 Drift Contribution of the various Components

Total Drift (D)	Plastic Drift $D-(0.00178)F$	Right Beam (θ_{br})	Left Beam (θ_{bl})	Top Column (θ_{ct})	Bottom Column (θ_{cb})	Joint Distortion from Eq.5.2 (γ_j)
+0.01	0.0050	0.0028	0.0043	0.0005	0.0005	0.0004
-0.01	-0.0052	-0.0028	-0.0033	-0.0008	-0.0005	-0.0009
+0.02	0.0145	0.0076	0.0125	0.0016	0.0013	0.0015
-0.02	-0.0143	-0.0097	-0.0080	-0.0033	-0.0014	-0.0008
+0.03	0.0246	0.0149	0.0210	0.0032	0.0022	0.0013
-0.03	-0.0245	-0.0173	-0.0143	-0.0036	-0.0022	-0.0029
+0.04	0.0356	0.0253	0.0294	0.0055	0.0022	0.0005
-0.04	-0.0350	-0.0300	-0.0276	-0.0041	-0.0018	-0.0002

it should be noted that the plastic rotation values of the beams and columns, tabulated in Table 5.2, are multiplied by their appropriate coefficients as seen in Eq. 5.2 before being presented graphically in Fig. 5.20. The plastic rotation contribution of the top and bottom columns is nearly one-eighth of that of the longitudinal beams. This shows that the

hinging is primarily restricted to the beams (Refer Fig. 5.21).

At the 3% drift cycle there was more joint distortion in the reverse than the forward direction (Refer Figs. 5.20-21).This deterioration of the fillet is further aggravated by the tendency of the bottom bars of the longitudinal beam to pull out at higher loads. The pinching of the hysteresis loops at the 3% drift cycle (Refer Fig. 5.17) is due to the partial loss of bond of the bottom longitudinal bars.

A comparison of rotation contribution of various components of the specimen before and after the retrofit (Refer Figs. 5.7, 5.20) indicate a clear change in the failure mode of the specimen. Figs. 5.6 and 5.7 show that there was no plastic rotation contribution from the longitudinal beams of the original as-built specimen. Results from Part II of the evaluation report series (Aycardi et al. 1992) show that the original as-built specimen top column failed, this would constitute a column side-sway mechanism in a full-scale structure. In contrast Figs. 5.20-21 show that the failure in the retrofitted specimen is due to hinging of the longitudinal beams; this would cause an entire structural frame to form a beam-sidesway mechanism.

5.7 Conclusions

Based on the observations of the previous testing of the original as-built specimen and the testing of the retrofitted specimen, the following conclusions are made:

1 The as-built specimen exhibited progressive damage in the columns, principally the top column, with no noticeable damage to the beams. This resulted in a weak column-strong beam failure mechanism. In contrast, the retrofitted specimen exhibited progressive damage to the beams near the joint fillet, with no noticeable damage to the columns; thus exhibiting a favorable weak beam-strong column mechanism.

2 Although it was not possible to detect visually, analysis showed that there was some inelastic joint shear distortion amounting to about 25% of total plastic displacement

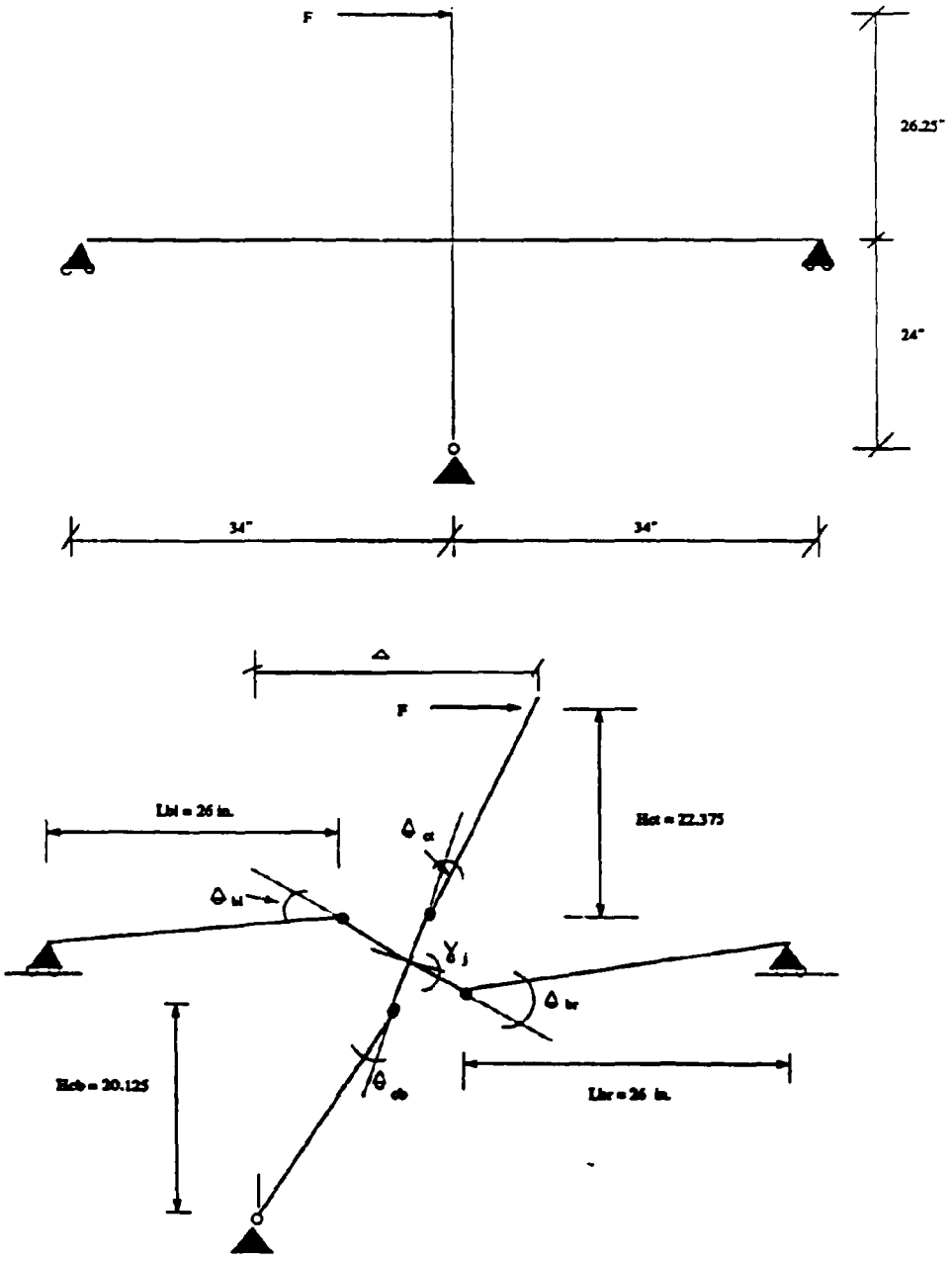

Fig. 5.16 Idealized Plastic Geometry of the Retrofitted Specimen

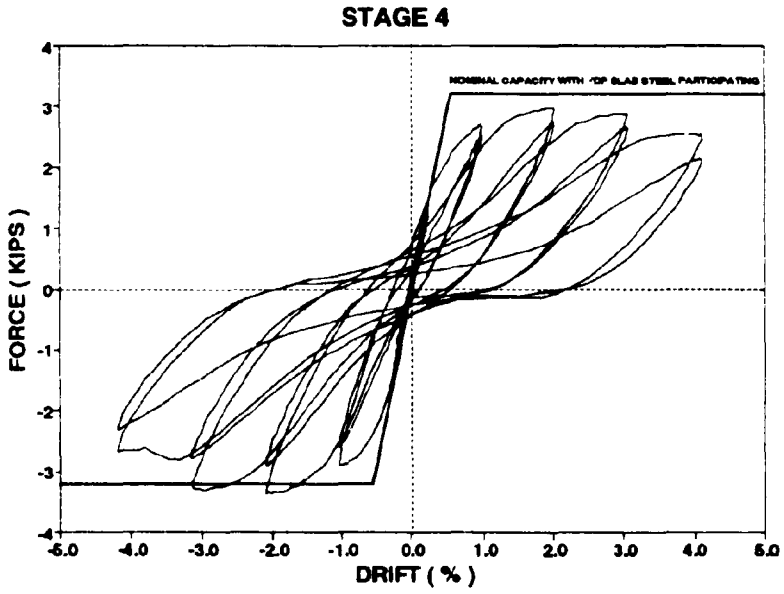

Fig. 5.17 Force - Drift of the Retrofitted Subassemblage

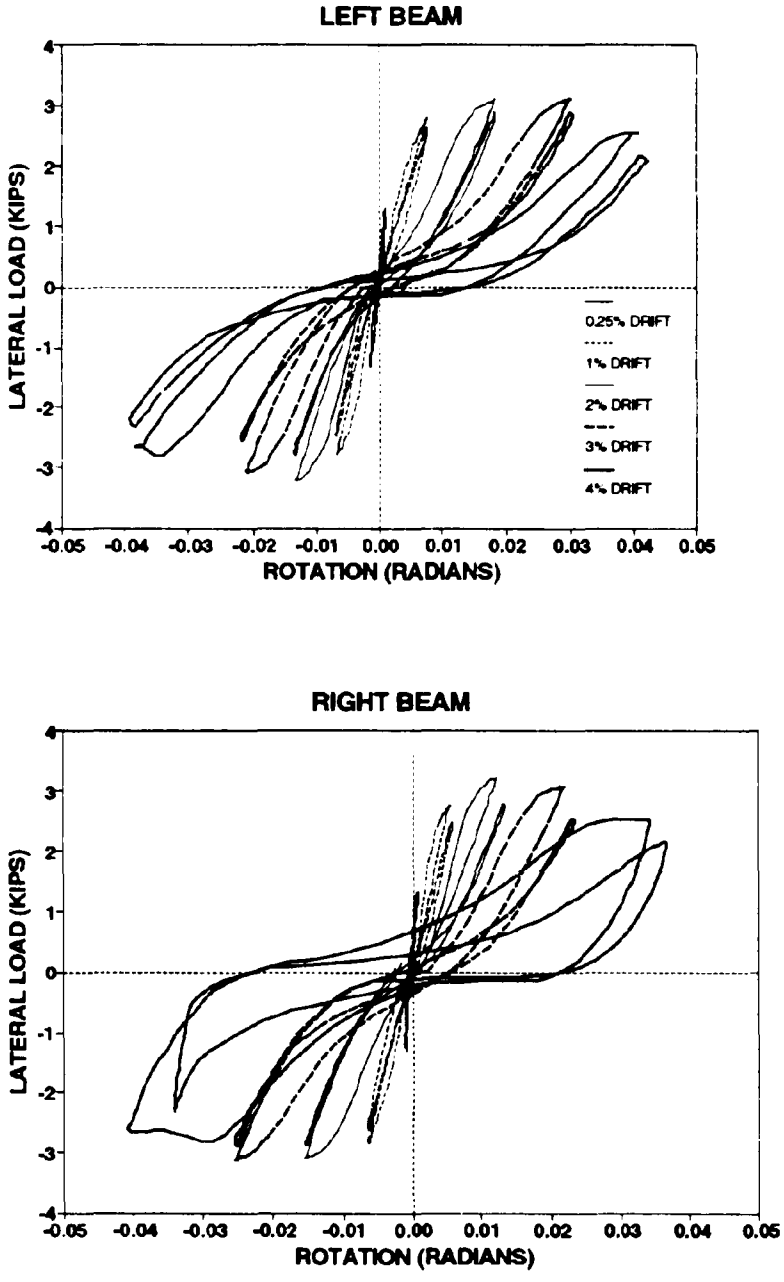

Fig. 5.18 Lateral Load vs. Rotation graphs for the Left and Right Longitudinal Beams of Retrofitted Specimen

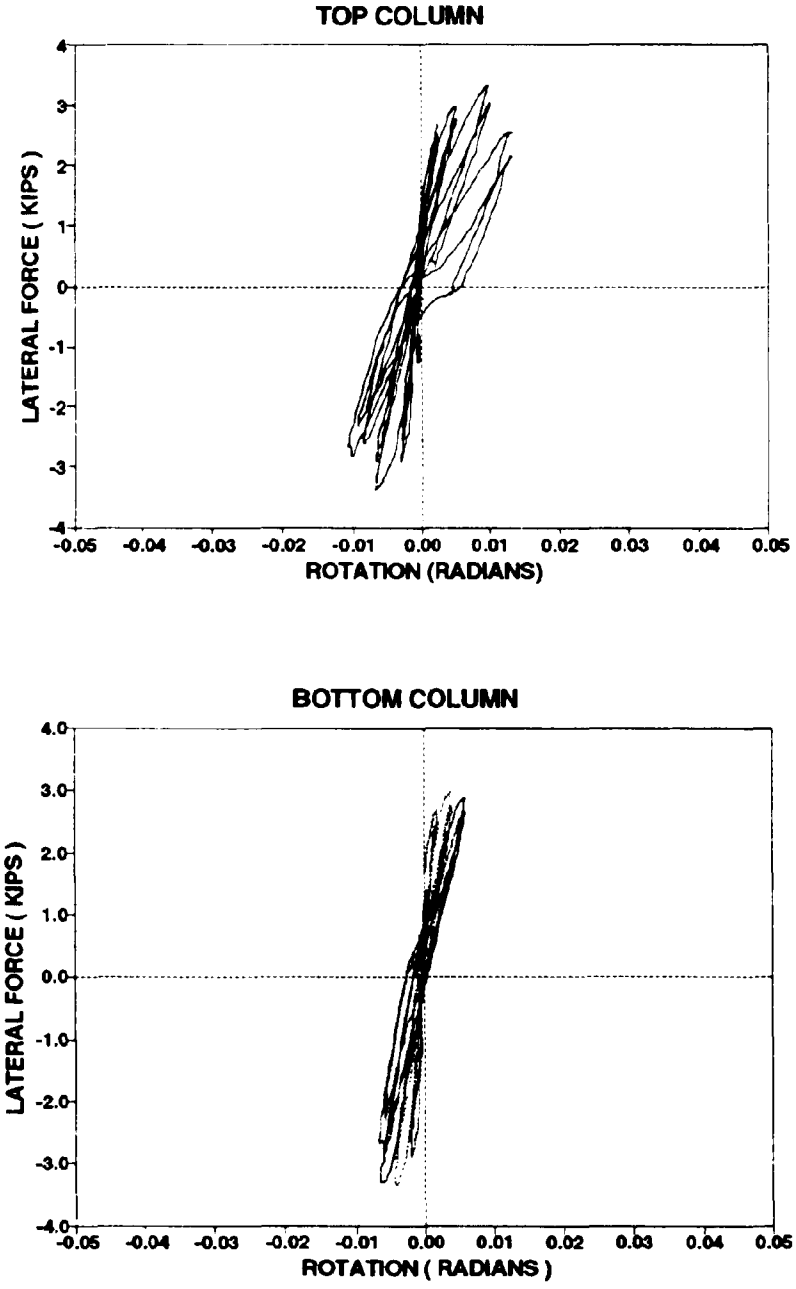

Fig. 5.19 Lateral Load vs. Rotation graphs for Top and Bottom Columns of the Retrofitted Specimen

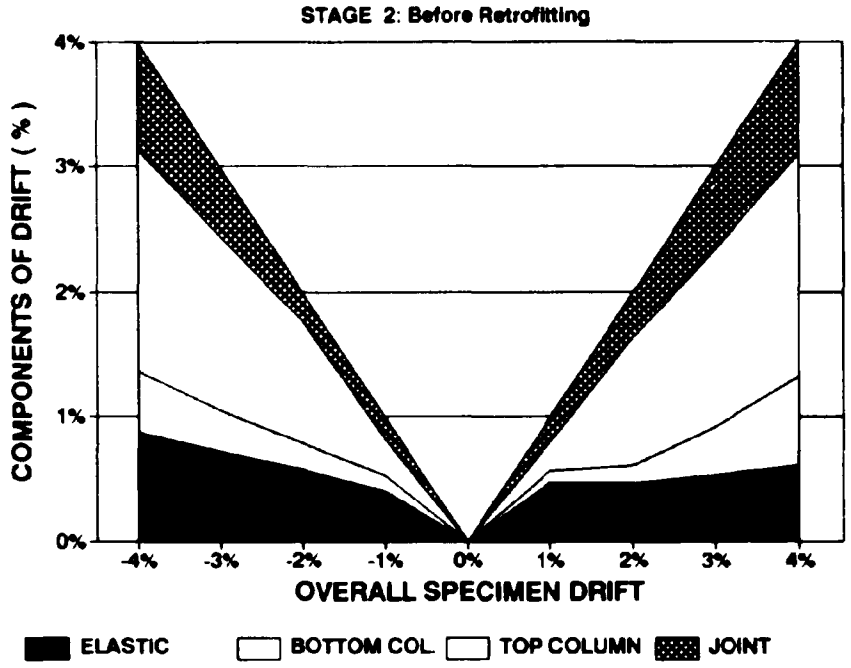

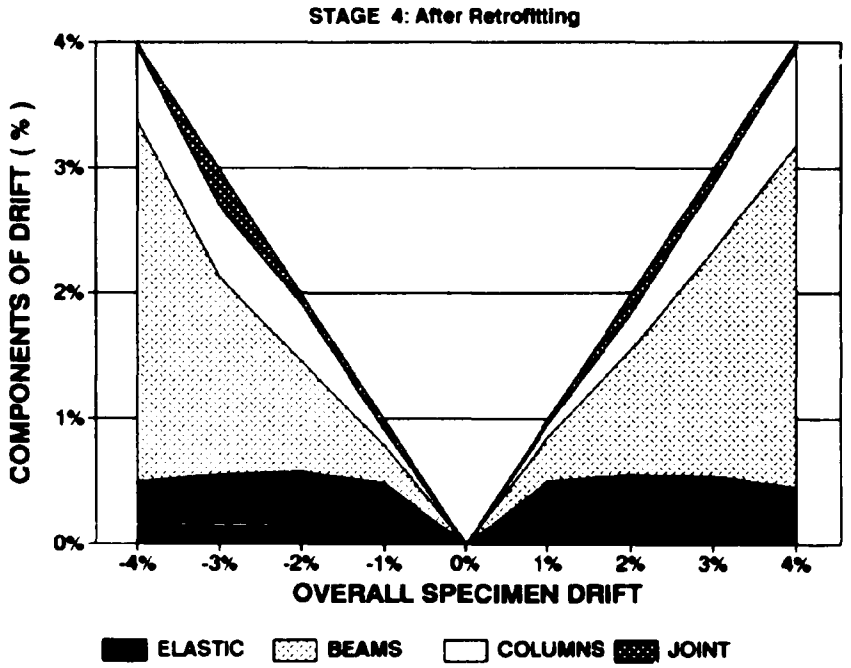

Fig. 5.20 Rotation Contributions Before and After Retrofitting

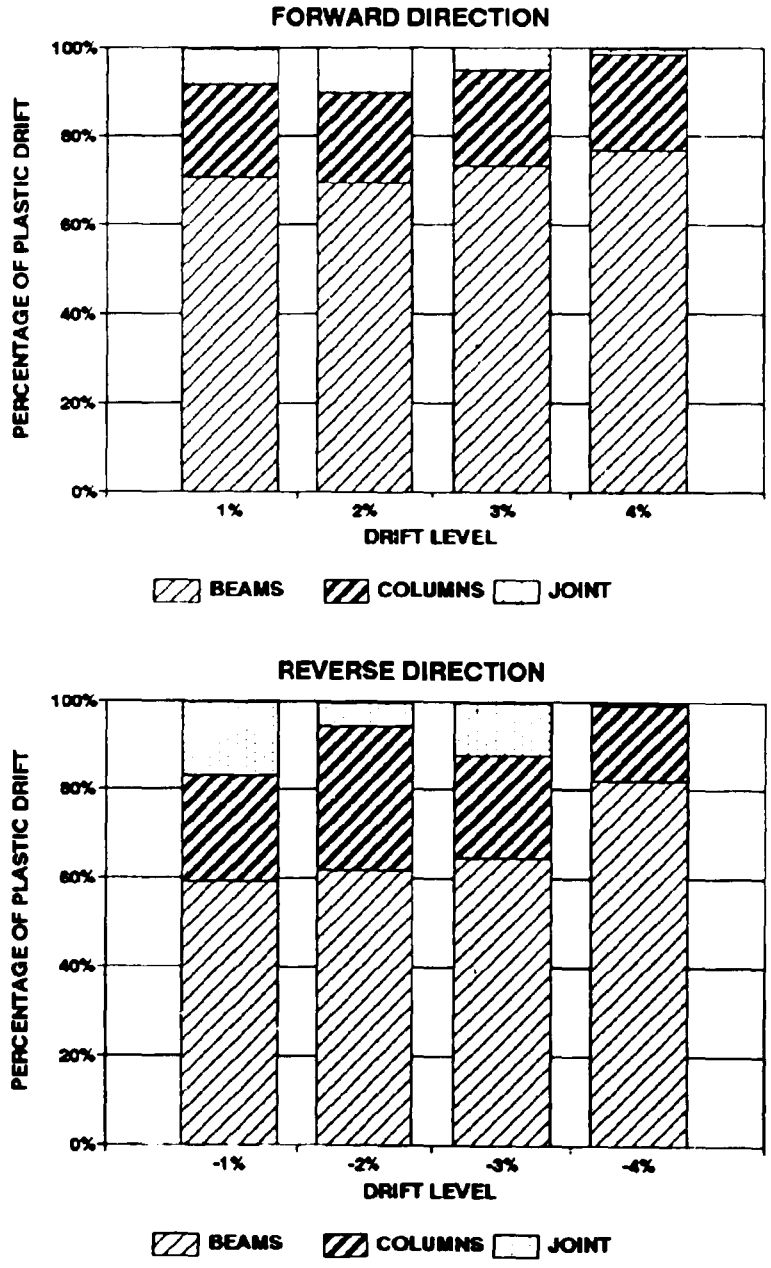

Fig. 5.21 Percentage Contribution of Plastic Drift by Components

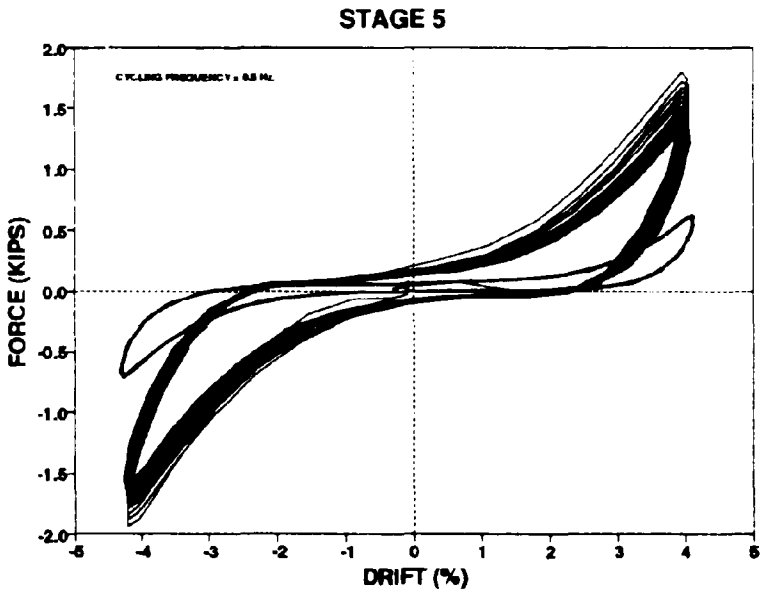

Fig. 5.22 Force - Drift for Quasi-Dynamic test at 4% drift

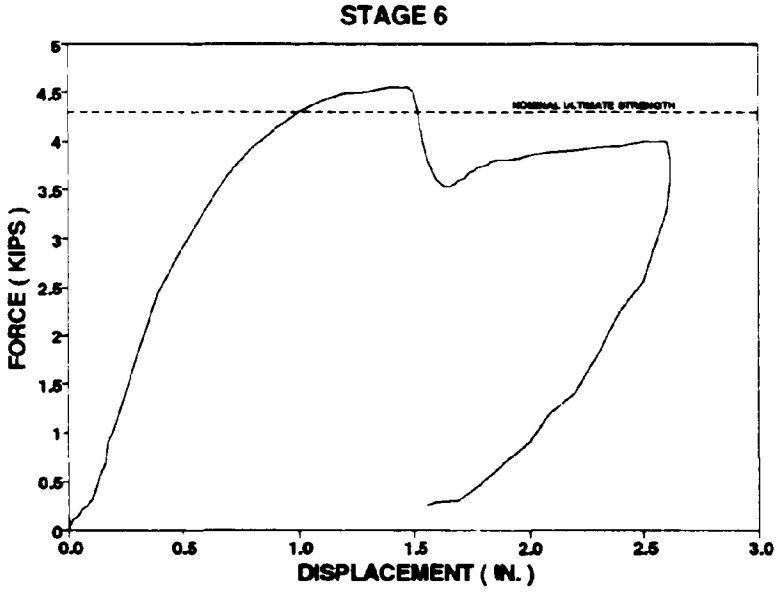

Fig. 5.23 Force-Displacement for the Pull Test

at large drifts in case of the as-built specimen. For the retrofitted specimen, a similar analysis showed that about 12% of the total plastic displacement was from inelastic joint shear distortion. This was partially observed due to cracking in the fillet region.

3. The construction of the joint fillet provided sufficient development length to the bottom reinforcement thus ensuring satisfactory anchorage to prevent pull-out under large drifts.

4. Post-tensioning the top column augmented the column strength in both moment and shear capacity ensuring elastic performance.

5. Maximum strengths for both the as-built and retrofitted specimen were achieved at 3% drift levels.

6. Concrete jacketing with a high strength mix provides a dependable and effective method of rehabilitating structures in which the columns have insufficient strength to prevent a column sidesway mechanism.

SECTION 6

CONCLUSIONS

Tables 6.1 and 6.2 summarize the experimental results. The remainder of this section presents a summary of conclusions presented at the end of Sections 2, 3, 4 and 5.

Table 6.1 Column Stiffnesses and Strengths Before and After Retrofitting

Specimen	Stiffness			Flexural Strength	
	Theor. Gross[*1] (EI_g)	Experime t. Observed[*2] (EI)	Experiment. Observed (ratio)[*3]	Nominal (Kips)	Achieved (Ratio)[*4]
Original	80200	52267	0.65	1.98	1.03
RC Jacket	426500	200064	0.47	5	1.2
PSC Jacket	426500	58068	0.14[*5]	3.34	0.94

[*1] The theoretical gross stiffness for the cantilever columns has been calculated using I_g moment of inertia of gross concrete section neglecting the reinforcement, and

$$E = 57000\sqrt{f'_c}\ psi$$

[*2] Observed experimental stiffness determined, from a secant slope, by $EI = \frac{PL^3}{3\Delta}$

where P is 75% of the nominal strength and Δ is the corresponding deflection.

[*3] Ratio with respect to the theoretical gross stiffness

[*4] Ratio with respect to the nominal strength

[*5] Specimen was severely damaged prior to retrofitting

Table 6.2 Subassemblage Stiffnesses and Strength Before and After Retrofitting

Specimen	Stiffness			Flexural Strength				
	Obs. Before Retrofit (K/in.)	Obs. After Retrofit (K/in.)	Ratio[*1]	Nominal for BSM[*2] (Kips)	Obs. Before Retrofit (Kips)	Obs. After Retrofit (Kips)	Ratio[*3]	
							Before	After
One-way beam column joint	3.90	6.90	.56	1.77	1.35	2.44	.76	1.8
Two-way beam column joint	4.91	10.23	.48	2.75	1.52	2.81	.55	1.02

[*1] Ratio of stiffness before to stiffness after retrofit.

[*2] Beam sidesway mechanism strength before retrofit.

[*3] Ratio with respect to BSM strength.

1. The capacity analysis and redesign demonstrated that it was of critical importance to provide dependable positive moment capacity in the longitudinal beams of the gravity load designed frame. A joint fillet is a recommended solution.

2. The use of prestressing for the flexural strength redesign of columns has multiple advantages, such as optimizing the section size and providing a strong elastic column. These obviate the need for additional transverse reinforcement, and afford easy pouring of concrete in tall enclosed spaces.

3. The principal objective of the retrofit redesign of column specimens was the augmentation of strength. This was achieved for both RC and PSC retrofits. A second objective for the RC column retrofit was to ensure a ductile post-ultimate behavior through the provision of transverse reinforcement. The specimen behaved well, showing excellent energy dissipation up to drift amplitudes of 5%. In spite of the absence of transverse reinforcement, there was no apparent distress due to shear in the PSC retrofit.

4. The controlling purpose of the seismic retrofit and redesign of the one-way beam column joint was to augment joint and column strength. This was achieved as corroborated by the essentially elastic behavior of the joint. Column strength was also adequately increased, preventing them from actively participating in the energy dissipating process.

5. The joint fillet design shifted the potential plastic hinge zone away from the column face to the edge of the joint fillet in an effective fashion and at the same time provided sufficient development length to preclude any possibility of pull-out of the bottom longitudinal beam reinforcement.

6. The bonding of the steel plates was effective in reducing the localized damage in the top portion on the south beam which was badly damaged due to previous testing. However, such a repair is good for only a limited number of load reversals.

7. The original subassemblage exhibited progressive damage in the columns, principally the top column, with no noticeable damage to the beams. This resulted in a weak column-strong beam failure mechanism. In contrast, the retrofitted specimen exhibited progressive damage to the beams near the joint fillet, with no noticeable damage to the columns; thus exhibiting a favorable weak beam-strong column mechanism.

8. Analysis showed that there was some inelastic joint shear distortion amounting to about 25% of total plastic displacement at large drifts in case of the as-built specimen. For the retrofitted specimen, a similar analysis showed that about 12% of the total plastic displacement was from inelastic joint shear distortion.

9. Post tensioning the top column augmented the column strength in both moment and shear capacity ensuring elastic performance. Concrete jacketing with a high strength mix provides a dependable and effective method of rehabilitating structures in which the columns have insufficient strength to prevent a column sidesway mechanism.

SECTION 7

REFERENCES

ACI Committee 318 (1989). "Building Code Requirements for Reinforced Concrete (ACI 318-89)", ACI, Detroit.

Aycardi, L.E., Mander, J.B., and Reinhorn, A.M. (1992). "Seismic Resistance of Reinforced Concrete Frame Structures Designed only for Gravity Loads: Part II - Experimental Performance of Subassemblages", Technical Report NCEER-92-0028, National Center for Earthquake Engineering Research, SUNY/Buffalo.

Augusti, G., Facardi, F., Grandano, S., and Manzini, E. (1980). "Rehabilitation of Damaged Reinforced Concrete Elements : an Experimental Investigation", *Proceedings of the Seventh WCEE*, Vol. 4, Part 1, 335-342, Istanbul, Turkey.

Bertero, V., and Brakken, S. (1980). "Effect of Infills in Seismic Resistant Buildings", Proceedings of the Second Seminar on Repair and Retrofit of Structures, Ann Arbor, Michigan, Vol. 2, 377-419.

Bracci, J.M., Mander, J.B., and Reinhorn, A.M. (1992a). "Seismic Resistance of Reinforced Concrete Frame Structures Designed only for Gravity Loads: Part I - Design and Properties of a One-Third Scale Model Structure", Technical Report NCEER-92-0027, National Center for Earthquake Engineering Research, SUNY/Buffalo.

Bracci, J.M., Mander, J.B., and Reinhorn, A.M. (1992b). "Seismic Resistance of Reinforced Concrete Frame Structures Designed only for Gravity Loads: Part III - Experimental Performance and Analytical Study of Study of Structural Model", Technical Report NCEER-92-0029, National Center for Earthquake Engineering Research, SUNY/Buffalo.

Bracci, J.M., Mander, J.B., and Reinhorn, A.M. (1992c). "Evaluation of Seismic Retrofit of Reinforced Concrete Frame Structures: Part II - Experimental Performance and Analytical Study of Retrofitted Structural Model", Technical Report NCEER-92-0031, National Center for Earthquake Engineering Research, SUNY/Buffalo.

Corazao, M., and Durrani, A.J. (1989). "Repair and Strengthening of Beam-to-Column Connections Subject to Earthquake Loading" , Technical Report NCEER-89-0013, National Center for Earthquake Engineering Research, SUNY/Buffalo.

Chai, Y.H., Priestley, M.J.N., and Seible, F. (1991). "Seismic Retrofit of Circular Bridge Columns for Enhanced Flexural Performance", *ACI Structural Journal*, V.88, No.5, September-October, 572-584.

El-Attar, A.G., White, R.N., and Gergely, P. (1991a). "Shaking Table Test of a 1/6 Scale Two-Story Lightly Reinforced Concrete Building", Technical Report NCEER-91-0017, National Center for Earthquake Engineering Research, SUNY/Buffalo.

El-Attar, A.G., White, R.N., and Gergely, P. (1991b). "Shaking Table Test of a 1/8 Scale Two-Story Lightly Reinforced Concrete Building", Technical Report NCEER-91-0018, National Center for Earthquake Engineering Research, SUNY/Buffalo.

Lao, Larry F. (1990). "The Effect of Detailing on the Seismic Performance of Gravity Load Dominated Reinforced Concrete Frames", MS Thesis, State University of New York at Buffalo.

Park, R. and Paulay, T. (1975). *Reinforced Concrete Structures*, John Wiley and Sons, Inc.

Paulay, T. (1989). "Equilibrium Criteria for Reinforced Concrete Beam-Column Joints", *ACI Structural Journal*, Vol.86, No. 6, November-December, 635-643.

Paulay, T. and Priestley, M.J.N. (1992). *Seismic Design of Reinforced Concrete and Masonry Buildings*, John Wiley and Sons, Inc., New York.

Park, R. (1986)."Ductile Design Approach for Reinforced Concrete Frames", *Earthquake Spectra*, Vol. 2, No.3, 565-619.

Paulay, T. (1988). "Seismic Design of Reinforced Concrete: The State of the Art in New Zealand", *Bulletin of the New Zealand National Society for Earthquake Engineering*, Vol. 21, No. 3, September, 208-232.

Stoppenhagen, D.R. and Jirsa, J.O. (1987). "Seismic Repair of a Reinforced Concrete Frame Using Encased Columns", University of Texas at Austin, PMFSEL Report No. 87-2.

NATIONAL CENTER FOR EARTHQUAKE ENGINEERING RESEARCH
LIST OF TECHNICAL REPORTS

The National Center for Earthquake Engineering Research (NCEER) publishes technical reports on a variety of subjects related to earthquake engineering written by authors funded through NCEER. These reports are available from both NCEER's Publications Department and the National Technical Information Service (NTIS). Requests for reports should be directed to the Publications Department, National Center for Earthquake Engineering Research, State University of New York at Buffalo, Red Jacket Quadrangle, Buffalo, New York 14261. Reports can also be requested through NTIS, 5285 Port Royal Road, Springfield, Virginia 22161. NTIS accession numbers are shown in parenthesis, if available.

NCEER 87-0001 "First Year Program in Research, Education and Technology Transfer," 3/5/87, (PB88-134275/AS).

NCEER 87-0002 "Experimental Evaluation of Instantaneous Optimal Algorithms for Structural Control," by R.C. Lin, T.T. Soong and A.M. Reinhorn, 4/20/87, (PB88-134341/AS).

NCEER 87-0003 "Experimentation Using the Earthquake Simulation Facilities at University at Buffalo," by A.M. Reinhorn and R.L. Ketter, to be published.

NCEER 87-0004 "The System Characteristics and Performance of a Shaking Table," by J.S. Hwang, K.C. Chang and G.C. Lee, 6/1/87, (PB88-134259/AS). This report is available only through NTIS (see address given above).

NCEER 87-0005 "A Finite Element Formulation for Nonlinear Viscoplastic Material Using a Q Model," by O. Gyebi and G. Dasgupta, 11/2/87, (PB88-213764/AS).

NCEER 87-0006 "Symbolic Manipulation Program (SMP) - Algebraic Codes for Two and Three Dimensional Finite Element Formulations," by X. Lee and G. Dasgupta, 11/9/87, (PB88-219522/AS).

NCEER 87-0007 "Instantaneous Optimal Control Laws for Tall Buildings Under Seismic Excitations," by J.N. Yang, A. Akbarpour and P. Ghaemmaghami, 6/10/87, (PB88-134333/AS).

NCEER-87-0008 "IDARC: Inelastic Damage Analysis of Reinforced Concrete Frame - Shear-Wall Structures," by Y.J. Park, A.M. Reinhorn and S.K. Kunnath, 7/20/87, (PB88-134325/AS).

NCEER-87-0009 "Liquefaction Potential for New York State: A Preliminary Report on Sites in Manhattan and Buffalo," by M. Budhu, V. Vijayakumar, R.F. Giese and L. Baumgras, 8/31/87, (PB88-163704/AS). This report is available only through NTIS (see address given above).

NCEER-87-0010 "Vertical and Torsional Vibration of Foundations in Inhomogeneous Media," by A.S. Veletsos and K.W. Dotson, 6/1/87, (PB88-134291/AS).

NCEER-87-0011 "Seismic Probabilistic Risk Assessment and Seismic Margins Studies for Nuclear Power Plants," by Howard H.M. Hwang, 6/15/87, (PB88-134267/AS).

NCEER-87-0012 "Parametric Studies of Frequency Response of Secondary Systems Under Ground-Acceleration Excitations," by Y. Yong and Y.K. Lin, 6/10/87, (PB88-134309/AS).

NCEER-87-0013 "Frequency Response of Secondary Systems Under Seismic Excitation," by J.A. HoLung, J. Cai and Y.K. Lin, 7/31/87, (PB88-134317/AS).

NCEER-87-0014 "Modelling Earthquake Ground Motions in Seismically Active Regions Using Parametric Time Series Methods," by G.W. Ellis and A.S. Cakmak, 8/25/87, (PB88-134283/AS).

NCEER-87-0015 "Detection and Assessment of Seismic Structural Damage," by E. DiPasquale and A.S. Cakmak, 8/25/87, (PB88-163712/AS).

NCEER-87-0016 "Pipeline Experiment at Parkfield, California," by J. Isenberg and E. Richardson, 9/15/87, (PB88-163720/AS). This report is available only through NTIS (see address given above).

NCEER-87-0017 "Digital Simulation of Seismic Ground Motion," by M. Shinozuka, G. Deodatis and T. Harada, 8/31/87, (PB88-155197/AS). This report is available only through NTIS (see address given above).

NCEER-87-0018 "Practical Considerations for Structural Control: System Uncertainty, System Time Delay and Truncation of Small Control Forces," J.N. Yang and A. Akbarpour, 8/10/87, (PB88-163738/AS).

NCEER-87-0019 "Modal Analysis of Nonclassically Damped Structural Systems Using Canonical Transformation," by J.N. Yang, S. Sarkani and F.X. Long, 9/27/87, (PB88-187851/AS).

NCEER-87-0020 "A Nonstationary Solution in Random Vibration Theory," by J.R. Red-Horse and P.D. Spanos, 11/3/87, (PB88-163746/AS).

NCEER-87-0021 "Horizontal Impedances for Radially Inhomogeneous Viscoelastic Soil Layers," by A.S. Veletsos and K.W. Dotson, 10/15/87, (PB88-150859/AS).

NCEER-87-0022 "Seismic Damage Assessment of Reinforced Concrete Members," by Y.S. Chung, C. Meyer and M. Shinozuka, 10/9/87, (PB88-150867/AS). This report is available only through NTIS (see address given above).

NCEER-87-0023 "Active Structural Control in Civil Engineering," by T.T. Soong, 11/11/87, (PB88-187778/AS).

NCEER-87-0024 "Vertical and Torsional Impedances for Radially Inhomogeneous Viscoelastic Soil Layers," by K.W. Dotson and A.S. Veletsos, 12/87, (PB88-187786/AS).

NCEER-87-0025 "Proceedings from the Symposium on Seismic Hazards, Ground Motions, Soil-Liquefaction and Engineering Practice in Eastern North America," October 20-22, 1987, edited by K.H. Jacob, 12/87, (PB88-188115/AS).

NCEER-87-0026 "Report on the Whittier-Narrows, California, Earthquake of October 1, 1987," by J. Pantelic and A. Reinhorn, 11/87, (PB88-187752/AS). This report is available only through NTIS (see address given above).

NCEER-87-0027 "Design of a Modular Program for Transient Nonlinear Analysis of Large 3-D Building Structures," by S. Srivastav and J.F. Abel, 12/30/87, (PB88-187950/AS).

NCEER-87-0028 "Second-Year Program in Research, Education and Technology Transfer," 3/8/88, (PB88-219480/AS).

NCEER-88-0001 "Workshop on Seismic Computer Analysis and Design of Buildings With Interactive Graphics," by W. McGuire, J.F. Abel and C.H. Conley, 1/18/88, (PB88-187760/AS).

NCEER-88-0002 "Optimal Control of Nonlinear Flexible Structures," by J.N. Yang, F.X. Long and D. Wong, 1/22/88, (PB88-213772/AS).

NCEER-88-0003 "Substructuring Techniques in the Time Domain for Primary-Secondary Structural Systems," by G.D. Manolis and G. Juhn, 2/10/88, (PB88-213780/AS).

NCEER-88-0004 "Iterative Seismic Analysis of Primary-Secondary Systems," by A. Singhal, L.D. Lutes and P.D. Spanos, 2/23/88, (PB88-213798/AS).

NCEER-88-0005 "Stochastic Finite Element Expansion for Random Media," by P.D. Spanos and R. Ghanem, 3/14/88, (PB88-213806/AS).

NCEER-88-0006 "Combining Structural Optimization and Structural Control," by F.Y. Cheng and C.P. Pantelides, 1/10/88, (PB88-213814/AS).

NCEER-88-0007 "Seismic Performance Assessment of Code-Designed Structures," by H.H-M. Hwang, J-W. Jaw and H-J. Shau, 3/20/88, (PB88-219423/AS).

NCEER-88-0008 "Reliability Analysis of Code-Designed Structures Under Natural Hazards," by H.H-M. Hwang, H. Ushiba and M. Shinozuka, 2/29/88, (PB88-229471/AS).

NCEER-88-0009 "Seismic Fragility Analysis of Shear Wall Structures," by J-W Jaw and H.H-M. Hwang, 4/30/88, (PB89-102867/AS).

NCEER-88-0010 "Base Isolation of a Multi-Story Building Under a Harmonic Ground Motion - A Comparison of Performances of Various Systems," by F-G Fan, G. Ahmadi and I.G. Tadjbakhsh, 5/18/88, (PB89-122238/AS).

NCEER-88-0011 "Seismic Floor Response Spectra for a Combined System by Green's Functions," by F.M. Lavelle, L.A. Bergman and P.D. Spanos, 5/1/88, (PB89-102875/AS).

NCEER-88-0012 "A New Solution Technique for Randomly Excited Hysteretic Structures," by G.Q. Cai and Y.K. Lin, 5/16/88, (PB89-102883/AS).

NCEER-88-0013 "A Study of Radiation Damping and Soil-Structure Interaction Effects in the Centrifuge," by K. Weissman, supervised by J.H. Prevost, 5/24/88, (PB89-144703/AS).

NCEER-88-0014 "Parameter Identification and Implementation of a Kinematic Plasticity Model for Frictional Soils," by J.H. Prevost and D.V. Griffiths, to be published.

NCEER-88-0015 "Two- and Three- Dimensional Dynamic Finite Element Analyses of the Long Valley Dam," by D.V. Griffiths and J.H. Prevost, 6/17/88, (PB89-144711/AS).

NCEER-88-0016 "Damage Assessment of Reinforced Concrete Structures in Eastern United States," by A.M. Reinhorn, M.J. Seidel, S.K. Kunnath and Y.J. Park, 6/15/88, (PB89-122220/AS).

NCEER-88-0017 "Dynamic Compliance of Vertically Loaded Strip Foundations in Multilayered Viscoelastic Soils," by S. Ahmad and A.S.M. Israil, 6/17/88, (PB89-102891/AS).

NCEER-88-0018 "An Experimental Study of Seismic Structural Response With Added Viscoelastic Dampers," by R.C. Lin, Z. Liang, T.T. Soong and R.H. Zhang, 6/30/88, (PB89-122212/AS). This report is available only through NTIS (see address given above).

NCEER-88-0019 "Experimental Investigation of Primary - Secondary System Interaction," by G.D. Manolis, G. Juhn and A.M. Reinhorn, 5/27/88, (PB89-122204/AS).

NCEER-88-0020 "A Response Spectrum Approach For Analysis of Nonclassically Damped Structures," by J.N. Yang, S. Sarkani and F.X. Long, 4/22/88, (PB89-102909/AS).

NCEER-88-0021 "Seismic Interaction of Structures and Soils: Stochastic Approach," by A.S. Veletsos and A.M. Prasad, 7/21/88, (PB89-122196/AS).

NCEER-88-0022 "Identification of the Serviceability Limit State and Detection of Seismic Structural Damage," by E. DiPasquale and A.S. Cakmak, 6/15/88, (PB89-122188/AS). This report is available only through NTIS (see address given above).

NCEER-88-0023 "Multi-Hazard Risk Analysis: Case of a Simple Offshore Structure," by B.K. Bhartia and E.H. Vanmarcke, 7/21/88, (PB89-145213/AS).

NCEER-88-0024 "Automated Seismic Design of Reinforced Concrete Buildings," by Y.S. Chung, C. Meyer and M. Shinozuka, 7/5/88, (PB89-122170/AS). This report is available only through NTIS (see address given above).

NCEER-88-0025 "Experimental Study of Active Control of MDOF Structures Under Seismic Excitations," by L.L. Chung, R.C. Lin, T.T. Soong and A.M. Reinhorn, 7/10/88, (PB89-122600/AS).

NCEER-88-0026 "Earthquake Simulation Tests of a Low-Rise Metal Structure," by J.S. Hwang, K.C. Chang, G.C. Lee and R.L. Ketter, 8/1/88, (PB89-102917/AS).

NCEER-88-0027 "Systems Study of Urban Response and Reconstruction Due to Catastrophic Earthquakes," by F. Kozin and H.K. Zhou, 9/22/88, (PB90-162348/AS).

NCEER-88-0028 "Seismic Fragility Analysis of Plane Frame Structures," by H.H-M. Hwang and Y.K. Low, 7/31/88, (PB89-131445/AS).

NCEER-88-0029 "Response Analysis of Stochastic Structures," by A. Kardara, C. Bucher and M. Shinozuka, 9/22/88, (PB89-174429/AS).

NCEER-88-0030 "Nonnormal Accelerations Due to Yielding in a Primary Structure," by D.C.K. Chen and L.D. Lutes, 9/19/88, (PB89-131437/AS).

NCEER-88-0031 "Design Approaches for Soil-Structure Interaction," by A.S. Veletsos, A.M. Prasad and Y. Tang, 12/30/88, (PB89-174437/AS). This report is available only through NTIS (see address given above).

NCEER-88-0032 "A Re-evaluation of Design Spectra for Seismic Damage Control," by C.J. Turkstra and A.G. Tallin, 11/7/88, (PB89-145221/AS).

NCEER-88-0033 "The Behavior and Design of Noncontact Lap Splices Subjected to Repeated Inelastic Tensile Loading," by V.E. Sagan, P. Gergely and R.N. White, 12/8/88, (PB89-163737/AS).

NCEER-88-0034 "Seismic Response of Pile Foundations," by S.M. Mamoon, P.K. Banerjee and S. Ahmad, 11/1/88, (PB89-145239/AS).

NCEER-88-0035 "Modeling of R/C Building Structures With Flexible Floor Diaphragms (IDARC2)," by A.M. Reinhorn, S.K. Kunnath and N. Panahshahi, 9/7/88, (PB89-207153/AS).

NCEER-88-0036 "Solution of the Dam-Reservoir Interaction Problem Using a Combination of FEM, BEM with Particular Integrals, Modal Analysis, and Substructuring," by C-S. Tsai, G.C. Lee and R.L. Ketter, 12/31/88, (PB89-207146/AS).

NCEER-88-0037 "Optimal Placement of Actuators for Structural Control," by F.Y. Cheng and C.P. Pantelides, 8/15/88, (PB89-162846/AS).

NCEER-88-0038 "Teflon Bearings in Aseismic Base Isolation: Experimental Studies and Mathematical Modeling," by A. Mokha, M.C. Constantinou and A.M. Reinhorn, 12/5/88, (PB89-218457/AS). This report is available only through NTIS (see address given above).

NCEER-88-0039 "Seismic Behavior of Flat Slab High-Rise Buildings in the New York City Area," by P. Weidlinger and M. Ettouney, 10/15/88, (PB90-145681/AS).

NCEER-88-0040 "Evaluation of the Earthquake Resistance of Existing Buildings in New York City," by P. Weidlinger and M. Ettouney, 10/15/88, to be published.

NCEER-88-0041 "Small-Scale Modeling Techniques for Reinforced Concrete Structures Subjected to Seismic Loads," by W. Kim, A. El-Attar and R.N. White, 11/22/88, (PB89-189625/AS).

NCEER 88 0042 "Modeling Strong Ground Motion from Multiple Event Earthquakes," by G.W. Ellis and A.S. Cakmak, 10/15/88, (PB89 174445/AS)

NCEER 88 0043 "Nonstationary Models of Seismic Ground Acceleration," by M. Grigoriu, S.E. Ruiz and E. Rosenblueth, 7/15/88, (PB89 189617/AS)

NCEER 88 0044 "SARCF User's Guide: Seismic Analysis of Reinforced Concrete Frames," by Y.S. Chung, C. Meyer and M. Shinozuka, 11/9/88, (PB89 174452/AS)

NCEER 88 0045 "First Expert Panel Meeting on Disaster Research and Planning," edited by J. Pantelic and J. Stoyle, 9/15/88, (PB89 174460/AS)

NCEER 88 0046 "Preliminary Studies of the Effect of Degrading Infill Walls on the Nonlinear Seismic Response of Steel Frames," by C.Z. Chrysostomou, P. Gergely and J.F. Abel, 12/19/88, (PB89-208383/AS)

NCEER 88 0047 "Reinforced Concrete Frame Component Testing Facility - Design, Construction, Instrumentation and Operation," by S.P. Pessiki, C. Conley, T. Bond, P. Gergely and R.N. White, 12/16/88, (PB89-174478/AS)

NCEER 89 0001 "Effects of Protective Cushion and Soil Compliancy on the Response of Equipment Within a Seismically Excited Building," by J.A. HoLung, 2/16/89, (PB89-207179/AS)

NCEER 89 0002 "Statistical Evaluation of Response Modification Factors for Reinforced Concrete Structures," by H.H.M. Hwang and J.W. Jaw, 2/17/89, (PB89-207187/AS)

NCEER 89 0003 "Hysteretic Columns Under Random Excitation," by G-Q. Cai and Y.K. Lin, 1/9/89, (PB89-196513/AS)

NCEER 89 0004 "Experimental Study of 'Elephant Foot Bulge' Instability of Thin-Walled Metal Tanks," by Z-H. Jia and R.L. Ketter, 2/22/89, (PB89-207195/AS)

NCEER-89-0005 "Experiment on Performance of Buried Pipelines Across San Andreas Fault," by J. Isenberg, E. Richardson and T.D. O'Rourke, 3/10/89, (PB89-218440/AS)

NCEER-89-0006 "A Knowledge-Based Approach to Structural Design of Earthquake-Resistant Buildings," by M. Subramani, P. Gergely, C.H. Conley, J.F. Abel and A.H. Zaghw, 1/15/89, (PB89-218465/AS)

NCEER-89-0007 "Liquefaction Hazards and Their Effects on Buried Pipelines," by T.D. O'Rourke and P.A. Lane, 2/1/89, (PB89-218481)

NCEER-89-0008 "Fundamentals of System Identification in Structural Dynamics," by H. Imai, C-B. Yun, O. Maruyama and M. Shinozuka, 1/26/89, (PB89-207211/AS)

NCEER-89-0009 "Effects of the 1985 Michoacan Earthquake on Water Systems and Other Buried Lifelines in Mexico," by A.G. Ayala and M.J. O'Rourke, 3/8/89, (PB89-207229/AS)

NCEER-89-R010 "NCEER Bibliography of Earthquake Education Materials," by K.E.K. Ross, Second Revision, 9/1/89, (PB90-125352/AS)

NCEER-89-0011 "Inelastic Three-Dimensional Response Analysis of Reinforced Concrete Building Structures (IDARC-3D), Part I - Modeling," by S.K. Kunnath and A.M. Reinhorn, 4/17/89, (PB90-114612/AS)

NCEER-89-0012 "Recommended Modifications to ATC-14," by C.D. Poland and J.O. Malley, 4/12/89, (PB90-108648/AS)

NCEER-89-0013 "Repair and Strengthening of Beam-to-Column Connections Subjected to Earthquake Loading," by M. Corazao and A.J. Durrani, 2/28/89, (PB90-109885/AS)

NCEER-89-0014 "Program EXKAL2 for Identification of Structural Dynamic Systems," by O. Maruyama, C.B. Yun, M. Hoshiya and M. Shinozuka, 5/19/89, (PB90-109877/AS).

NCEER-89-0015 "Response of Frames With Bolted Semi-Rigid Connections, Part I - Experimental Study and Analytical Predictions," by P.J. DiCorso, A.M. Reinhorn, J.R. Dickerson, J.B. Radziminski and W.L. Harper, 6/1/89, to be published.

NCEER-89-0016 "ARMA Monte Carlo Simulation in Probabilistic Structural Analysis," by P.D. Spanos and M.P. Mignolet, 7/10/89, (PB90-109893/AS).

NCEER-89-P0017 "Preliminary Proceedings from the Conference on Disaster Preparedness - The Place of Earthquake Education in Our Schools," Edited by K.E.K. Ross, 6/23/89.

NCEER-89-0017 "Proceedings from the Conference on Disaster Preparedness - The Place of Earthquake Education in Our Schools," Edited by K.E.K. Ross, 12/31/89, (PB90-207895). This report is available only through NTIS (see address given above).

NCEER-89-0018 "Multidimensional Models of Hysteretic Material Behavior for Vibration Analysis of Shape Memory Energy Absorbing Devices, by E.J. Graesser and F.A. Cozzarelli, 6/7/89, (PB90-164146/AS).

NCEER-89-0019 "Nonlinear Dynamic Analysis of Three-Dimensional Base Isolated Structures (3D-BASIS)," by S. Nagarajaiah, A.M. Reinhorn and M.C. Constantinou, 8/3/89, (PB90-161936/AS). This report is available only through NTIS (see address given above).

NCEER-89-0020 "Structural Control Considering Time-Rate of Control Forces and Control Rate Constraints," by F.Y. Cheng and C.P. Pantelides, 8/3/89, (PB90-120445/AS).

NCEER-89-0021 "Subsurface Conditions of Memphis and Shelby County," by K.W. Ng, T.S. Chang and H.H.M. Hwang, 7/26/89, (PB90-120437/AS).

NCEER-89-0022 "Seismic Wave Propagation Effects on Straight-Jointed Buried Pipelines," by K. Elhmadi and M.J. O'Rourke, 8/24/89, (PB90-162322/AS).

NCEER-89-0023 "Workshop on Serviceability Analysis of Water Delivery Systems," edited by M. Grigoriu, 3/6/89, (PB90-127424/AS).

NCEER-89-0024 "Shaking Table Study of a 1/5 Scale Steel Frame Composed of Tapered Members," by K.C. Chang, J.S. Hwang and G.C. Lee, 9/18/89, (PB90-160169/AS).

NCEER-89-0025 "DYNA1D: A Computer Program for Nonlinear Seismic Site Response Analysis - Technical Documentation," by Jean H. Prevost, 9/14/89, (PB90-161944/AS). This report is available only through NTIS (see address given above).

NCEER-89-0026 "1/4 Scale Model Studies of Active Tendon Systems and Active Mass Dampers for Aseismic Protection," by A.M. Reinhorn, T.T. Soong, R.C. Lin, Y.P. Yang, Y. Fukao, H. Abe and M. Nakai, 9/15/89, (PB90-173246/AS).

NCEER-89-0027 "Scattering of Waves by Inclusions in a Nonhomogeneous Elastic Half Space Solved by Boundary Element Methods," by P.K. Hadley, A. Askar and A.S. Cakmak, 6/15/89, (PB90-145699/AS).

NCEER-89-0028 "Statistical Evaluation of Deflection Amplification Factors for Reinforced Concrete Structures," by H.H.M. Hwang, J.-W. Jaw and A.L. Ch'ng, 8/31/89, (PB90-164633/AS).

NCEER-89-0029 "Bedrock Accelerations in Memphis Area Due to Large New Madrid Earthquakes," by H.H.M. Hwang, C.H.S. Chen and G. Yu, 11/7/89, (PB90-162330/AS).

NCEER-89-0030 "Seismic Behavior and Response Sensitivity of Secondary Structural Systems," by Y.Q. Chen and T.T. Soong, 10/23/89, (PB90-164658/AS).

NCEER-89-0031 "Random Vibration and Reliability Analysis of Primary-Secondary Structural Systems," by Y. Ibrahim, M. Grigoriu and T.T. Soong, 11/10/89, (PB90-161951/AS).

NCEER-89-0032 "Proceedings from the Second U.S. - Japan Workshop on Liquefaction, Large Ground Deformation and Their Effects on Lifelines, September 26-29, 1989," Edited by T.D. O'Rourke and M. Hamada, 12/1/89, (PB90-209388/AS).

NCEER-89-0033 "Deterministic Model for Seismic Damage Evaluation of Reinforced Concrete Structures," by J.M. Bracci, A.M. Reinhorn, J.B. Mander and S.K. Kunnath, 9/27/89.

NCEER-89-0034 "On the Relation Between Local and Global Damage Indices," by E. DiPasquale and A.S. Cakmak, 8/15/89, (PB90-173865).

NCEER-89-0035 "Cyclic Undrained Behavior of Nonplastic and Low Plasticity Silts," by A.J. Walker and H.E. Stewart, 7/26/89, (PB90-183518/AS).

NCEER-89-0036 "Liquefaction Potential of Surficial Deposits in the City of Buffalo, New York," by M. Budhu, R. Giese and L. Baumgrass, 1/17/89, (PB90-208455/AS).

NCEER-89-0037 "A Deterministic Assessment of Effects of Ground Motion Incoherence," by A.S. Veletsos and Y. Tang, 7/15/89, (PB90-164294/AS).

NCEER-89-0038 "Workshop on Ground Motion Parameters for Seismic Hazard Mapping," July 17-18, 1989, edited by R.V. Whitman, 12/1/89, (PB90-173923/AS).

NCEER-89-0039 "Seismic Effects on Elevated Transit Lines of the New York City Transit Authority," by C.J. Costantino, C.A. Miller and E. Heymsfield, 12/26/89, (PB90-207887/AS).

NCEER-89-0040 "Centrifugal Modeling of Dynamic Soil-Structure Interaction," by K. Weissman, Supervised by J.H. Prevost, 5/10/89, (PB90-207879/AS).

NCEER-89-0041 "Linearized Identification of Buildings With Cores for Seismic Vulnerability Assessment," by I-K. Ho and A.E. Aktan, 11/1/89, (PB90-251943/AS).

NCEER-90-0001 "Geotechnical and Lifeline Aspects of the October 17, 1989 Loma Prieta Earthquake in San Francisco," by T.D. O'Rourke, H.E. Stewart, F.T. Blackburn and T.S. Dickerman, 1/90, (PB90-208596/AS).

NCEER-90-0002 "Nonnormal Secondary Response Due to Yielding in a Primary Structure," by D.C.K. Chen and L.D. Lutes, 2/28/90, (PB90-251976/AS).

NCEER-90-0003 "Earthquake Education Materials for Grades K-12," by K.E.K. Ross, 4/16/90, (PB91-113415/AS).

NCEER-90-0004 "Catalog of Strong Motion Stations in Eastern North America," by R.W. Busby, 4/3/90, (PB90-251984)/AS.

NCEER-90-0005 "NCEER Strong-Motion Data Base: A User Manual for the GeoBase Release (Version 1.0 for the Sun3)," by P. Friberg and K. Jacob, 3/31/90 (PB90-258062/AS).

NCEER-90-0006 "Seismic Hazard Along a Crude Oil Pipeline in the Event of an 1811-1812 Type New Madrid Earthquake," by H.H.M. Hwang and C-H.S. Chen, 4/16/90(PB90-258054).

NCEER-90-0007 "Site-Specific Response Spectra for Memphis Sheahan Pumping Station," by H.H.M. Hwang and C.S. Lee, 5/15/90, (PB91-108811/AS).

NCEER-90-0008 "Pilot Study on Seismic Vulnerability of Crude Oil Transmission Systems," by T. Ariman, R. Dobry, M. Grigoriu, F. Kozin, M. O'Rourke, T. O'Rourke and M. Shinozuka, 5/25/90, (PB91-108837/AS).

NCEER-90-0009 "A Program to Generate Site Dependent Time Histories: EQGEN," by G.W. Ellis, M. Srinivasan and A.S. Cakmak, 1/30/90, (PB91-108829/AS).

NCEER-90-0010 "Active Isolation for Seismic Protection of Operating Rooms," by M.E. Talbott, Supervised by M. Shinozuka, 6/8/9, (PB91-110205/AS).

NCEER-90-0011 "Program LINEARID for Identification of Linear Structural Dynamic Systems," by C-B. Yun and M. Shinozuka, 6-25-90, (PB91-110312/AS).

NCEER-90-0012 "Two-Dimensional Two-Phase Elasto-Plastic Seismic Response of Earth Dams," by A.N. Yiagos, Supervised by J.H. Prevost, 6/20/90, (PB91-110197/AS).

NCEER-90-0013 "Secondary Systems in Base-Isolated Structures: Experimental Investigation, Stochastic Response and Stochastic Sensitivity," by G.D. Manolis, G. Juhn, M.C. Constantinou and A.M. Reinhorn, 7/1/90, (PB91-110320/AS).

NCEER-90-0014 "Seismic Behavior of Lightly Reinforced Concrete Column and Beam-Column Joint Details," by S.P. Pessiki, C.H. Conley, P. Gergely and R.N. White, 8/22/90, (PB91-108795/AS).

NCEER-90-0015 "Two Hybrid Control Systems for Building Structures Under Strong Earthquakes," by J.N. Yang and A. Danielians, 6/29/90, (PB91-125393/AS).

NCEER-90-0016 "Instantaneous Optimal Control with Acceleration and Velocity Feedback," by J.N. Yang and Z. Li, 6/29/90, (PB91-125401/AS).

NCEER-90-0017 "Reconnaissance Report on the Northern Iran Earthquake of June 21, 1990," by M. Mehrain, 10/4/90, (PB91-125377/AS).

NCEER-90-0018 "Evaluation of Liquefaction Potential in Memphis and Shelby County," by T.S. Chang, P.S. Tang, C.S. Lee and H. Hwang, 8/10/90, (PB91-125427/AS).

NCEER-90-0019 "Experimental and Analytical Study of a Combined Sliding Disc Bearing and Helical Steel Spring Isolation System," by M.C. Constantinou, A.S. Mokha and A.M. Reinhorn, 10/4/90, (PB91-125385/AS).

NCEER-90-0020 "Experimental Study and Analytical Prediction of Earthquake Response of a Sliding Isolation System with a Spherical Surface," by A.S. Mokha, M.C. Constantinou and A.M. Reinhorn, 10/11/90, (PB91-125419/AS).

NCEER-90-0021 "Dynamic Interaction Factors for Floating Pile Groups," by G. Gazetas, K. Fan, A. Kaynia and E. Kausel, 9/10/90, (PB91-170381/AS).

NCEER-90-0022 "Evaluation of Seismic Damage Indices for Reinforced Concrete Structures," by S. Rodríguez-Gomez and A.S. Cakmak, 9/30/90, PB91-171322/AS).

NCEER-90-0023 "Study of Site Response at a Selected Memphis Site," by H. Desai, S. Ahmad, E.S. Gazetas and M.R. Oh, 10/11/90, (PB91-196857/AS).

NCEER-90-0024 "A User's Guide to Strongmo: Version 1.0 of NCEER's Strong-Motion Data Access Tool for PCs and Terminals," by P.A. Friberg and C.A.T. Susch, 11/15/90, (PB91-171272/AS).

NCEER-90-0025 "A Three-Dimensional Analytical Study of Spatial Variability of Seismic Ground Motions," by L-L. Hong and A.H.-S. Ang, 10/30/90, (PB91-170399/AS).

NCEER 90-0026 "MUMOID User's Guide - A Program for the Identification of Modal Parameters," by S. Rodriguez-Gomez and E. DiPasquale, 9/30/90, (PB91-171298/AS).

NCEER 90-0027 "SARCF-II User's Guide - Seismic Analysis of Reinforced Concrete Frames," by S. Rodriguez-Gomez, Y.S. Chung and C. Meyer, 9/30/90, (PB91-171280/AS).

NCEER 90-0028 "Viscous Dampers: Testing, Modeling and Application in Vibration and Seismic Isolation," by N. Makris and M.C. Constantinou, 12/20/90 (PB91-190561/AS).

NCEER 90-0029 "Soil Effects on Earthquake Ground Motions in the Memphis Area," by H. Hwang, C.S. Lee, K.W. Ng and T.S. Chang, 8/2/90, (PB91-190751/AS).

NCEER 91-0001 "Proceedings from the Third Japan-U.S. Workshop on Earthquake Resistant Design of Lifeline Facilities and Countermeasures for Soil Liquefaction, December 17-19, 1990," edited by T.D. O'Rourke and M. Hamada, 2/1/91, (PB91-179259/AS).

NCEER 91-0002 "Physical Space Solutions of Non-Proportionally Damped Systems," by M. Tong, Z. Liang and G.C. Lee, 1/15/91, (PB91-179242/AS).

NCEER 91-0003 "Seismic Response of Single Piles and Pile Groups," by K. Fan and G. Gazetas, 1/10/91, (PB92-174994/AS).

NCEER 91-0004 "Damping of Structures: Part 1 - Theory of Complex Damping," by Z. Liang and G. Lee, 10/10/91, (PB92-197235/AS).

NCEER 91-0005 "3D-BASIS - Nonlinear Dynamic Analysis of Three Dimensional Base Isolated Structures: Part II," by S. Nagarajaiah, A.M. Reinhorn and M.C. Constantinou, 2/28/91, (PB91-190553/AS).

NCEER 91-0006 "A Multidimensional Hysteretic Model for Plasticity Deforming Metals in Energy Absorbing Devices," by E.J. Graesser and F.A. Cozzarelli, 4/9/91, (PB92-108364/AS).

NCEER 91-0007 "A Framework for Customizable Knowledge-Based Expert Systems with an Application to a KBES for Evaluating the Seismic Resistance of Existing Buildings," by E.G. Ibarra-Anaya and S.J. Fenves, 4/9/91, (PB91-210930/AS).

NCEER 91-0008 "Nonlinear Analysis of Steel Frames with Semi-Rigid Connections Using the Capacity Spectrum Method," by G.G. Deierlein, S-H. Hsieh, Y-J. Shen and J.F. Abel, 7/2/91, (PB92-113828/AS).

NCEER 91-0009 "Earthquake Education Materials for Grades K-12," by K.E.K. Ross, 4/30/91, (PB91-212142/AS).

NCEER 91-0010 "Phase Wave Velocities and Displacement Phase Differences in a Harmonically Oscillating Pile," by N. Makris and G. Gazetas, 7/8/91, (PB92-108356/AS).

NCEER 91-0011 "Dynamic Characteristics of a Full-Size Five-Story Steel Structure and a 2/5 Scale Model," by K.C. Chang, G.C. Yao, G.C. Lee, D.S. Hao and Y.C. Yeh," 7/2/91.

NCEER 91-0012 "Seismic Response of a 2/5 Scale Steel Structure with Added Viscoelastic Dampers," by K.C. Chang, T.T. Soong, S-T. Oh and M.L. Lai, 5/17/91 (PB92-110816/AS).

NCEER 91-0013 "Earthquake Response of Retaining Walls; Full-Scale Testing and Computational Modeling," by S. Alampalli and A-W.M. Elgamal, 6/20/91, to be published.

NCEER 91-0014 "3D-BASIS-M: Nonlinear Dynamic Analysis of Multiple Building Base Isolated Structures," by P.C. Tsopelas, S. Nagarajaiah, M.C. Constantinou and A.M. Reinhorn, 5/28/91, (PB92-113885/AS).

NCEER-91-0015 "Evaluation of SEAOC Design Requirements for Sliding Isolated Structures," by D. Theodossiou and M.C. Constantinou, 6/10/91, (PB92-114602/AS).

NCEER-91-0016 "Closed-Loop Modal Testing of a 27-Story Reinforced Concrete Flat Plate-Core Building," by H.R. Somaprasad, T. Toksoy, H. Yoshiyuki and A.E. Aktan, 7/15/91, (PB92-129980/AS).

NCEER-91-0017 "Shake Table Test of a 1/6 Scale Two-Story Lightly Reinforced Concrete Building," by A.G. El-Attar, R.N. White and P. Gergely, 2/28/91, (PB92-222447/AS).

NCEER-91-0018 "Shake Table Test of a 1/8 Scale Three-Story Lightly Reinforced Concrete Building," by A.G. El-Attar, R.N. White and P. Gergely, 2/28/91.

NCEER-91-0019 "Transfer Functions for Rigid Rectangular Foundations," by A.S. Veletsos, A.M. Prasad and W.H. Wu, 7/31/91.

NCEER-91-0020 "Hybrid Control of Seismic-Excited Nonlinear and Inelastic Structural Systems," by J.N. Yang, Z. Li and A. Danielians, 8/1/91, (PB92-143171/AS).

NCEER-91-0021 "The NCEER-91 Earthquake Catalog: Improved Intensity-Based Magnitudes and Recurrence Relations for U.S. Earthquakes East of New Madrid," by L. Seeber and J.G. Armbruster, 8/28/91, (PB92-176742/AS).

NCEER-91-0022 "Proceedings from the Implementation of Earthquake Planning and Education in Schools: The Need for Change - The Roles of the Changemakers," by K.E.K. Ross and F. Winslow, 7/23/91, (PB92-129998/AS).

NCEER-91-0023 "A Study of Reliability-Based Criteria for Seismic Design of Reinforced Concrete Frame Buildings," by H.H.M. Hwang and H.-M. Hsu, 8/10/91, (PB92-140235/AS).

NCEER-91-0024 "Experimental Verification of a Number of Structural System Identification Algorithms," by R.G. Ghanem, H. Gavin and M. Shinozuka, 9/18/91, (PB92-176577/AS).

NCEER-91-0025 "Probabilistic Evaluation of Liquefaction Potential," by H.H.M. Hwang and C.S. Lee," 11/25/91, (PB92-143429/AS).

NCEER-91-0026 "Instantaneous Optimal Control for Linear, Nonlinear and Hysteretic Structures - Stable Controllers," by J.N. Yang and Z. Li, 11/15/91, (PB92-163807/AS).

NCEER-91-0027 "Experimental and Theoretical Study of a Sliding Isolation System for Bridges," by M.C. Constantinou, A. Kartoum, A.M. Reinhorn and P. Bradford, 11/15/91, (PB92-176973/AS).

NCEER-92-0001 "Case Studies of Liquefaction and Lifeline Performance During Past Earthquakes, Volume 1: Japanese Case Studies," Edited by M. Hamada and T. O'Rourke, 2/17/92, (PB92-197243/AS).

NCEER-92-0002 "Case Studies of Liquefaction and Lifeline Performance During Past Earthquakes, Volume 2: United States Case Studies," Edited by T. O'Rourke and M. Hamada, 2/17/92, (PB92-197250/AS).

NCEER-92-0003 "Issues in Earthquake Education," Edited by K. Ross, 2/3/92, (PB92-222389/AS).

NCEER-92-0004 "Proceedings from the First U.S. - Japan Workshop on Earthquake Protective Systems for Bridges," 2/4/92, to be published.

NCEER-92-0005 "Seismic Ground Motion from a Haskell-Type Source in a Multiple-Layered Half-Space," A.P. Theoharis, G. Deodatis and M. Shinozuka, 1/2/92, to be published.

NCEER-92-0006 "Proceedings from the Site Effects Workshop," Edited by R. Whitman, 2/29/92, (PB92-197201/AS).

NCEER-92-0007 "Engineering Evaluation of Permanent Ground Deformations Due to Seismically Induced Liquefaction," by M.H. Baziar, R. Dobry and A-W.M. Elgamal, 3/24/92, (PB92-222421/AS).

NCEER-92-0008 "A Procedure for the Seismic Evaluation of Buildings in the Central and Eastern United States," by C.D. Poland and J.O. Malley, 4/2/92, (PB92-222439/AS).

NCEER-92-0009 "Experimental and Analytical Study of a Hybrid Isolation System Using Friction Controllable Sliding Bearings," by M.Q. Feng, S. Fujii and M. Shinozuka, 5/15/92, (PB93-150282/AS).

NCEER-92-0010 "Seismic Resistance of Slab-Column Connections in Existing Non-Ductile Flat-Plate Buildings," by A.J. Durrani and Y. Du, 5/18/92.

NCEER-92-0011 "The Hysteretic and Dynamic Behavior of Brick Masonry Walls Upgraded by Ferrocement Coatings Under Cyclic Loading and Strong Simulated Ground Motion," by H. Lee and S.P. Prawel, 5/11/92, to be published.

NCEER-92-0012 "Study of Wire Rope Systems for Seismic Protection of Equipment in Buildings," by G.F. Demetriades, M.C. Constantinou and A.M. Reinhorn, 5/20/92.

NCEER-92-0013 "Shape Memory Structural Dampers: Material Properties, Design and Seismic Testing," by P.R. Witting and F.A. Cozzarelli, 5/26/92.

NCEER-92-0014 "Longitudinal Permanent Ground Deformation Effects on Buried Continuous Pipelines," by M.J. O'Rourke, and C. Nordberg, 6/15/92.

NCEER-92-0015 "A Simulation Method for Stationary Gaussian Random Functions Based on the Sampling Theorem," by M. Grigoriu and S. Balopoulou, 6/11/92, (PB93-127496/AS).

NCEER-92-0016 "Gravity-Load Designed Reinforced Concrete Buildings: Seismic Evaluation of Existing Construction and Detailing Strategies for Improved Seismic Resistance," by G.W. Hoffmann, S.K. Kunnath, J.B. Mander and A.M. Reinhorn, 7/15/92, to be published.

NCEER-92-0017 "Observations on Water System and Pipeline Performance in the Limón Area of Costa Rica Due to the April 22, 1991 Earthquake," by M. O'Rourke and D. Ballantyne, 6/30/92, (PB93-126811/AS).

NCEER-92-0018 "Fourth Edition of Earthquake Education Materials for Grades K-12," Edited by K.E.K. Ross, 8/10/92.

NCEER-92-0019 "Proceedings from the Fourth Japan-U.S. Workshop on Earthquake Resistant Design of Lifeline Facilities and Countermeasures for Soil Liquefaction," Edited by M. Hamada and T.D. O'Rourke, 8/12/92.

NCEER-92-0020 "Active Bracing System: A Full Scale Implementation of Active Control," by A.M. Reinhorn, T.T. Soong, R.C. Lin, M.A. Riley, Y.P. Wang, S. Aizawa and M. Higashino, 8/14/92, (PB93-127512/AS).

NCEER-92-0021 "Empirical Analysis of Horizontal Ground Displacement Generated by Liquefaction-Induced Lateral Spreads," by S.F. Bartlett and T.L. Youd, 8/17/92.

NCEER-92-0022 "IDARC Version 3.0: Inelastic Damage Analysis of Reinforced Concrete Structures," by S.K. Kunnath, A.M. Reinhorn and R.F. Lobo, 8/31/92, to be published.

NCEER-92-0023 "A Semi-Empirical Analysis of Strong-Motion Peaks in Terms of Seismic Source, Propagation Path and Local Site Conditions, by M. Kamiyama, M.J. O'Rourke and R. Flores-Berrones, 9/9/92, (PB93-150266/AS).

NCEER-92-0024 "Seismic Behavior of Reinforced Concrete Frame Structures with Nonductile Details, Part I: Summary of Experimental Findings of Full Scale Beam-Column Joint Tests," by A. Beres, R.N. White and P. Gergely, 9/30/92, to be published.

NCEER-92-0025 "Experimental Results of Repaired and Retrofitted Beam-Column Joint Tests in Lightly Reinforced Concrete Frame Buildings," by A. Beres, S. El-Borgi, R.N. White and P. Gergely, 10/29/92, to be published.

NCEER 92-0026 "A Generalization of Optimal Control Theory: Linear and Nonlinear Structures," by J.N. Yang, Z. Li and S. Vongchavalitkul, 11/2/92.

NCEER 92-0027 "Seismic Resistance of Reinforced Concrete Frame Structures Designed Only for Gravity Loads: Part I - Design and Properties of a One-Third Scale Model Structure," by J.M. Bracci, A.M. Reinhorn and J.B. Mander, 12/1/92, to be published.

NCEER 92-0028 "Seismic Resistance of Reinforced Concrete Frame Structures Designed Only for Gravity Loads: Part II - Experimental Performance of Subassemblages," by L.E. Aycardi, J.B. Mander and A.M. Reinhorn, 12/1/92, to be published.

NCEER 92-0029 "Seismic Resistance of Reinforced Concrete Frame Structures Designed Only for Gravity Loads: Part III - Experimental Performance and Analytical Study of a Structural Model," by J.M. Bracci, A.M. Reinhorn and J.B. Mander, 12/1/92, to be published.

NCEER 92-0030 "Evaluation of Seismic Retrofit of Reinforced Concrete Frame Structures: Part I - Experimental Performance of Retrofitted Subassemblages," by D. Choudhuri, J.B. Mander and A.M. Reinhorn, 12/8/92.